Computational models for the study of responses to infections

Dissertation zur Erlangung des

naturwissenschaftlichen Doktorgrades

der Bayrischen Julius-Maximilians-Universität Würzburg

vorlegt von

Juilee Thakar

Aus Pune, Indien und Limerick, Irland

Würzburg 2005

Eingereicht am: ……………………………………………………………………

Mitglieder der Promotionskommission:

Vorsitzender:

Erster Gutachter: Professor Thomas Dandekar

Zweiter Gutachter : Professor Christoph Borner

Tag des Promotionskolloguiums: ....

Doktorurkunde ausghändigt am: ....

Erklärung

Hiermit erkläre ich ehrenwörtlich, daß ich die vorliegende Dissertation selbständig angefertigt und keine anderen als die angegeben Quellen und Hilfsmittel verwendet habe.

Die Dissertation wurde bisher weder in gleicher noch ähnlicher Form in einem anderen Prüfungsverfahren vorgelegt.

Außer dem Masters in Mikrobiologie von der Universität Pune, Indien habe ich bisher keine weiteren akademischen Grade erworben oder versucht zu erwerben.

Würzburg, December 2005   Juilee Thakar

Acknowledgement

Foremost I want to thank Professor Thomas Dandekar, for giving me enough freedom to think and develop ideas and yet guiding me whenever necessary during my thesis. This thesis would not have been possible without his support.
I would like to thank Professor Christoph Borner for his crucial suggestions and his willingness to serve on my thesis committee and also Dorothée Walter from his group for providing experimental data to validate our apoptosis model. I am also grateful to Dr. Gareth Griffith and Dr. Mark Kühnel for extremely useful discussions during the development of phagosome related models. I also want to thank Dr. Karin Schleinkofer for her guidance during structural analysis and for being a friend. I am thankful to Chunguang Liang for developing the openGL program for the phagosome spatial simulation.

I am extremely grateful to Professor Thomas Dandekar for allowing me to do a summer school in the Pennsylvania State University. I am equally thankful to Professor Réka Albert for her guidance and for providing me fellowship during this internship.

I would love to express my gratitude to Dr. Milind Watve who plays a guru's role in my career, who has always shown me direction and whose advice in my career I have always valued.

I am grateful to everyone in the Department of Bioinformatics, Wuerzburg for creating a great ambience for working. I would really like to thank Birgit Pils, Elisa Monzon Casanova, Julia Engelmann, Gudrun Dandekar, Stefan Pinkert and Torben Friedrich for their valuable companionship. I would specially like to thank Julia for reading my thesis. I am thankful to our administrative officer Karin Lustre for being patient with my limited German knowledge.

Last but not the least I am grateful to my parents Dinanath Thakar and Suvarna Thakar for imparting the right attitude to achieve my goals, to my sister Rama Thakar for always being my best friend and my fiancé Yogeshwar Kelkar for listening to my difficulties and for invaluable discussions during my Thesis. Without their backing this would have been very difficult. I would also like to give an attribute to all my friends and relatives whose names I can not list because of the limited space, but their love and affection plays a great role in my present position.

Table of contents

Results

Results Part I: Apoptosis: Analysis of the pathway and its components

Results Part II: Phagosome and Lysosome: Signaling and fusion

Results Part III: Host pathogen interplay exemplified by *Bordetella*: A heuristic approach

1. Introduction

The goal of this cumulative thesis is to study host responses to pathogens. Biological background (chapter 2), theoretical foundation, material and methods are sequentially organized followed by three parts of results and general discussion at the end. The chapter 3 'Theoretical foundation' describes modeling approaches used in the thesis. In spite of the complex regulated host immune system some pathogens still succeed in invasion. Versatile bioinformatical and modeling approaches are applied to understand different cascades of interactions in infections. Boolean networks, time step simulations, ordinary differential equations (ODEs) with domain and structure analysis are combined to study apoptosis, phagosome-lysosome fusion and interactions between host and pathogen. All components studied here are involved in different processes during pathogen invasion.

Biological cascades are studied in this thesis at different levels:

(i) Proteins - recognizing the important interacting surfaces involved in protein-protein interactions,

(ii) Pathway - recognizing different components involved in the pathway from literature, the effect of their topology and their role, by performing *in silico* deletions and by comparing with experimental observations.

(iii) Organelles (phagosome, lysosome) and networks - studying the important factors (actin polymerization) directing the fusion, effect of different molecules affecting fusion (phospholipids regulate actin polymerization and here the effect of combination of phospholipids on actin polymerization is studied).

(iv) System's responses – The immunological responses of the host in the case of *Bordetella* infections are studied in detail. Here we analyse the cascade of interactions between the virulence factors and the host immunological components upon pathogen invasion.

The results section is divided in to three parts, in part I the apoptosis pathway and its relation with a proliferation pathway is studied in detail. In the

section part I, chapter 5 and 6 describe the study of protein-protein interactions and a model of the apoptosis pathway respectively. Proteins in the apoptosis pathway have a set of domains in common collectively called the death domain superfamily. In chapter 5 interactions between proteins containing one of these domains are studied. Some of these proteins are known to play a role in the decision between proliferation/ survival or apoptosis. They are studied using phylogenetic, sequence and structural analysis. Some of the important amino acids in the interactions are also predicted. In the chapter 6 of part I the complete apoptosis pathway of *C. elegans*, *Drosophila melanogaster* and *Mus musculus* is then compared and used for qualitative modeling. ODEs are used to develop the model which was then used in a dynamic simulation for this purpose; further the results from the simulation are compared with experimental observations to test the success of the simulation.

In the second part a model is built to study the fusion between phagosome and lysosome. As seen in chapter 2 *M. tuberculosis* inhibits this fusion making it possible to live inside the phagosome. This step of fusion is essential in removal of pathogens. In chapter 7 the cascade of phospholipid reactions that take place in the phagosome membrane is modeled. It plays an important role in *de novo* actin polymerization. Actin polymerization in particular is known to be inhibited by *M. tuberculosis*. The simulation predicts the effect of the combination of phospholipids on the actin polymerization. The predictions of this model are checked and used in experiments. Spatial and analytical models are developed in chapter 8. These two models try to address the question of optimization of energy (ATPs), the effect of diffusion and time. The analytical model probabilistically calculates the time necessary for a successful event (fusion), taking into consideration the time taken by unsuccessful events. In contrary the spatial model actually tries to address the optimal length of F-actin necessary for efficient fusion.

In part III, chapter 9 a heuristic approach is used to study the host pathogen interactions exemplified by mammals and *Bordetella* species. A qualitative simulation is developed using logical operators. The results are compared with experiments proving the success of the model. Further the dynamic simulation is used to make some predictions about regulatory hot spots in immune responses. Conclusions at the each result chapter briefly discuss and summarize the main implications as well as the limitations of the specific approaches.

In the general discussion section the different approaches used in the thesis for modeling biologically complex systems are compared with similar approaches used by others. This also includes the implications of such work in answering biological questions and in drug discovery. We have also mentioned the advantages and disadvantages of the approaches.

2. Biological Background

2.1   The challenges of infectious diseases

About 15 million of 57 million annual deaths worldwide are estimated to be related directly to infectious diseases; this figure does not include the additional millions of deaths that occur as a consequence of past infections or because of complications associated with chronic infections, such as liver failure and hepatocellular carcinoma in people infected with hepatitis C or B viruses (figure 1). Infections in general can be classified as newly emerging infections, reemerging or deliberately emerging infections. Emerging infections (EIs) can be defined as "infections that have newly appeared in a population or have existed previously but are rapidly increasing in incidence or geographic range (Merrell and Falkow, 2004)"

Infectious diseases	Annual deaths (million)
Respiratory infections	3.96
HIV/AIDS	2.77
Diarrhoeal diseases	1.80
Tuberculosis	1.56
Vaccine-preventable childhood diseases	1.12
Malaria	1.27
STDs (other than HIV)	0.18
Meningitis	0.17
Hepatitis B and C	0.16
Tropical parasitic diseases	0.13
Dengue	0.02
Other infectious diseases	1.76
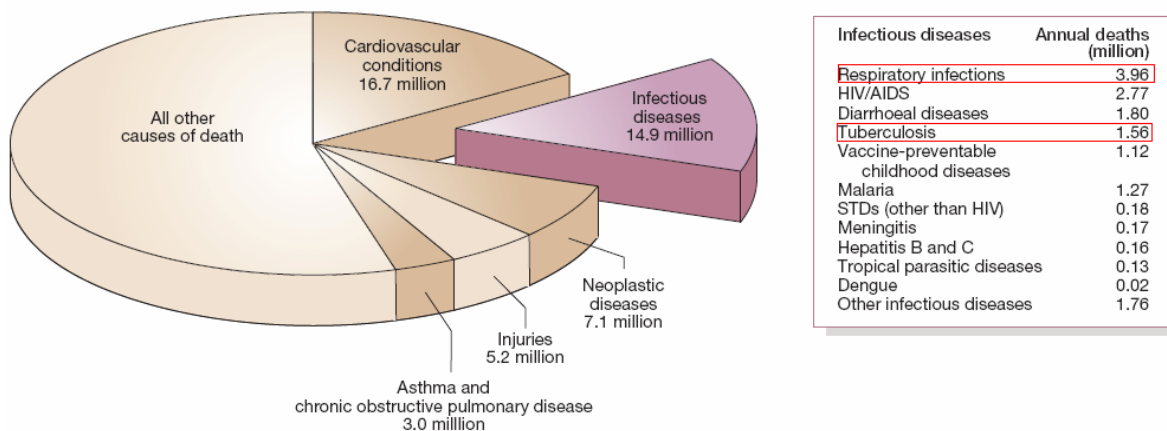
Figure 1: Leading causes of death worldwide. About 15 million (>25%) of 57 million annula deaths worldwide are the direct result if infectious disease. Figures published by the World Health Organization.

Environmentally persistent organisms:

Infectious agents indirectly transmitted to or between humans by way of human-modified environments account for emerging zoonoses, as well as certain non-zoonotic diseases. For example, legionnaires' disease is caused by *Legionella*

pneumophila, whose emergence as a human pathogen might not have occurred were it not for the environmental niche provided by air-conditioning systems (Committee on Emerging Microbial Threats to Health in the 21st Century. Microbial Threats to Health in the United States: Emergence). *Campylobacter jejuni* and Shiga-toxin-producing *Escherichia coli* (*E. coli* O157:H7 and other agents of haemolytic−uraemic syndrome) infect agricultural animals, gaining access to humans through food, milk, water or direct animal contact. Other enteric pathogens, such as the vibrios causing classical cholera (re-emerging; see below) and serogroup O139 cholera, and the zoonotic protozoa *Cryptosporidium parvum* and *Cyclospora cayetanensis* (Committee on Emerging Microbial Threats to Health in the 21st Century. Microbial Threats to Health in the United States: Emergence), seem to have come from environmental or animal organisms that have adapted to human-to-human 'faecal−oral' transmission through water.

Old microbes cause new diseases:

Some EIs come from microorganisms that once caused familiar diseases, but which now cause new or previously uncommon diseases. *Streptococcus pyogenes* caused a fatal pandemic of scarlet and puerperal fevers between 1830 and 1900(Katz and Morens, 1992). Scarlet fever, then the leading cause of death in children, is now rare, but has been largely supplemented by other streptococcal complications such as streptococcal toxic shock syndrome, necrotizing fasciitis and re-emergent rheumatic fever (Musser and Selander, 1990). Although the bases of emergences of new and more severe diseases caused by *S. pyogenes* and *H. influenzae* biogroup *aegyptius* are not fully known, in both cases complex microbial genetic events are suspected. The distinctive clonal variants associated with severe *H. influenzae* biogroup *aegyptius* disease have been shown by PCR (polymerase chain reaction)-based subtractive genome hybridization to contain not only a unique plasmid, but also unique

chromosomal regions, some of which are encoded by bacteriophages (Li et al., 2003).

Microbial agents and chronic diseases:

Infectious agents that are associated with chronic diseases are one of the most challenging categories of newly emerging (or at least newly appreciated) infections. Examples include the associations of hepatitis B and C with chronic liver damage and hepatocellular carcinoma, of certain genotypes of human papillomaviruses with cancer of the uterine cervix, of Epstein−Barr virus with Burkitt's lymphoma (largely in Africa) and nasopharyngeal carcinoma (in China), of human herpesvirus 8 with Kaposi sarcoma, and of *Helicobacter pylori* with gastric ulcers and gastric cancer (Chang et al., 1994; Sanders and Peura, 2002). Some data even suggest infectious aetiologies for cardiovascular disease and diabetes mellitus, major causes of death and disability worldwide. Other associations between infectious agents and idiopathic chronic diseases will inevitably be found.

Re-emerging infections (Tuberculosis):

Re-emerging and resurging infections are those that existed in the past but are now rapidly increasing either in incidence or in geographical or human host range. For example Tuberculosis is one of the most deadly re-emerging diseases (Figure 1). The discovery of isoniazid and other drugs initially led to effective tuberculosis cures, empty sanitoria and the dismantling of public health control systems in developed nations. Consequently, by the 1980s, when tuberculosis had re-emerged in the era of HIV/AIDS, local and state health departments in the United States lacked field, laboratory and clinical staff and so had to reinvent tuberculosis-control programmes (Committee on Emerging Microbial Threats to Health in the 21st Century. Microbial Threats to Health in the United States: Emergence). The remarkable re-emergence of tuberculosis was fuelled by the

immune deficiencies of people with AIDS, which greatly increases the risk of latent *Mycobacterium tuberculosis* infections progressing to active disease, and being transmitted to others. Inadequate courses of anti-tuberculosis therapy compound the problem, leading to the emergence and spread of drug-resistant and multidrug-resistant strains (Espinal, 2003), and a need for more expensive treatment strategies such as directly observed therapy. It has been known for over a century that tuberculosis is a disease of poverty, associated with crowding and inadequate hygiene. The continuing expansion of global populations living in poverty makes tuberculosis more difficult to control.

2.1.1   Pathogens and introduction to their strategies of invasion and survival

Wide range of microbe-host relationships can lead to disease. Host and pathogens constantly evolve to out-compete each others strategies. Recently two most general strategies are described in military term as 'frontal' and 'stealth' assaults(Merrell and Falkow, 2004). Frontal assault strategies require that the infecting microbes rapidly replicate, induce disease symptoms that overwhelm the innate defenses of the host, and find a new host before engagement of the adaptive immune system. The stealth assaults on the other hand, typically involve slower infection processes in which microbes subvert the host's innate and adaptive immune systems to set up a chronic or persistent infection. One example of the pathogen that uses a frontal assault strategy is *Vibro cholerae*, a potent epidemic adversary in many developing areas of the world. The ability of V. *cholerae* to rapidly cause disease before eliciting productive immune responses is shared by many organisms including the most common cause of diarrhoeal disease in infants, the rotavirus family, which is responsible for 600,000 deaths a year. The understanding of the strategies used by pathogens to set up persistent infections remains fairly limited compared with our knowledge of the frontal assault strategies discussed above. Some of the known strategies used by bacteria with examples are described in table 1.

Table 1: An overview of mechanisms used by bacteria to avoid host immune responses(Merrell and Falkow, 2004).

Immune response affected	Pathogen	Bacterial factor/mechanism
Induction of apoptosis/cytotoxicity	*Shigella flexneri* *Yersinia*	IpaB activation of pro-caspase 1 YopJ/P injection into macrophages
Inhibition of apoptosis	*Chlamydia* *Mycobacterium tuberculosis*	IL-10-induced TNF-α suppression Increased expression of *bcl2* and Rb
Inhibition of cytokine production	*Bartonella* *Vibrio cholerae*	IL-10 induction suppresses other cytokines CT inhibition of IL-12 secretion
Cytokine overproduction	*Bordetella pertussis* *Helicobacter pylori*	Pertussis toxin induction of IL-1 and IL-4 IL-8 induction
Complement evasion	*Streptococcus pyogenes* *Porphyromonas gingivalis*	M protein binding of C4BP Protease inactivation of C3 and C5
Evasion of host antibodies	*Staphylococcus aureus* *Peptostreptococcus magnus*	Protein A binding of IgG blocks phagocytosis Protein L binding of κ light chains
Inhibition of antigen presentation	*Helicobacter pylori* *Mycobacterium tuberculosis*	VacA targeting of antigen-presenting cells Downregulation of MHC class II and CD1
Inhibition of phagocytosis	*Pseudomonas* *Yersinia*	ExoT, ExoS targeting of Rho, Rac and Cdc42 YopO targeting of RhoA, Rac and actin
Survival in phagocytes	*Legionella* *Coxiella burnetii*	Dot/ICM genes inhibit phagolysosome fusion Acid tolerance allows survival in acidified lysosomes
Phase/antigenic variation	*Neisseria gonorrhoeae* *Helicobacter pylori*	Modulation of pilin Modulation of PAI and CagA

2.2 The host defense system an introduction

Pathogens invade the host and further spread by various routes for example through air, food, close contact etc. The host system recognizes the virulence factors expressed by pathogens and produce various cytokines in response. Cytokines are usually produced by cells which come in contact with pathogens for example epithelial cells. The two components of the immune system 'innate' and 'adaptive' immunity are essential for the protection against infection. Invasion of pathogens activate innate immune responses which is the retort to foreign material. These responses help in elimination or slow the spread of the pathogen. The effector mechanisms used by the host to control infection include production of pro-inflammatory cytokines and chemokines, recruitment of inflammatory cells to the site of infection and activation of lymphocytes and natural killer cells. If the pathogen persists, antigen specific adaptive immune

responses are activated. The adaptive immunity is further divided in to humoral and cellular responses. Humoral immunity refers to the antibody mediated responses against pathogen. Cellullar immunity involves activation of macrophages and NK cells and the production of various cytokines in response to antigen.

In Humoral immunity B cells are activated by T cell subtype called TH2 cells. B cells then undergo clonal expansion and produce antigen specific antibodies. Some antibodies for example IgG and IgM opsonize pathogens and activate classical complement pathway. Antibody opsonized pathogens also go through Fc receptor mediated phagocyosis. T cells are activated by interactions between dendritic cells and T naïve cells. Depending on the cytokines produced during interaction T naïve cells develop in to TH1 cells or TH2 cells. Th1 cells produce cytokines that activate large amount of phagocytic cells and especially macrophages. Macrophages are very essential phagocytic cells required for pathogen removal.

2.3 Microbial countermeasures

Humans live in harmony with much of the microbial world, thanks to a sophisticated immune system. The infiltrators still exist and they make use of the loop holes in the very same sophisticated immune system to survive and cause infections. Here we discuss microorganisms that survive in phagocytic cells. As seen in section 1.2 phagocytic cells actually remove microorganisms from our body. They are activated during innate and adaptive immunity.

Following microbial internalization, the newly formed phagosome proceeds through numerous steps of maturation accompanied by continuous remodeling of its protein composition. Moreover, the late phagosome is characterized by its fusion with late endosomes transporting endocytosed materials. Finally, the late phagosome forms a phagolysosome by fusing with pre-existing lysosomes. Within the lysosomal vacuoles are potent hydrolytic

enzymes that function optimally at acidic pH (4.5-5.0) and are capable of degrading microorganisms. The family of acid hydrolases includes nucleases, proteases, glycosidases, lipases, phosphatases, sulfatases and phospholipases. The degradation of intracellular microorganisms by intralysosomal acidic hydrolases constitutes a significant antimicrobial mechanism of phagocytes. In addition, the process of microbial degradation by lysosomes results in the generation of antigenic peptides suitable for presentation by class II MHC molecules and activation of CD4+ T lymphocytes. It appears that the antimicrobial activity of the phagolysosome is mediated, at least in part, by the degradative function of lysosomal enzymes and/or the direct or indirect effect of acidification. However, the precise mechanisms by which the hydrolases and acidification mediate antimicrobial activity, as well as the process of acidification of the various endocytic compartments, are not completely understood.

Various microbes exploit distinct intracellular niches for survival and proliferation within host cells (Table 1). In this section different microbial evasion strategies at different stages of infection will be discussed.

(A)   **(B)**

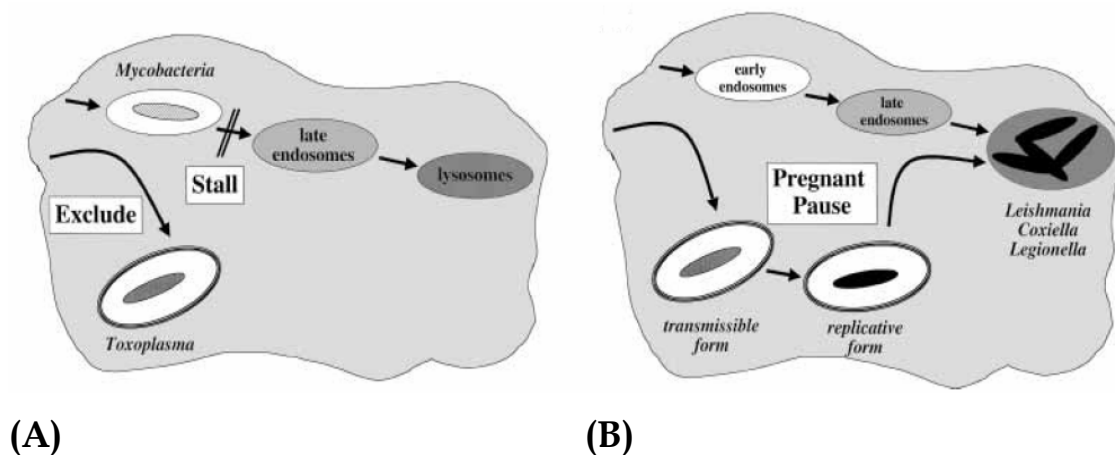**Figure 2: To avoid death in the lysosomes, pathogens short-circuit phagosome maturation. (A)** *Mycobacterium tuberculosis* **stalls maturation of its phagosome and replicates within an early endosomal compartment, whereas** *Toxoplasma gondii* **assembles a vacuole that excludes host trans-membrane proteins. (B) The transmissible forms of** *Leishmania* **spp.,** *Coxiella burnetii***, and** *Legionella pneumophila*

establish vacuoles that are separate from the endosomal pathway, but later differentiate to replicative forms that thrive in acidic lysosomes.

Inhibition of phagosome-lysosome fusion

Prevention of phagosome-lysosome fusion (Figure 2A) not only favors bacterial viability inside phagosomes, but also avoids antigen presentation and stimulation of CD4+ T lymphocytes. In cultivated human macrophage-like cells, *E. chaffeensis* resides in early endosomes that selectively accumulate the transferrin receptor and do not fuse with lysosomes, thereby preventing exposure to hydrolytic enzymes of the lysosomes (Barnewall et al., 1999). Furthermore, *ehrlichiae* prevent accumulation of vacuolar ATPase, which results in relatively high intraphagosomal pH (6.5). This pH is critical for obtaining iron from transferrin and for blunting the action of lysosomal hydrolases. Similarly, *M. tuberculosis* (Clemens et al., 2000), *L. pneumophila* (Clemens et al., 2000), *Chlamydia psittaci* and *C. trachomatis* occupy unique compartments which are distinct from late endosomes or phagolysosomes. The *L. pneumophila* phagosome exists completely outside the endolysosomal pathway, and the *M. tuberculosis* phagosome displays maturational arrest at an early endosomal stage (Sinai and Joiner, 1997) and does not fuse with lysosomes. These compartments neither acidify nor contain late endosomal markers such as cathepsin D and rab7 (Clemens et al., 2000). The exclusion of the vacuolar ATPase proton pump from phagosomes containing live *M. tuberculosis* or *M. avium* provides a mechanism for the relative lack of acidification of mycobacterial phagosomes. Similarly, *Chlamydia* spp. resides and replicate in a non-acidic compartment, the inclusion body. The localization of these pathogens within the host cell might depend on their route of internalization. For example, the intracellular parasite *T. gondii* actively invades its host cell and forms a vacuole that does not fuse with other intracellular compartments. However, antibody-opsonized *T. gondii* is engulfed via the FcR without active participation by the parasite and subsequently ends up in a phagolysosome (Mordue and Sibley, 1997).

Survival in the phagolysosome

Salmonella, *Leishmania*, and *Coxiella* survive and even replicate in the acidic and hydrolytic environment of the late endosomal/lysosomal compartments. Importantly, the phagolysosomal compartment may provide an essential source of nutrients for these organisms. Live *Salmonella typhimurium* resides in late endosomal/phagolysosomal vacuoles characterized by the presence of cathepsin L and other late endosomal markers without significant loss in bacterial viability. *Leishmania amastigotes* (Figure 2B) appear to be covered with lipidoglycans that are relatively resistant to all hydrolases. In addition, *Leishmania* parasites have nucleotidases on their surfaces that allow them to extract purines from autophagosomes in the cell necessary for their survival (Debrabant et al., 2000).

C. burnetii, the causative agent of Q fever, not only replicates within the phagolysosome of host cells, but also can transport and incorporate nutrients at a mildly acidic but not at a neutral pH (Howe and Mallavia, 2000). There is evidence to suggest, however, that *C. burnetii* is able to modify its environment. Supernatants from disrupted *C. burnetii* possess acid phosphatase activity that inhibits the metabolic burst of formyl-Met-Leu-Phe (fMLP)-stimulated human neutrophils.

Escape into the cytosol

This mechanism of evasion is employed by *Listeria*, *Shigella* and *Rickettsia*. Such a strategy not only protects these pathogens from harsh phagolysosomal conditions and associated host defense mechanisms, but also provides them with a nutrient-rich environment as discussed earlier. *L. monocytogenes* produces LLO that forms pores in the phagosomal membrane, thus allowing access of *Listeria* to the cytosol. *Shigella flexneri* displays hemolytic activity upon close contact with erythrocytes. This contact-mediated hemolytic activity seems to be necessary to lyse the phagocytic vacuole and is mediated by IpaB in the invasion- mediating protein complex.

Rickettsia spp. escape quickly from the phagosome into the host cell cytosol, but the mechanism of how this is achieved remains unclear. Phospholipase A activity possibly related to cell invasion and escape into the cytoplasm is associated with rickettsiae.

Once in the cytoplasm, the bacteria replicate in the cytosol of host cells. Many cytosolically replicating intracellular bacteria seem to possess the ability to spread from the primary infected cell into neighboring cells by inducing formation of host-derived F-actin tails that propel the bacteria through the cytoplasm and the cell membrane of the host cell. By using this cell-to-cell spread without extracellular exposure, these bacteria avoid extracellular host defenses, such as complement and antibodies.

During growth in the cytosol, some bacteria can induce or repress the expression of specific host genes and can influence pre-existing cytosolic gene products. The observed downregulation of host genes involved in the generation of MHC class II molecules and of the receptors for IFN-Q and TNF- α by cytosolically replicating *L. monocytogenes* may positively affect cytosolic *listerial* replication under in vivo conditions. Furthermore, activation of NF- κB by specific virulence factors produced by the replicating bacteria takes place after escape of *Rickettsia rickettsii* (Clifton et al., 1998) as well as *L. monocytogenes* (Hauf et al., 1997) into the host cell cytosol. NF-κB activation results in inhibition of apoptosis, allowing prolonged multiplication of intracellular bacteria in the cytosol.

Inhibition of generation of reactive nitrogen and oxygen intermediates

Many pathogenic microorganisms are known to inhibit generation of O_2^- radicals in neutrophils or monocytes. For example, the human granulocytic ehrlichiosis agent, *Anaplasma phagocytophila*, which is an obligatory intracellular bacterium that replicates in neutrophils, subverts the ability of human neutrophils to generate O_2^- in response to both soluble stimuli (e.g., phorbol

myristic acid or fMLP) and particulate stimuli (*Escherichia coli*), which activate the NADPH oxidase through different signaling pathways (Mott and Rikihisa, 2000). *M. tuberculosis* produces catalase and superoxide dismutase, two gene products capable of degrading reactive oxygen species. Additionally, *M. tuberculosis* avoids host defense through binding to CR1 or CR3, which do not trigger the oxidative burst and inflammatory response (Schorey et al., 1997).

Lack of production of proinflammatory cytokines

Certain intracellular pathogens have the intrinsic ability to down regulate the production of proinflammatory cytokines by infected macrophages. For example, macrophages infected with *E. chaffeensis* do not secrete IL-6 or granulocyte macrophage colony stimulation factor GM-CSF, and TNF-α production is not upregulated (Lee and Rikihisa, 1996). Similarly, different intracellular bacteria have varying abilities to stimulate macrophages or immune lymphocytes to produce TNF-α. For example, viable *Orientia tsutsugamushi*, although able to grow to high titers in both murine peritoneal macrophages and a macrophage-like cell line, does not stimulate the production of detectable TNF-α by these cells. In contrast, infection of macrophages with *R. conorii* results in production of high levels of TNF-α.

Inhibition of apoptotic cell death

Cells infected with *T. gondii* are resistant to both Fas dependent and Fas-independent CTL-mediated cell death. The ability to extend the life of infected host cells would be a substantial advantage to intracellular pathogens for enhancing their own survival.

2.4 Apoptosis and host homeostasis

Apoptosis and cell cycle are highly conserved mechanisms by which eukaryotic cells commit suicide and replicate themselves respectively. Apoptosis enables an organism to eliminate unwanted and defective cells through an orderly process of cellular disintegration that has the advantage of not inducing an undesirable inflammatory response (Jacobson et al., 1997). Apoptotic elimination of cells occurs during normal development and turnover, as well as in a variety of pathological conditions. Improper regulation of apoptosis contributes to disorders such as cancer, viral infection, autoimmune diseases, neurodegenerative disorders, stroke, anemia and AIDs (Wyllie, 1997). Apoptosis can be triggered by a wide number of signals. These include FAS ligand, tumor necrosis factor, growth factor withdrawal, viral or bacterial infection, oncogenes, irradiation, ceramide and chemotherapeutic drugs (Wyllie, 1997). The morphological changes characteristic of apoptotic process are mainly due to caspases, a family of cysteine proteases that act as effectors of the cell death pathway (Golstein, 1997). Their activation leads to the cleavage of specific proteins that include some cell regulators. The process of cell loss and cell gain must be homeostatically balanced in order to generate and maintain the complex architechture of tissues. One way in which this connection may be achieved is through the coupling of cell cycle and programmed cell death, perhaps by using or controlling a shared set of factors (King and Cidlowski, 1995). One evidence is that apoptosis is regulated by genes that are involved in cell cycle progression. Here, in this thesis I study apoptosis inducing ligands, the components of cell cycle that are involved in activating or inhibiting apoptosis, the conservation of apoptosis pathway in *C. elegans*, *Drosophila melanogaster* and *M. musculus*. Below there are some examples of proteins and their regulation studied in this thesis; that are affected during diseases.

Apoptosis in disease and the responses to disease

It is evident that apoptosis provides a powerful regulatory mechanism for many aspects of normal tissue growth and function. This section extends the discussion to describe how apoptosis regulates the responses to disease and how defective regulation of apoptosis may be central to the pathogenesis of many important disorders.

Inflammation

The response to injury or infection has itself considerable potential to damage tissue and it is therefore tightly regulated. Neutrophils, eosinophils and monocytes die by apoptosis within a relatively short period (e.g. 3-4 days for eosinophils in culture), however death can be significantly delayed by proinflammatory cytokines such as C5a (neutrophils), IL-1β, TNF-α, IFN-γ (monocytes) and IL-5 (eosinophils) (Mangan and Wahl, 1991; Stern et al., 1992). In contrast TGF-β and TNF-α accelerate eosinophil and neutrophil apoptosis respectively (Alam et al., 1994; Takeda et al., 1993). This suggests a potential mechanism *in vivo* for control of the survival and ultimately the removal of these potentially dangerous cells from sites of inflammation when the inflammatory stimulus subsides. Defects in these mechanisms or in the clearance of apoptotic cells may underlie some chronic inflammatory diseases (e.g. hypereosinophilic syndromes) due to inappropriate persistence of inflammatory cells with continued release of toxic cellular contents perpetuating tissue injury and inflammation. Of interest in this regard is the multifocal inflammatory disease and tissue necrosis that occurs in mice without functional TGF β1 (Shull et al., 1992).

Cytotoxic lymphocyte (CTL) killing

Cell-mediated cytotoxicity is an integral component of specific host defenses, for example against virally infected cells, and apoptosis is believed to be the mode of death in a proportion of CTL-induced target cell killing (Squier

and Cohen, 1994). Evidence suggests that activation of target cell fas by the CTL is an important mechanism for this cell-mediated apoptosis, although engagement of target cell TNF receptors may also act to trigger apoptosis in some instances (Ratner and Clark, 1993; Rouvier et al., 1993). The finding that activation of surface fas on hepatocytes triggers apoptosis(Ogasawara et al., 1993) suggests a potential pathogenetic mechanism for viral or perhaps autoimmune hepatitis that may have implications for new strategies of therapy. It is of relevance to note that CTL can kill by a mechanism that involves perforin insertion into target cell membranes and granule exocytosis (Squier and Cohen, 1994). The relative importance and interactions of these different modes of killing is not established.

AIDS

The gradual depletion of CD4+T cells during HIV infection that leads to clinical AIDS is thought to be due to excessive apoptosis (Ogasawara et al., 1993). HIV-infected cells express a viral envelope transmembrane gp120-gp41 complex which binds the CD4 D1 domain of uninfected T cells and triggers apoptosis directly(Ameisen, 1992). Furthermore HIV particles shed gp120 which, although unable to trigger apoptosis itself, can bind CD4 and program uninfected T cells for apoptosis (instead of proliferation) in response to subsequent T cell receptor stimulation by antigen (Gougeon and Montagnier, 1993). The deletion of naive and memory T cell clones on encountering their specific antigen abolishes the individual's ability to mount a specific immune response to infections (Gougeon and Montagnier, 1993).

Oncogenic viruses

Oncogenic viruses have developed strategies to prevent host cell apoptosis that have shed light on control pathways. The Epstein Barr virus BHRFI protein is a bcl-2 homologue, whilst the LMP-1 protein upregulates bcl-2

expression and induces the A20 zinc finger protein that confers resistance to TNFα cytotoxicity (Henderson et al., 1993; Henderson et al., 1991). The adenovirus E1B gene encodes a functional homologue of bcl-2 and a protein that inactivates the p53 oncosuppressor (Debbas and White, 1993; White et al., 1992). In fact several viruses inhibit p53 function in different ways, including SV40 (large T antigen), Epstein Barr virus (EBNA 5), human papillomavirus types 16 and 18 (E6 protein) and hepatitis B virus (HBx protein) (Selter and Montenarh, 1994). This is a testament to the importance of that molecule in countering abnormal cell proliferation. Interestingly, many oncogenic viruses contain genes that activate cells from the growth arrested state (SV40 T antigen, adenovirus E1A, HPV E7) probably via inactivation of Rb protein, release of transcription factor E2F and activation of c-myc. At least some of these changes also imply increased susceptibility to apoptosis, as discussed earlier. The combination therefore of pro-apoptotic oncogenes with others having anti-apoptotic activity appears to be an essential part of the viral strategy to induce cell proliferation without also activating cell death.

Cancer therapy implications

Apoptosis is a physiological process to regulate tissue homeostasis, and a defect in its execution may lead to cancer. Moreover, evading apoptosis is considered as one of the six steps leading to malignant growth as the ability to modify sensitivity to apoptosis through the regulatory pathways has clear implications for the treatment of malignancy (Hickman, 1992). Potential strategies fall into three categories—direct triggering of apoptosis by cytotoxic agents, enhancing susceptibility to apoptosis to increase the efficacy of other therapies, and boosting the resistance of normal cells to apoptosis (with survival factors). Restoration of function of interrupted apoptotic pathways, e.g. *p53*-dependent apoptosis, with consequent self-deletion by tumour cells would be a most attractive strategy. Bcl-2 antagonists might likewise be expected to cause

regression of follicular lymphomas or at least to increase their radio- or chemosensitivity. Induction of a high turnover state (with survival factor dependence) or antagonism of tumour survival factors (e.g. antiandrogens for prostate carcinoma, tamoxifen for oestrogen receptor-expressing breast carcinomas) is other approaches to therapy. Boosting normal cell resistance to apoptosis with exogenous survival factors can be used after ablative therapy to improve restoration of the normal cell population, (Sachs and Lotem, 1993) reducing treatment morbidity and allowing greater frequency of cytotoxic treatments.

3. Theoretical foundations

3.1 Modeling: From proteomics to systems biology
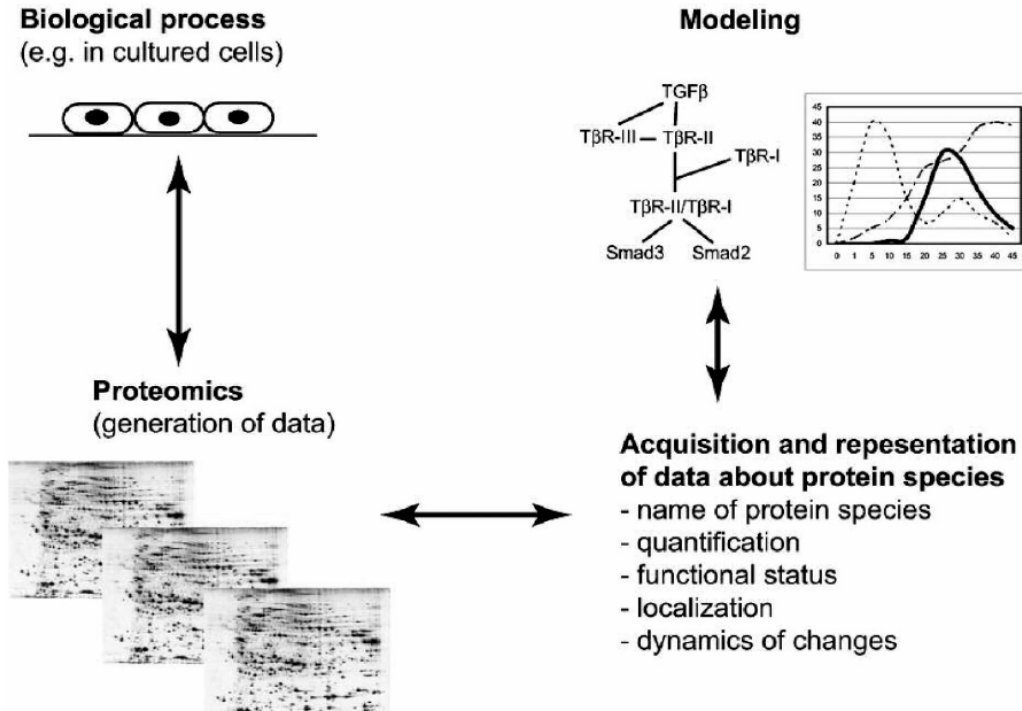
Figure 3: Steps of biological modeling using proteomics data. In this figure, experimental models include any biologically relevant processes in living systems, and are represented by cultured cells as an example. Proteomics is exemplified by 2-D gels. Further proteomics datasets have to be acquired and represented in formats that are compatible with modeling tools. It is represented by listing information which is required for representation of biological data. Proteomics datasets which are translated into modeling compatible formats can be then used for modeling. Here, modeling is represented by a relation network between TGF β, its receptors (TβR-I, TβR-II, TβR-III) and receptor substances (Smad2 and Smad3), and a graph which illustrates changes in protein concentrations. The arrows between the main steps are double-headed, as modeling tools influence requirements for data deposition and representation. Data deposition and representation also affect designing of proteomics experiments, and proteomics technologies may affect selection of a biological model.

Proteomics is a large scale technology which provides a global overview of proteomes (de Hoog and Mann, 2004; Gorg et al., 2004). Information about

28

protein expression, rates of synthesis and degradation, enzymatic activities, structure, localization and interacting partners can be generated by modern proteomics techniques, although with various degree of preciseness. In general the study of proteomics can be divided in to (i) quantification of proteins, (ii) functional status of proteins (activity and interactions), (iii) localization and (iv) the dynamics of proteomes. This information can be used heuristically for building and analysis of models of biological processes. A number of modeling tools addresses biological complexity on the level of biochemical reactions and cell physiology and evolution (Papin et al., 2005) (Figure 3). The term 'model' refers to the description of biological processes in the mathematical terms, without discrimination of mathematical tools. Consequently modeling is defined as "the application of methods to analyse complex, real world problems to make predictions about what might happen with various actions". Modeling tools cover a broad range of mathematical methods (Figure 4), from system of differential equations to statistical correlation tools. Some tools require detailed knowledge about components, For example, to build a system of differential equations for modeling of signaling pathway, knowledge of concentration of components and kinetic parameters of reactions in this pathway is required. Data with less precise information can be analyzed by other tools For example, to build a model based on Bayesian network it is sufficient to know relations between studied components of a model. However, common for all modeling tools is the requirement of information about quantity and identity of components of a model, and knowledge of dependencies and dynamics of relation between these components (Souchelnytskyi, 2005). Once a model has been developed it has to be tested for different parameter to find the best fitting parameters. Parameters are many times unknown constants which can be standardized by simulations. In many instances the model is tested across time such simulations are called dynamic simulations.

29
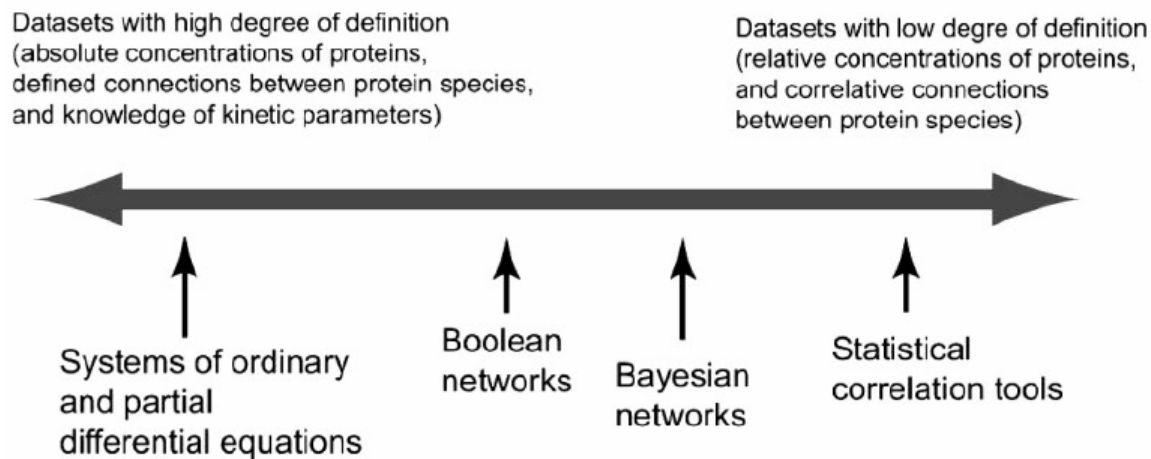
Figure 4: Application of modeling tools to datasets with various degree of definition. **Proteomics produces data of various degrees of definition of protein species, e.g., various levels of details about absolute or relative concentrations of proteins, their activities, localization and dynamics of changes of these proteins. Each set of such data can be most efficiently analyzed by modeling tools designed to process data with various definitions of details in the description of proteomes as indicated. As examples, differential equations, Boolean and Bayesian networks, and statistical correlation tools are indicated. They are shown in relation to the required level of details about datasets to be efficiently analyzed with those tools.**

I will focus here on the categories functional status (ii) and dynamics of proteins (iv) from the proteomics section described above as they are important for the computational approach used here. In the functional status of proteins along with the experimental work for identification of interacting partners, their modifications (For example: phosphorylation, methylation etc.) and their activity; the bioinformatical approach is essential to predict new interaction partners, modification sites and novel interacting surfaces. Various bioinformatical approaches mainly include, (i) sequence analysis of whole proteins or domains (functional units of proteins): comparison across the species in a multiple alignment and (ii) structural analysis: Prediction of structures from sequence alignment, comparison of structures of proteins and active sites from various organisms and study of evolution of structure. In both of these approaches, slow evolving and fast evolving sites are predicted by multiple

alignment of sequences. Ofcourse experimental results are necessary to confirm these predictions. The data on dynamics of proteins has to be obtained from experiments. The timescale of biological processes varies from milliseconds to days. The experimental data in such cases includes reaction rates, kinetic constants and concentrations *in vivo*. As mentioned above these details are important for qualitative simulations that are many times performed using ODEs. Qualitative modeling can be performed without these details, the information about relative concentrations of components and relative rates of reaction are sufficient.

Most of the proteins especially proteins associated with cell cycle, apoptosis and immune responses to the pathogens are not constitutively produced but are induced when necessary.

3.2 Approaches to study biological regulatory networks

Current Opinion in Chemical Biology
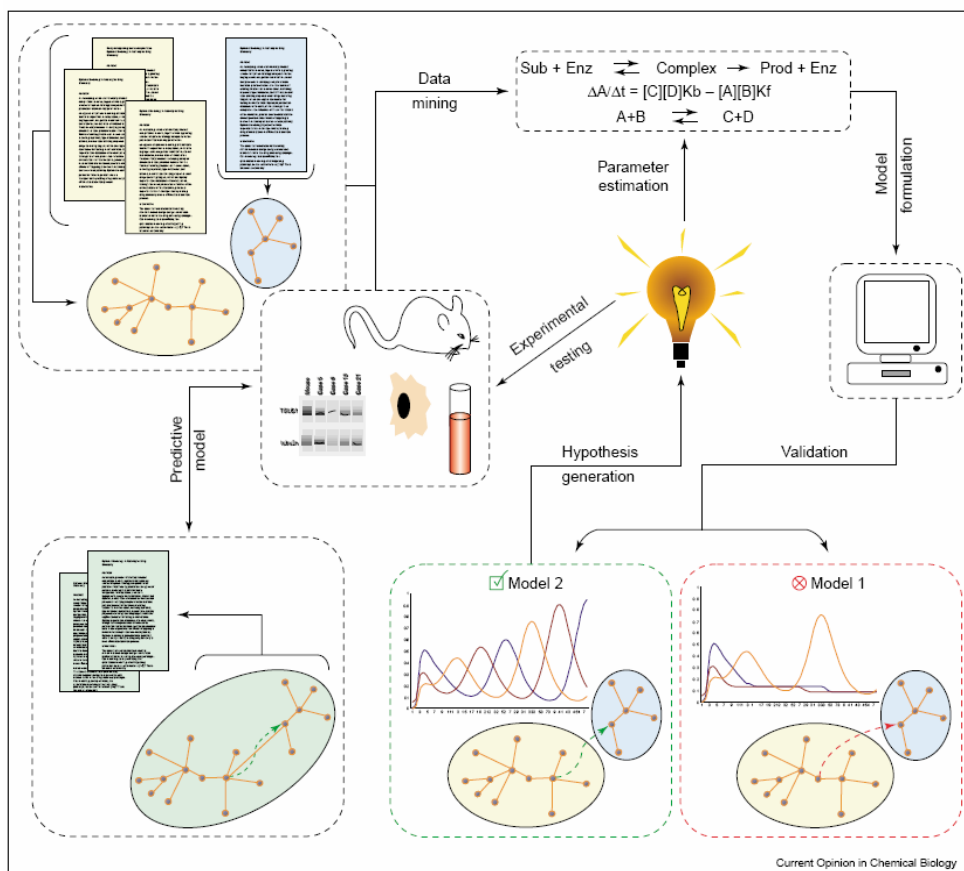
Figure 5: Iterative process of modeling a biological signaling system. Data are collated from literature and experiments, and parameters are estimated where necessary. Models are considered to be valid when simulation results match a significant set of experimental observations. Finally, the model is used to generate hypothesis, which can be experimentally tested (Rajasethupathy et al., 2005).

The process of modeling a biological signaling system begins with extensive data mining from literature to obtain parameters (Figure 5). Other specific inputs to the model might be: details of key regulatory pathways, known interactions with pharmacological agents, tissue specificity, and so on. Often, it is necessary to use indirect data or even educated guesses to set a parameter for which direct data do not exist. The model is considered valid if it can explain a substantial set of experimental observations. Finally, the model is used to generate hypotheses that can then be tested. Through this iterative process, one gains a better understanding of the biological system and insights into possible therapeutic interventions.

The most traditional approach to study biological networks is to employ ODEs such as Michaelis-Menten equations. This approach provides mathematically well founded and fine interpretations of biological networks, especially for enzyme reactions. Gepasi (Mendes, 1993) is a software package based on this approach for modeling biochemical systems and it aims at assisting users in translating reaction processes to matrices and ODEs. E-cell (Tomita et al., 1999) is a system for representation and simulation with a GUI and, with this tool, a model of a hypothetical cell with only 127 genes sufficient for transcription, translation, energy production and phospholipids synthesis has been constructed. Use of ODEs is often restricted due to the need of various rate constants. A Petri net is a stoichiometrical approach, developed by Reisig in 1985 and was first used in 1993 for modeling metabolic pathways (Reddy et al., 1993).

Petri net is a network consisting of place, transition, arc and token. A place can hold tokens as its contents. A transition has arcs coming from places and arcs going out from transition to some places. A transition with these arcs defines a

firing rule in terms of the contents of the places where the arcs are attached. Firing speed is given as a function of values in the places in the model. Hybrid Petri nets (HPN) (Alla and David, 1998) and hybrid dynamic net (HDN) (Drath, 1998) and hybrid functional Petri nets (HFPN) (Matsuno et al., 2003) are improved versions of original Petri nets. Biological pathways essentially consist of discrete parts such as a genetic switch control and continuous parts such as a metabolic reaction. These discrete and continuous parts can be represented by discrete elements (discrete place and discrete transition) and continuous elements (continuous place and continuous transition). Continuous transition fires continuously. For example: if discrete place has a token, the protein necessary for activating the operator site has bound to the operator that means the gene expression is turned on.

Another approach to represent metabolic pathway is by a stoichiometric matrix m * n where m corresponds to the number of metabolites and n corresponds to the number of reactions or fluxes taking place within the network. The analysis of such matrix is performed by representation of fluxes by basis vectors in the null space (Horiuti and Nakamura, 1957; Reder, 1988). Taking in to consideration the irreversibility of the reaction the region of admissible steady state flux vectors shrink to a subset of null space. Elementary the mode analysis was developed to find basis vectors of this subset which are of interest to understand metabolic pathways (Heinrich et al., 2002). In other words the elementary mode is a minimal set of enzymes that could operate at steady state, with the enzyme weighted by the relative flux they need to carry for mode to function. Here the concept of Petri net and elementary mode analysis converge in the study of feasible metabolic fluxes. The stoichiometric matrix of a metabolic network corresponds to the incidence matrix of Petri net so that the stoichiometric coefficients are described by arc weights. The concept of T invariants in Petri net is similar to the flux modes and conservations in later representation (Zevedei-Oancea and Schuster, 2003).

In these models the proportion of fluxes is fixed whereas the magnitudes are indeterminate, thus avoiding the need of kinetic data. The methods described above have been proven successful in modeling metabolic pathways where products can be stoichametrically balanced and proportion of fluxes can be decided. These properties can not be formulated in signal transduction pathways. Thus the mathematical representations of signal transduction pathways are difficult to formulate due to large number of unknown factors such as rate constants, concentrations of components etc. But even before such data becomes available simulations can enhance our understanding of regulatory principles and pinpoint critical behavior and parameters for further experimental tests.

Though efforts to study the signal transduction pathway are still in early stages, some approaches have been developed. A simple linear cascade of protein kinases was mathematically represented to understand the key steps in kinase and phosphatase regulation (Heinrich et al., 2002). The approach developed analytical solutions to understand the effect limited number of key parameters on the regulation. In spite of vigorous mathematical formulations the model can describe very simple and linear pathways and further has restricted applications.

3.3 Dynamic simulation

Dynamic modeling (Batt et al., 2005; Bentele et al., 2004; Bhalla et al., 2002; Heinrich et al., 2002) is used in this thesis in chapters 6, 7 and 9 for understanding biological networks. It inludes two steps, in the first step all the interactions are described by a mathematical formalism. In the second step the evolution of these interactions is studied in time. Understanding of the system is necessary to make a decision about which mathematical formalism to use. Further they can evolve continuously or discontinuous in time. This is often dependent on which mathematical formulism is used in the first step, the

information available about the rate constants and the development of the network (for example: if the network is complete a continuous function can be used, but if some of the components in the network are missing then a discontinuous function may be more useful).

In chapter 6 a Michaelis Menten type simplification is used to describe a set of key interactions in the apoptosis pathway. The system evolves as a continuous function of time, thus ODEs are used for this purpose. Though concentrations are calculated at discrete time steps, the system is based on a continuous curve. For example, if:

X_1 and X_2 are two components in the pathway and X_2 is activated in presence of X_1, then I can write,

IF $(X_1[t]>$THRESHOLD$)$
      $dX_2/dt= (X_1[t]*$MAX_UNIT$)/(K + X_1[t])$
ELSE
      $dX_2/dt=0$

$X_2[t] = X_2[t-1] + dX_2/dt$

Where X[t], indicates the concentration at time t, K is the Michaelis Menten constant.

In contrast to chapter 6, in chapter 7 and 9 logical operators are used for the mathematical formalism of the interactions. Here the evolution of components is the step function of time, which gives discrete values to the components (that is 0 or 1) at each time step. For example:

In the phagosomal membrane, PI4P is activated by PI, so I can write,

    If (PI[t]>Threshould)

    Then,

    PI4P [t+1] = PI [t]

where PI4P and PI both take either the value '1' or '0'.

Such formalism can be improved by adding weights, for example above reaction can be written as,

If (PI[t]>Threshould)

Then,

PI4P [t+1] = K * PI [t]

By using different values of K the description of biological system can be improved and use the biological information as much as possible.

4. **Material and Methods**

4.1 Sequence analysis

We searched for all DD containing proteins and retrieved their DD (SMART accession number SM00005) sequences in FASTA format according to the SMART (Letunic et al., 2004) domain database version 4.0 (http://smart.embl-heidelberg.de/). This collection is continuously updated screening a non redundant database of all major primary databases, a BLAST cutoff of 0.01 together with a number of further quality (checks regarding conserved residues and motifs as well as hand curation) to include only *bona fide* domains of this type. We used clustal W (Thompson et al., 1994) for multiple sequence alignment and seaview (Galtier et al., 1996) to edit the alignment manually taking into consideration structural data. CHROMA (Goodstadt and Ponting, 2001) (http://www.lg.ndirect.co.uk/chroma/) was used to format the alignment. Further we used PHYLIP 3.62 (phylogeny inference package Seattle, WA, USA) (Felsenstein, 1997) (http://evolution.genetics.washington.edu/ phylip.html/) which uses a neighbor joining matrix for generating a phylogenetic tree.

TreeView 32 (Page, 1996) (http://taxonomy.zoology.gla.ac.uk/rod/ -treeview.html/) was used to analyze phylogenetic trees.

4.2 Structure analysis

SWISS MODEL (Guex et al., 1999; Guex and Peitsch, 1997) (http://swissmodel.expasy.org/), an automated comparative protein modeling server was applied to predict structures for DDs which had no resolved structure in the PDB database (http://www.rcsb.org/pdb/). SWISS MODEL predicts a structure applying a template from the PDB database, this template was provided manually. FADD (PDB code 1E3Y, chain A) and P55TNFR1 (PDB code

1ICH, chain A) were used as templates to model TRADD (modeled with 1E3Y chain A, RMSD=0.08A°, average pairwise score: 25, Percent target sequence length modeled with template: 92.0%), RIP (modeled with 1E3Y chain A, RMSD=0.63A°, average pairwise score: 27, Percent target sequence length modeled with template: 95.8%), NFκB (modeled with 1ICH chain A, RMSD=0.37°; average pairwise score: 32, Percent target sequence length modeled with template: 98.7%) and CRADD (modeled with 1E3Y chain A, RMSD=0.11A°, average pairwise score: 18, Percent target sequence modeled with template: 100%, all residues) structures. PDB files of all modeled protein will be available upon request to authors. Structures were analyzed manually and by applying the docking procedure described below. Structures were viewed by Swiss Pdb Viewer version 3.7 and Rasmol version 2.6.

4.3. Docking

Best results were obtained by the program 3D-DOCK (Smith and Sternberg, 2003) (http://www.bmm.icnet.uk/). This program is composed of four routines: The first one is ftdock: Here a global scan of the translational and rotational space of possible positions of the two molecules, limited by surface complementarity (SCscore) and electrostatic filtering is done. In the second routine, rpdock, an empirical scoring of possible complexes using residue level pair potentials is performed. In the third one, complexes are filtered using biological information such as distance between two interacting proteins in the complex or involvement of specific residues in interactions. We did not use the filter option in routine 3 as the goal of the study was to look for new interacting surfaces. In the fourth one, energy minimization is performed. However, further information about conformational changes after interactions is unavailable. To avoid bias, energy minimization was thus not taken in to consideration (Weber and Vincenz, 2001).

For each protein-protein interaction we considered in each case the five complexes with highest rpscore obtained from rpdock. Pelle-Tube and FAS-FADD monomers were docked by the same procedure as a control. Pelle and Tube are DD containing proteins found in *D. melanogaster*, their structure and interacting surfaces have been experimentally solved. The predicted complex by 3D-Dock was in its topological details similar to the actual complex as annotated in PDB database (1D2Z) (SCscore: 190 and rpscore: 4.810). The other protein complexes were docked in the same order as the interactions follow each other in the signal cascade (Figure 6). Docking pairs were: (i) p55TNFRI-TRADD, (ii) TRADD-FADD, (iii) TRADD-RIP, (iv) RIP-CRADD or RIP-NFκB. We assumed that interaction surfaces involved in one interaction are less likely to be involved in the interaction with a protein consecutive in the cascade. We always used the highest RPscoring complex consistent with this assumption of partly overlapping and consecutively used interaction surfaces. The possible number of complexes were minimized by this to decide on important residues for specific complexes in the DD of proteins under study.

The RPscores of the complexes used in this study were as follows: p55TNFR1-TRADD: 4.740, TRADD-FADD: 5.240, TRADD-RIP: 5.120 (involved in TRADD-RIP-NFκB interaction), 5.080 (involved in TRADD-RIP-CRADD interaction), RIP-CRADD: 5.590, RIP-NFκB: 4.860. Each complex was one of the three highest RPscoring complexes and always the only one of these three offering an interaction surface not yet taken by earlier cascade interactions. Alternative docking strategies (Patchdock, Smoothdock, Cluspro) were also tested but performed not similar well (see results).

Further we used Swiss Pdb Viewer version 3.7 to superimpose complexes and look for possible steric hindrance and overlapping interaction surfaces.

4.4 Experimental methods for study of apoptosis pathway

Extraction of FASL

Neuro 2A cells (N2A cells) are cultivated in a media containing 10%FCS. After cells are confluent they are starved by changing a media to the one containing 10% FCS.   FASL is then harvested after one week.

Fluorogenic Caspase-3 activity assay

Primary *M. musculus* hepatocytes were treated with 25% FasL/CHX for different time points. Cytosolic extracts were made and aliquots were mixed with activity buffer and the fluorogenic Caspase-3 substrate DEVD-AMC The fluorescence was measured with a Microplate Fluoroskan Ascent Reader.

Fluorescence activated cell sorting assay

Primary *M. musculus* hepatocytes (app. 400.000 cells/well) were seeded onto a 6-well plate. Cells were then treated with apoptotic stimuli for different time points. The media (with detached cells) were collected in 15ml Falcon tubes. The cells still attached to the plate were washed twice in AnnexinV-binding buffer. The buffer was then removed and added to the appropriate falcon tube containing the detached cells/media. The cells were centrifuged at 700 rpm for 5 min. The supernatant was removed and the remaining pellet was washed twice in AnnexinV-binding buffer. Cells still attached to the plate were labelled with 500 µl AnnexinV-GFP (diluted 1:500) and Propidium Iodide (5µg/ml, diluted 1:1000) in Annexin V-binding buffer for max.15-30 min at 37ºC. The plate was carefully swayed. After the indicated incubation time, the labelling was not thrown away. Instead, it was added to the detached cells obtained in. Meanwhile, the attached cells remain in Annexin V-binding buffer. The detached cells were incubated for 15-30 min at RT (protect from light). The cells were centrifuged at 700 rpm for 5 min, washed twice in Annexin V-binding buffer and the pellet was resuspended in 50 µl AnnexinV-binding buffer. The attached cells

were washed twice in Annexin V-binding buffer and the supernatant was completely removed. The cells were fixed with 500 μl Fixative (formaldehyde solution, e.g. 4% PFA) for 5 min at 37ºC. Cells were washed twice in 1x PBS, the supernatant was removed. Cells were detached from the plate with 0.375% trypsin at 37ºC. The incubation time depends on the detachment of the cells (max.15 min). The trypsin was removed and added to the appropriate falcon tube. Cells were centrifuged at 700 rpm for 5 min and washed twice in 1x PBS. The pellet was resuspended in 200 μl AxV- binding buffer (Note that Annexin V-binding buffer was added without any Annexin V-GFP or PI at this step) and the cells were mixed with detached cells to a final volume of 250 μl. FACS analysis was performed using a FACSCalibur™ machine from BD Biosciences. The data were analysed with the Cell-Quest Pro program supplied by the manufacturer.

4.5 Development of the dynamic simulation for apoptosis pthway

The interaction network of *C. elegans* and *D. melanogaster* pathways was reconstituted from interaction information after a broad screen of literature. The components for the *M. musculus* apoptosis cascade were first obtained from a recent version of KEGG (Kyoto Encyclopedia of Genes and Genomes; release 36.0, October 2005). Furthermore, for modeling the information for all three organisms on positive and negative regulation of components in the cascade is essential (and e.g. not available from KEGG). This was retrieved from literature. The network was further drawn using SMART DRAW version 7, to depict topological differences and functional position (Figure 1). The oval nodes are the components playing a role in the apoptosis pathway. Square node shows the consequence of the action of effector components. The arrows indicate activation (→) or inhibition (—|) of the node with an incoming arrow by the node from which the arrow is originated.

Table 2: The table describes ordinary differential equations used for the activation of all components in Figure 13.

No	Ordinary differential equations
C. elegans	
1	d[egl2]/dt = ((A * MAX_UNIT) / (K + A))
2	d[ced4]/dt = ((egl2[t] * MAX_UNIT) / (K + egl2[t])) - ced9[t]
3	d[ced9]/dt = 0.01*((A * ced4[t]) / (K + A))
4	d[ced3]/dt = ((ced4[t] * MAX_UNIT) / (5 + ced4[t]))
D. melanogaster	
5	d[dapaf]/dt = ((A * MAX_UNIT) / (K + A)) – BCLXL[t]
6	d[BCLXL]/dt = 0.1*((A * dapaf[t]) / (K + A))
7	d[casp8]/dt = ((dapaf[t] * MAX_UNIT) / (4 + dapaf[t]))
8	d[casp]/dt = ((dapaf[t] * MAX_UNIT) / (4 + dapaf[t]))
9	d[casp3]/dt = ((casp8[t] * (MAX_UNIT/2)) / (5 + casp8[t])) + ((casp[t] * (MAX_UNIT/2)) / (5 + casp[t])) – IAP[t]
10	d[casp7]/dt = ((casp8[t] * (MAX_UNIT/2)) / (15 + casp8[t])) + ((casp[t] * (MAX_UNIT/2)) / (15 + casp[t])) – IAP[t]
11	d[IAP]/dt=((A * (casp3[t]+casp7[t])) / (K + A))
M. musculus	
12	d[FASL]/dt = ((A* MAX_UNIT) / (K +A))
13	d[TRAIL]/dt = ((A* MAX_UNIT) / (K +A))
14	d[TNFA]/dt = ((A* MAX_UNIT) / (K +A))

15	d[IL1]/dt = ((A * MAX_UNIT) / (K + A))
16	d[FADD]/dt = ((TRAILR[t] * (MAX_UNIT/4)) / (K + TRAILR[t])) + ((FASR[t] * (MAX_UNIT/4)) / (K + FASR[t])) + ((TNFAR[t] * (MAX_UNIT/4)) / (K + TNFAR[t])) + ((ILR[t] * (MAX_UNIT/4)) / (K + ILR[t])) – (prob * FLIP[t])
17	d[TRADD]/dt = ((TNFAR[t] * (MAX_UNIT/2)) / (K + TNFAR[t])) + ((ILR[t] * (MAX_UNIT/2)) / (K + ILR[t]))
18	d[sur]/dt = 0.1*((TNFAR[t] * MAX_UNIT) / ((K + TNFAR[t])))
19	d[MYD88]/dt =0.1* ((ILR[t] * MAX_UNIT) / ((K + ILR[t])))
20	d[NFKB]/dt =((MYD88[t]+sur[t])*(MAX_UNIT/2))/(K+(MYD88[t]+sur[t]))
21	d[FLIP]/dt = 0.1*((NFKB[t] * FADD[t]) / (K + NFKB[t]))
22	d[casp8]/dt = ((FADD[t] * (MAX_UNIT/2)) / (4 + FADD[t])) + ((TRADD[t] * (MAX_UNIT/2)) / (4 + TRADD[t]))
23	d[bid]/dt = ((casp8[t] * MAX_UNIT) / ((K) + casp8[t]))
24	d[casp3]/dt = ((casp8[t] * (MAX_UNIT/2)) / (5 + casp8[t])) + ((casp9[t] * (MAX_UNIT/2)) / (5 + casp9[t])) - (prob * IAP[t])
25	d[casp7]/dt = ((casp8[t] * (MAX_UNIT/2)) / (15 + casp8[t])) + ((casp9[t] * (MAX_UNIT/2)) / (15 + casp9[t])) - (prob * IAP[t])
26	d[apaf]/dt = ((bid[t] * MAX_UNIT) / ((K) + bid[t])) – (prob * BCLXL[t])
27	d[casp9]/dt = ((apaf[t] * MAX_UNIT) / (408 + apaf[t])) – (prob * IAP[t])
28	d[BCLXL]/dt = (NFKB[t] * apaf[t]) / (K + NFKB[t])
29	d[IAP]/dt = 0.5*((NFKB[t]* (casp9[t])) / (K + NFKB[t])) + 0.5*((NFKB[t]* (casp3[t]+casp7[t])) / (K + NFKB[t]))

The model was developed writing ordinary differential equations (Table 2) for each interaction in the apoptosis cascade assuming Michaelis Menten kinetics to simplify complex regulatory interactions. The dynamic simulation program implementing all the features of these topological differences was developed in C language to study the evolution of this model in time. The program was compiled by Borland C++ compiler. Ms Excel was used for plotting graphs of compound concentrations.

RESULTS PART I

Apoptosis: Analysis of the pathway and its components

Results and chapter discussion

5. Analysis of death domain containing proteins

5.1 Background to death domain containing proteins in the apoptosis pathway.
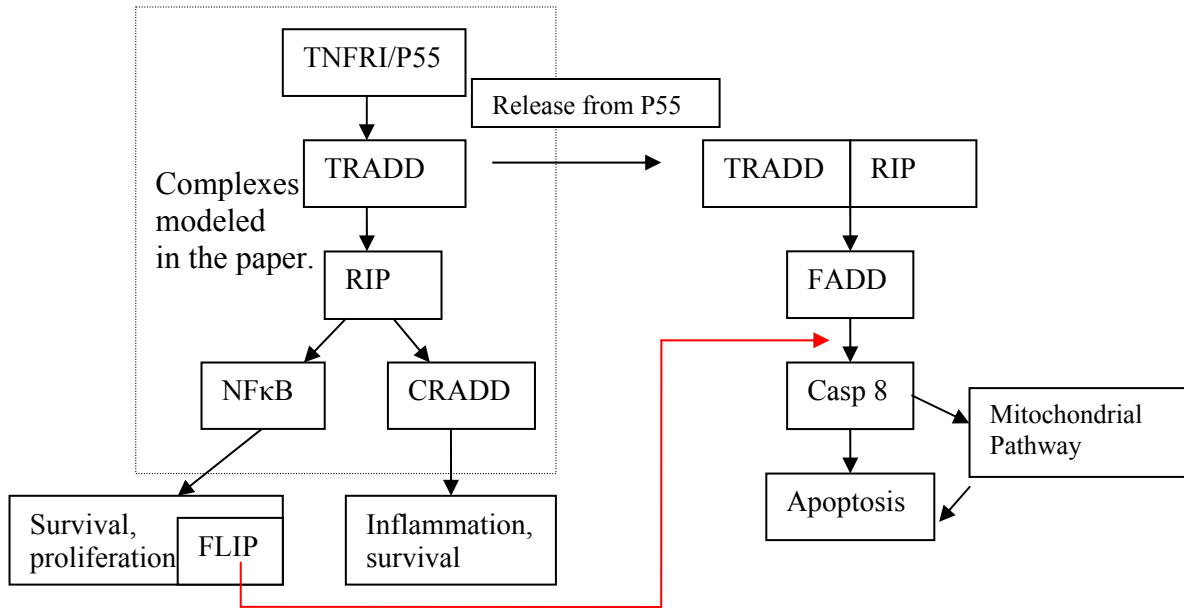
Figure 6: Scheme of the TNFRI induced pathway. The dotted square represents the interactions modeled in the present study. The figure also includes further interactions known from the literature (Micheau and Tschopp, 2003).

Death domains (DD) mediate interactions between signaling molecules. The DD superfamily includes the death domain (DD), the death effector domain (DED) and the caspase-recruitment domain (CARD).

Apoptosis induction proceeds through two major signaling pathways, the extrinsic death receptor and the intrinsic mitochondrial pathway.

In the *extrinsic pathway*, after binding FasL, the Fas receptor recruits at its intracellular site the adaptor protein FADD (FAS-associating death domain-containing protein) via a DD-DD interaction (Nagata, 1998; Wajant, 2002). FADD in turn binds to the initiator pro-caspases-8 or -10 via DED motifs and thereby allows proximity-induced activation of the caspases (Aravind et al., 1999;

Kischkel et al., 1995). Subsequent cleavage and activation of the executioner caspases-3 and -7 by caspase-8/10 leads to the proteolysis of numerous cellular substrates that govern the cell's demise.

In the *intrinsic*, mitochondrial *pathway*, a multimeric complex, called the apoptosome is formed via CARD-CARD domain interactions between the cytochrome c-activated adaptor Apaf-1 and initiator pro-caspase-9.

Signals for *proliferation and survival* are also mediated by DD-containing proteins. This is typified by the signaling pathway induced by TNF through the TNF receptor I (p55TNFR1). Here, activated p55TNFR1 first assembles a survival/proliferation signaling complex via TRADD-TRAF2-RIP (complex I) that leads to the activation of NFκB (Figure 6). This complex then dislodges from the receptor and either maintains survival signaling by recruiting the competitive caspase-8 inhibitor FLIP or, in the absence of FLIP, assembles FADD and caspase-8 into the complex for death signaling (Figure 6). Thus, the TRADD protein, essentially known to signal for death, can also signal for survival depending on the level of auxiliary molecules. Both TRADD and RIP contain DDs for interactions. RIP additionally possesses a serine/threonine protein kinase activity.

Aim of the study: It was interesting to know whether DD domains diverge between signaling molecules involved in apoptosis and proliferation/survival.

(i) Sequence analysis was performed of all DD containing proteins in the TNF pathway. DD specific features (residues in secondary structure elements) were identified for activating and inhibitory adaptors and receptors from these phylogenetic sequence comparisons.

(ii) Key homotypic DD interactions were modeled in the TNF pathway by comparing the structures and interaction sequences between the domains. Based on the known cascade, the delayed displacement of complex I from p55TNFR1 was tried to represent and the effect of homotypic DD interactions between DD
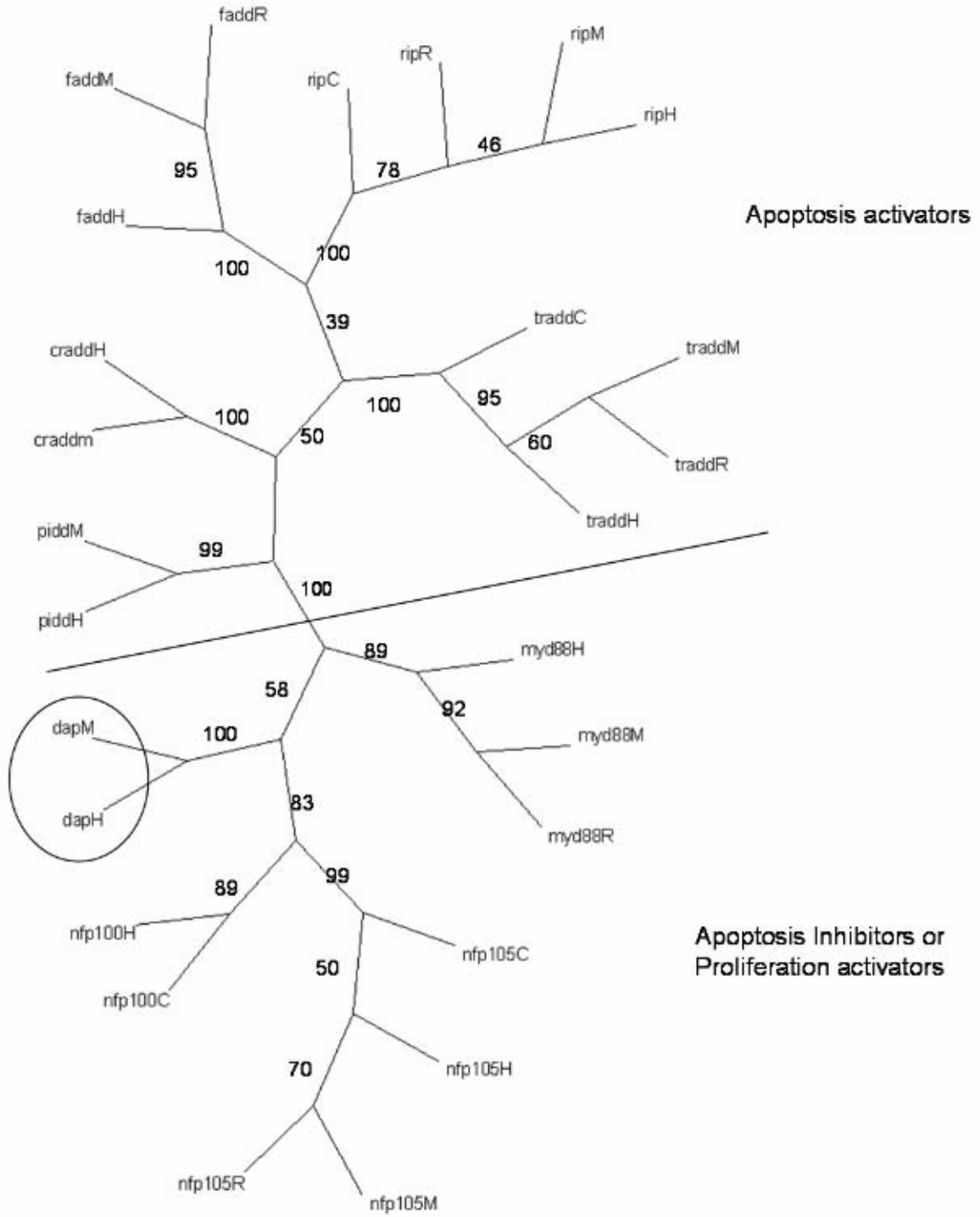
containing proteins from our results. The models were used to predict and identify critical residues involved in these DD mediated interactions. Their compatibility with available mutational data from genetics was showed. It suggests; how for proliferation key interactions are available and mediated via differential binding of RIP to TRADD. The structural complexes modeled lead to the hypothesis that depending on how RIP interacts with TRADD, it further binds to either NFκB or CRADD downstream in the pathway.

Table 3: Proteins and protein DDs used in our analysis and their functional significance in human[1]. (M: *M. musculus*, R: Rat, H: Human, C: Chicken,)

Common name used in the analysis	Identifiers	Complete name/ standard name	Functional significance in human
Adaptors:			
TRADD	M:XP_134502	TNFR1-associated death domain protein	Interacts with P55TNFR1. The interaction can signal for cell death activation and inhibition.
	R: XP_341672		
	H: Q15628		
	C: XP_414067		
FADD	M: Q61160	FAS-associating death domain-containing protein	Interacts with FASR via death domain and is involved signaling for cell death.
	R: Q8R2E7		
	H: Q13158		
RIP	M: Q60855	Receptor-interacting serine/threonine-protein kinase 1	RIP can interact with FAS, FADD, P55TNFR1, TRADD and CRADD. It is involved in cell death and survival signaling, but the exact mechanism is unknown.
	H: Q13546		
	C: Q7ZZX8		
Pidd	H: Q9HB75	PIDD	Induced by p53 and activates caspase 2. Caspase 2 is known to be activator or inhibitor of cell death in different tissues.
	M: Q9ERV7		
Cradd	H: P78560	Death domain containing protein CRADD	Adaptor protein interacting with Caspase and RIP. It is involved in cell death and inflammation signaling.
	M: O88843		
NFκBp105	M: P25799	Nuclear factor NF-kappa-B p105 subunit	Interaction partner in cytosol, it plays role in survival signaling.
	R: Q63369		
	H: P19838		
	C: Q04861		
NFκBp100/ 49	H: Q00653	Nuclear factor NF-kappa-B p100/p49 subunits	Interaction partner in cytosol, plays role in survival signaling.
	C: P98150		

Myd88	M: P22366	Myeloid differentiation primary response protein	Adapter protein involved in the Toll-like receptor and IL-1 receptor signaling. It is known to transfer survival signal.
	R: AAO919		
	H: Q99836		
Dap	H: P53355	Death-associated protein kinase	Calcium/calmodulin-dependent serine/threonine kinase which acts as a positive regulator of apoptosis.
	M: Q80YE7		
Receptors:			
FAS	M: P25446	Tumor necrosis factor receptor superfamily member 6	Receptor inducing apoptosis signal after binding to FAS adaptor.
	R: Q63199		
	H: P25445		
	Mn: Q9GK28		
	P: O77736		
	B: P51867		
P55TNFR1	P: P50555	Tumor necrosis factor receptor superfamily member 1A	Receptor that can activate two signaling cascades, cell death and cell survival signaling.
	B: O19131		
	H: P19438		
	M: P25118		
	R: P22934		
DR3	M: Q8VD70	Tumor necrosis factor receptor superfamily member 25	Interacts with P55TNFR1, Receptor for TNFSF12/APO3L/TWEAK.
	H: Q99831		
DR4	H: O00220	Tumor necrosis factor receptor superfamily member 10A	Receptor for the cytotoxic adaptor TNFSF10/TRAIL.
DR5	H: O14763	Tumor necrosis factor receptor superfamily member 10B	Receptor for the cytotoxic adaptor TNFSF10/TRAIL.
	M: Q9QZM4		
DR6	H: O75509	Tumor necrosis factor receptor superfamily member 29	May activate NF-kappa-B and JNK and promote apoptosis.
	C: Q98SM6		
TVBs1	C: Q9PW79	TVBs1	TNFR related receptor found in chicken.
NGF	M: Q9Z0W1	Tumor necrosis factor receptor superfamily member 16	Interact with TRAF and transfers survival signal.
	R: P07174		
	H: P08138		
	C: P18519		

5.2 Phylogeny of death domain sequences

(A)
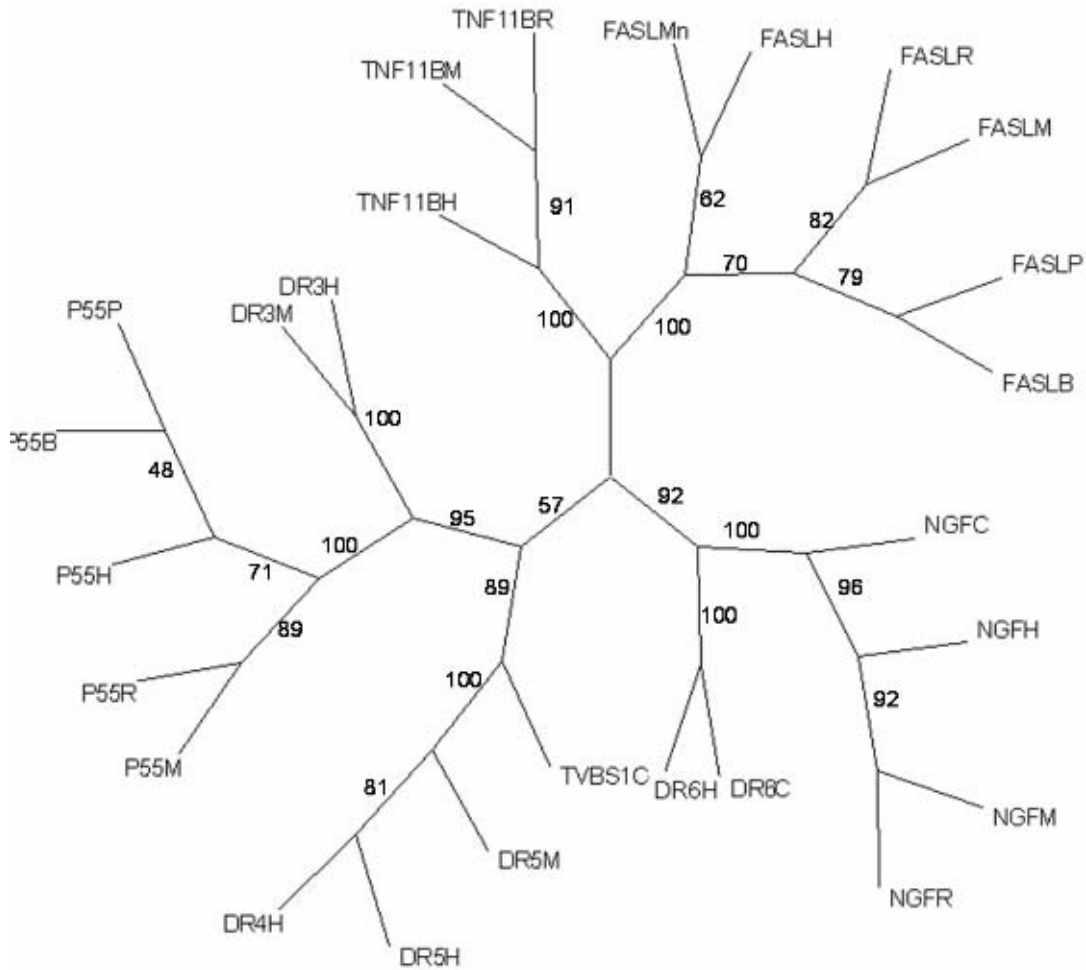
(B)

Figure 7: Phylogeny of A) adaptors with DD and B) receptors with DD, involved in apoptosis in humans based on the degree of their sequence homology. This tree was constructed using the neighbor-joining algorithm of the program NEIGHBOR in the PHYLIP (phylogeny inference package) program (Seattle, WA, USA). Bootstrap support out of 100 is indicated. In A) the divergence of activators of the apoptosis pathway from the inhibitors of the pathway is indicated by a line. Death associated protein kinase (DAP) is an exception as it is grouped with inhibitors though it is known to activate apoptosis. B) describes the receptor phylogeny tree and shows the diversion in receptor DDs in correlation with their functional categories as described by (Bridgham et al., 2003).
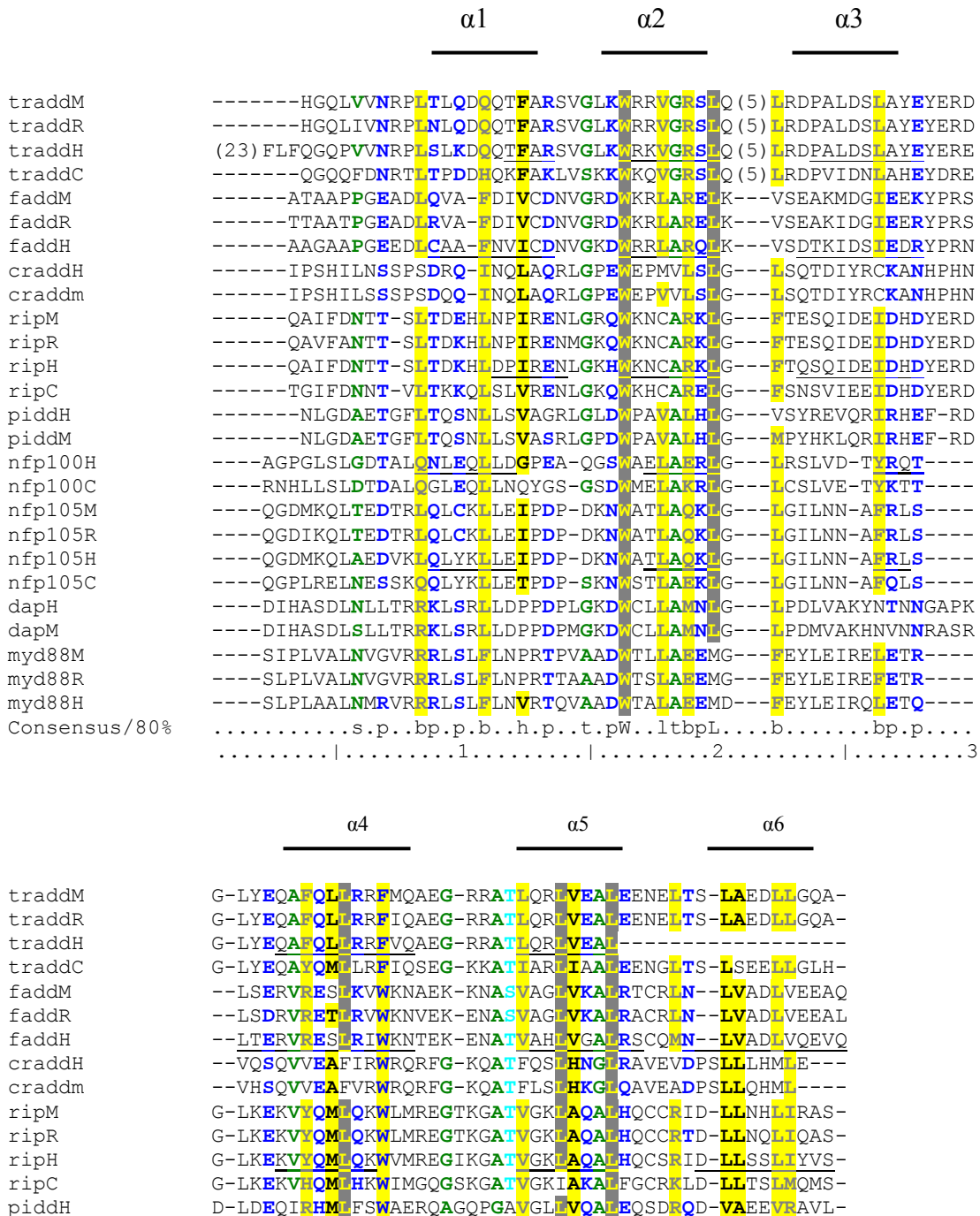
DD proteins which play an important role in the decision between caspase-dependent apoptosis and survival/proliferation in death receptor signaling are listed in Table 3. We performed sequence and phylogenetic analysis

of the DD domains to reveal characteristics of activators and inhibitors of the pathway. Phylogenetic analysis of adaptor DDs (Figure 7A/B) shows that DD proteins implicated in apoptosis signaling (for example TRADD and FADD) diverge from those mediating exclusively inhibition of this pathway or the induction of proliferation (for example MYD88 and NFκB). DAP (Death associated Serine/ threonine protein kinase) was the only exception of this phylogenetic clustering, as it is a kinase that activates apoptosis but groups with inhibitory DD containing proteins (Figure 7A). DAP normally localizes to the nucleus where it regulates transcription rather than apoptosis. However, for apoptosis induction, it has to relocate to the cytoplasm with the help of the pro-apoptotic protein Par-4 (Preuss et al., 2003). In recent studies ERK (extracellular signal regulated kinase), a protein involved in proliferation signaling has been shown to interact with DAP through a docking sequence within its DD domain (Chen et al., 2004). These observations might explain why DAP is an exception. According to our phylogenetic analysis, the DD of apoptosis inhibitors/ proliferation activators are thus well diverged from the adaptors that can activate apoptosis.

TRADD is essentially known as an apoptosis activator; however, recently there has been speculation about its role in temporarily activating apoptosis inhibitory processes (Micheau and Tschopp, 2003). Given such suggestions about double roles for DD proteins, a bioinformatics approach is helpful to develop new predictions and models. In the following work we concentrated on the study of death adaptors in order to identify specific interactions (Figure 7A). For the purpose of comparison were-analyzed the death receptor study by Bridgham et al (2003) (Bridgham et al., 2003) focusing on DDs involved in the Fas and TNF signaling pathways. The DD receptor results confirm the functional sub-categories for receptors (EDAR-like receptors with DR6 versus non-EDAR like such as TNFR1, FAS) (Figure 7B). Our analysis further reveals that DD sequences of receptors are more conserved than those of adaptors. The average pairwise

score for receptors is 21.49 % (n=23) and for adaptors it is 19.57 % (n=26). The t-value (1.386814) according to t-statistics indicates for this difference a significant trend (p < 0.1).

5.3 Identifying critical residues in death domain

```
                        α1                α2                α3
                  _____        _____        _____

traddM       -------HGQLVVNRPLTLQDQQTFARSVGLKTRRVGRSLQ(5)LRDPALDSLAYEYERD
traddR       -------HGQLIVNRPLNLQDQQTFARSVGLKTRRVGRSLQ(5)LRDPALDSLAYEYERD
traddH       (23)FLFQGQPVVNRPLSLKDQQTFARSVGLKTRKVGRSLQ(5)LRDPALDSLAYEYERE
traddC       -------QGQQFDNRTLTPDDHQKFAKLVSKKTKQVGRSLQ(5)LRDPVIDNLAHEYDRE
faddM        ------ATAAPPGEADLQVA-FDIVCDNVGRDTKRLARELK---VSEAKMDGIEEKYPRS
faddR        ------TTAATPGEADLRVA-FDIVCDNVGRDTKRLARELK---VSEAKIDGIEERYPRS
faddH        ------AAGAAPGEEDLCAA-FNVICDNVGKDTRRLARQLK---VSDTKIDSIEDRYPRN
craddH       ------IPSHILNSSPSDRQ-INQLAQRLGPETEPMVLSLG---LSQTDIYRCKANHPHN
craddm       ------IPSHILSSSPSDQQ-INQLAQRLGPETEPVVLSLG---LSQTDIYRCKANHPHN
ripM         ------QAIFDNTT-SLTDEHLNPIRENLGRQWKNCARKLG---FTESQIDEIDHDYERD
ripR         ------QAVFANTT-SLTDKHLNPIRENMGKQWKNCARKLG---FTESQIDEIDHDYERD
ripH         ------QAIFDNTT-SLTDKHLDPIRENLGKHWKNCARKLG---FTQSQIDEIDHDYERD
ripC         ------TGIFDNNT-VLTKKQLSLVRENLGKQWKHCARELG---FSNSVIEEIDHDYERD
piddH        -------NLGDAETGFLTQSNLLSVAGRLGLDWPAVALHLG---VSYREVQRIRHEF-RD
piddM        -------NLGDAETGFLTQSNLLSVASRLGPDWPAVALHLG---MPYHKLQRIRHEF-RD
nfp100H      ----AGPGLSLGDTALQNLEQLLDGPEA-QGSWAELAERLG---LRSLVD-TYRQT----
nfp100C      ----RNHLLSLDTDALQGLEQLLNQYGS-GSDWMELAKRLG---LCSLVE-TYKTT----
nfp105M      ----QGDMKQLTEDTRLQLCKLLEIPDP-DKNWATLAQKLG---LGILNN-AFRLS----
nfp105R      ----QGDIKQLTEDTRLQLCKLLEIPDP-DKNWATLAQKLG---LGILNN-AFRLS----
nfp105H      ----QGDMKQLAEDVKLQLYKLLEIPDP-DKNWATLAQKLG---LGILNN-AFRLS----
nfp105C      ----QGPLRELNESSKQQLYKLLETPDP-SKNWSTLAEKLG---LGILNN-AFQLS----
dapH         ----DIHASDLNLLTRRKLSRLLDPPDPLGKDWCLLAMNLG---LPDLVAKYNTNNGAPK
dapM         ----DIHASDLSLLTRRKLSRLLDPPDPMGKDWCLLAMNLG---LPDMVAKHNVNNRASR
myd88M       ----SIPLVALNVGVRRRLSLFLNPRTPVAADWTLLAEEMG---FEYLEIRELETR----
myd88R       ----SLPLVALNVGVRRRLSLFLNPRTTAAADWTSLAEEMG---FEYLEIREFETR----
myd88H       ----SLPLAALNMRVRRRLSLFLNVRTQVAADWTALAEEMD---FEYLEIRQLETQ----
Consensus/80% ............s.p..bp.p..h.p..t.pW..ltbpL....b.......bp.p....
              .........|.........1.........|.........2.........|.........3
```

```
                        α4            α5            α6
                  _____      _____      _____

traddM       G-LYEQAFQLLRRFMQAEG-RRATLQRLVEALEENELTS-LAEDLLGQA-
traddR       G-LYEQAFQLLRRFIQAEG-RRATLQRLVEALEENELTS-LAEDLLGQA-
traddH       G-LYEQAFQLLRRFVQAEG-RRATLQRLVEAL------------------
traddC       G-LYEQAYQMLLRFIQSEG-KKATIARLIAALEENGLTS-LSEELLGLH-
faddM        --LSERVRESLKVWKNAEK-KNASVAGLVKALRTCRLN--LVADLVEEAQ
faddR        --LSDRVRETLRVWKNVEK-ENASVAGLVKALRACRLN--LVADLVEEAL
faddH        --LTERVRESLRIWKNTEK-ENATVAHLVGALRSCQMN--LVADLVQEVQ
craddH       --VQSQVVEAFIRWRQRFG-KQATFQSLHNGLRAVEVDPSLLLHMLE---
craddm       --VHSQVVEAFVRWRQRFG-KQATFLSLHKGLQAVEADPSLLQHML----
ripM         G-LKEKVYQMLQKWLMREGTKGATVGKLAQALHQCCRID-LLNHLIRAS-
ripR         G-LKEKVYQMLQKWLMREGTKGATVGKLAQALHQCCRTD-LLNQLIQAS-
ripH         G-LKEKVYQMLQKWVMREGIKGATVGKLAQALHQCSRID-LLSSLIYVS-
ripC         G-LKEKVHQMLHKWIMGQGSKGATVGKIAKALFGCRKLD-LLTSLMQMS-
piddH        D-LDEQIRHMLFSWAERQAGQPGAVGLLVQALEQSDRQD-VAEEVRAVL-
```

```
piddM          D-LDGQVRHMLFSWAERQTGQPGAVGHLVQALEQSDRRD-VAEEVRAIL-
nfp100H        ---TSPSGSLIRSY-ELAG---GDLAGLLEALSDMGLEE-GVRLLRGPE-
nfp100C        ---PSP-ASALRSY-ELPG---GSLGGLLEALDSMGLRG-AVRMLRKPE-
nfp105M        ---PAPSKTLMDNY-EVSG---GTIKELMEALQQMGYTE-AIEVIQAAF-
nfp105R        ---PAPSKTLMDNY-EVSG---GTIKELVEALRQMGYTE-AIEVIQAAF-
nfp105H        ---PAPSKTLMDNY-EVSG---GTVRELVEALRQMGYTE-AIEVIQAAS-
nfp105C        ---PSPSKTLLDNY-KISG---GTGQELIAAFTQMDHTE-AIEVIQKAL-
dapH           DFLPSPLHALLREWTTYPE---STVGTLMSKLRELGRRD-AADLLLKAS-
dapM           DFLPSPVHALLQEWTSYPE---STVGILISKLRELGRRD-AADFLLKAS-
myd88M         ---PDPTRSLLDAWQGRSG---ASVGRLLELLALLDRED-ILKELKSRI-
myd88R         ---PDPTRSLLDAWQGRSG---SSVGRLLELLALLDRED-ILYELKDRI-
myd88H         ---ADPTGRLLDAWQGRPG---ASVGRLLELLTKLGRDD-VLLELGPSI-
Consensus/80%  ....p.sbphLp.a....s...t*l..LhptLp...bp..hh..lb....
               .........|.........4.........|.........5.........|
```

(A)

```
                                   α1          α2          α3
                                  _____    _____    _____

FASLH          -ETVAINLSDVDLSK----YITTIAGVMTLSQVKGFVRKNG-VNEAKIDEIKND-NVQDT
FASLMn         -PETAINLSDVDLSK----YITTIAGAMTLSQVKDFVRKNG-VSEAKIDEIKNH-NVQDT
FASLP          ---EVPMIKDVDLGK----YITRIAEQMKITEVKDFVRKNG-IEETKIDEIMHD-NPKDT
FASLB          ---RQLNLTDVDLGK----YIPSIAEQMRITEVKEFVRKNG-MEEAKIDDIMHD-NVHET
FASLM          ---IPMNASNLSLSK----YIPRIAEDMTIQEAKKFARENN-IKEGKIDEIMHD-SIQDT
FASLR          ---VPMNVSDVNLNK----YIWRTAEKMKICDAKKFARQHK-IPESKIDEIEHN-SPQDA
P55P           -HSAPAQLADADP-----ATLYAVVDGVPPTRWKEFVRRLG-LSEHEIERLELQ-NGRCL
P55B           -PSAPDQLADADP-----ATLYAVVDGVPPSRWKELVRRLG-LSEHEIERLELE-NGRHL
P55H           -AHKPQSLDTDDP-----ATLYAVVENVPPLRWKEFVRRLG-LSDHEIDRLELQ-NGRCL
P55M           -SAHPQRPDNADL-----AILYAVVDGVPPARWKEFMRFMG-LSEHEIERLEMQ-NGRCL
P55R           -AAQPQRLDTADP-----AMLYAVVDGVPPTRWKEFMRLLG-LSEHEIERLELQ-NGRCL
TNF25M         PAGSPAAVLQPGPQ------LYDVMDAVPARRWKEFVRTLG-LREAEIEAVEVE-ICR-F
TNF25H         PAGSPAMMLQPGPQ------LYDVMDAVPARRWKEFVRTLG-LREAEIEAVEVE-IGR-F
TNF10AH        -PANGADPTETLMLF-----FDKFANIVPFDSWDQLMRQLD-LTKNEIDVVRAG-TAG-P
TNF10BH        -PANEGDPTETLRQC-----FDDFADLVPFDSWEPLMRKLG-LMDNEIKVAKAE-AAG-H
TNF10BM        -PVNGNDSADDLKFI-----FEYCSDIVPFDSWNRLMRQLG-LTDNQIQMVKAE-TLV-T
TVBS1C         -PVLGENPIALLHRS-----FNTFVDYVPFPEWKRFGRALD-LQENDLYLAEQH-DRV-S
TNF29H         GLKKSMTPTQNREKW(8)IDILKLVAAQVGSQWKDIYQFLCNASEREVAAFSNG-YTA-D
TNF29C         IMKKSTTPTQNREKW(8)IDILKPVAAQVGSQWKDIYQFLCNASEREVAAFSNG-YAA-D
TNF16M         GNLYSSLPLTKRE------EVEKLLN---GDTWRHLAGELG-YQPEHIDSFTH------E
TNF16R         GNLYSSLPLTKRE------EVEKLLN---GDTWRHLAGELG-YQPEHIDSFTH------E
TNF16H         GGLYSSLPPAKRE------EVEKLLNGSAGDTWRHLAGELG-YQPEHIDSFTH------E
TNF16C         GSLYASLPPSKQE------EVEKLLSSSAEETWRQLAGELG-YKEDLIDCFTR------E
Consensus/80%  ....s....p...........l..hhs..s.pph+pbhppbs.hpc.cl-.hp........
               .........|.........1.........|.........2.........|.........3
```

```
                  α4          α5          α6
                 _____    _____    _____

FASLH          AEQKVQLLRNWHQLHGK-KEAYDTLIKDLKKANLCTLAEKIQTII---
FASLMn         AEQKVQLLRNWYQLHGK-KDACDTLIKGLKTADLCTLAEKIHAVI---
FASLP          AEQKVQLLRNWYLYHGK-KDAYCTLIQGLRKAKLSALADKINDIV---
FASLB          AEQKVQLLRNWYQSHGK-KNAYCTLTKSLPKA----LAEKICDIV(4)
FASLM          AEQKVQLLLCWYQSHGK-SDAYQDLIKGLKKAECRRTLDKFQDMV---
FASLR          AEQKIQLLQCWYQSHGK-TGACQALIQGLRKANRCDIAEEIQAMV---
P55P           REAQYSMLAEWRRRTSRREATLELLGSVLRDMDLLGCLEDIEEAL---
P55B           REAQYSMLAAWRRRTPRREATLELLGRVLRDMDLLGCLENIEEAL---
P55H           REAQYSMLATWRRRTPRREATLELLGRVLRDMDLLGCLEDIEEAL---
P55M           REAQYSMLEAWRRRTPRHEDTLEVVGLVLSKMNLAGCLENILEAL---
P55R           REAHYSMLEAWRRRTPRHEATLDVVGRVLCDMNLRGCLENIRETL---
TNF25M         RDQQYEMLKRWRQQQP---AGLGAIYAALERMGLEGCAEDLRSRL---
TNF25H         RDQQYEMLKRWRQQQP---AGLGAVYAALERMGLDGCVEDLRSRL---
```

```
TNF10AH        GDALYAMLMKWVNKTGR-NASIHTLLDALERMEERHAKEKIQDLL---
TNF10BH        RDTLYTMLIKWVNKTGR-DASVHTLLDALETLGERLAKQKIEDHL---
TNF10BM        REALYQMLLKWRHQTGR-SASINHLLDALEAVEERDAMEKIEDYA---
TVBS1C         CEPFYQMLNTWLNQQGS-KASVNTLLETLPRIGLSGVADIIASEL---
TNF29H         HERAYAALQHWTIRGPE--ASLAQLISALRQHRRNDVVEKIRGLM---
TNF29C         HERAYAALQHWTIRGPE--ASLAQLISALRQHRRNDVVEKIRGLM---
TNF16M         ACPVRALLASWGAQDS---ATLDAILAALRRIQRADIVESLCSES---
TNF16R         ACPVRALLASWGAQDS---ATLDAILAALRRIQRADIVESLCSES---
TNF16H         ACPVRALLASWATQDS---ATLDAILAALRRIQRADLVESLCSES---
TNF16C         ESPARALLADWSAKET---ATLDAILVALRKIQRGDIAESLYSES---
Consensus/80%  .-...b.bL..W..pps...ssbphLh.sLcch.b..hh-plpp.h...
               .........|.........4.........|.........5.......
```

(B)

Figure 8: Sequence alignment of death domains of A) adaptors and B) receptors from Table 3 were performed separately using the program ClustalW. This analysis was performed to understand the differences in receptor and adaptor sequences and their consequences for maintaining specificity. The significance of the conserved residues obtained from the detailed sequence comparison was studied further in interactions with other DDs by structural analysis. The 80% consensus sequence is written at the end of each block of the sequence alignment. α helix numbering is shown at the top of the alignment block. Underlined are the positions of α helices in the protein families which were studied in detail below. Every tenth residue in the alignment is denoted by '|' and each twentieth residue is denoted by a number at the end of the sequence alignment. Residue key: -negative, * : ser/thr, l: aliphatic, +: positive, t: tiny, a: aromatic, c: charged, s: small, p: polar, b: big, h: hydrophobic.

Considering the alignments of our analysis and exploiting the available structural information on the sequences of the DDs allows the following findings (Figure 8A, 8B; the numbering of helices is indicated by α1 to α5): Three residues are completely conserved in the receptor family (L68:α4, W71: α4 C terminal, L89: α5) whereas only one residue is completely conserved in adaptors (W33: α2). The sequence composition of adaptor DDs is different from that in the receptor domains. For example while in adaptors alpha-helix 3 shows large sequence variations, in receptors the residues are mostly conserved (helices are underlined in sequences of human proteins that are analyzed structurally). This helix has been shown to be important in interaction of the Fas receptor with the adaptor FADD (Jeong et al., 1999). Moreover, residues S84 or T84 (α5 N terminus) are conserved in all adaptors except PIDD and NFκBp100/49, which might suggest the possibility of regulation by phosphorylation. Finally, stretches of charged residues are well conserved in receptors at three places; in particular

the conservation of negatively charged residues at three places (49: α3, 62: α4, 99: α6) and positively charged residues at one place (34: α2) indicate the importance of electrostatic interactions and the maintenance of specificity through adaptors. In receptors and adaptors many stretches of hydrophobic residues are conserved. These are results from sequence and structure analysis of individual DD adabtors and receptors. They build on our phylogenetic analysis and known, well resolved structures of DD (Pelle-Tube (1D2Z: chain A, B, C, D), FAS (1DDF), FADD (1E3Y: chain A), p55TNFRI (1ICH: chain A)).

5.4 Structural modeling of death domain interaction surfaces

Are adaptors responsible for specific interactions and the selection of the downstream signaling pathway? In particular, are there DD interaction surfaces, of which one can bind to an upstream component that determines the downstream component interacting with the other interaction surface? To answer these questions, the structural interactions involved in the TNFR1-TRADD-RIP pathway leading to survival/proliferation are examined and compared it to interaction modules known from Fas-FADD DD interactions. Docking was performed to study important interacting surfaces using homology models (RIP, TRADD, CRADD, NFκB), known three dimensional structures (Pelle, Tube) and known interacting surfaces (FAS, FADD and p55TNFRI, TRADD). We have to stress that thus the structure of Pelle / Tube as well as interacting residues and surface of FAS/ FADD are known experimentally and were used to test the method. In contrast, RIP, TRADD and CRADD as well as the complexes they participate in are modeled.

Choice and reliability of 3D-Dock:

The interaction partners of the protein complexes docked together are thus experimentally verified, but neither their interacting surfaces nor all their structures are exactly known. Considering the fact that varied interacting

surfaces are known to be used in DD-DD homotypic interactions, we explored the possibility of new interfaces involved in the interactions. 3D Dock proved to be the most reliable method for this purpose for the following reasons: (i) some of the docking programs use complementarity principles (Patchdock). However, this can not be applied for docking of homotypic interactions between domains of the same type. (ii) Other docking programs are specifically designed to dock adaptors on receptors (Smoothdock). This was inappropriate in this case as we wanted to dock adaptors with adaptor, DD adaptors are known to interact with each other in the cytosol. (iii) we also tested Cluspro (http:// nrc.bu.edu/cluster). This program is also designed for receptor-ligand docking, but advanced options in the software allowed us to use it for our purpose. However, when tested, this server could not predict correctly the known interaction surfaces for Pelle-Tube (PDB code of the complex: 1D2Z), FAS-FADD (PDB code of the complex: FAS: 1DDF, FADD: 1E3Y) and p55TNFRI-TRADD (here only p55TNFR1 is known in its crystal structure 1ICH). (iv) This positive control experiment was well passed by 3D-Dock, the interaction surfaces were correctly predicted and with high rpscores mentioned in materials and methods. The rpscore improved the complex selection procedure, it has been proven to be successful in similar tasks before (Lett et al., 2004). Experimental validation will be the strongest proof of the results presented here. However, the success of 3D-Dock in the correct prediction of homotypic interacting surfaces in the case of Pelle-Tube(Xiao et al., 1999), FAS-FADD(Hill et al., 2004; Weber and Vincenz, 2001) and p55TNFRI-TRADD, the experimental evidence that all binding partners examined here do dock to each other in the cell and the strong rpdock scores for the complexes presented here support the validity of our predicted complexes. Furthermore, the templates used have a high level of similarity to the crystal structure: TRADD (modeled with 1E3Y chain A, average pairwise score: 25, Percent target sequence length modeled with template: 92.0%), RIP (modeled with 1E3Y chain A, average pairwise score: 27, Percent target sequence length

modeled with template: 95.8%), NFκB (modeled with 1ICH chain A, average pairwise score: 32, Percent target sequence length modeled with template: 98.7%) and CRADD (modeled with 1E3Y chain A, average pairwise score: 18, Percent target sequence modeled with template: 100%, all residues) structures. Moreover, several of the interacting residues identified do so robustly even if the docking surface is slightly modified, e.g. tilted.
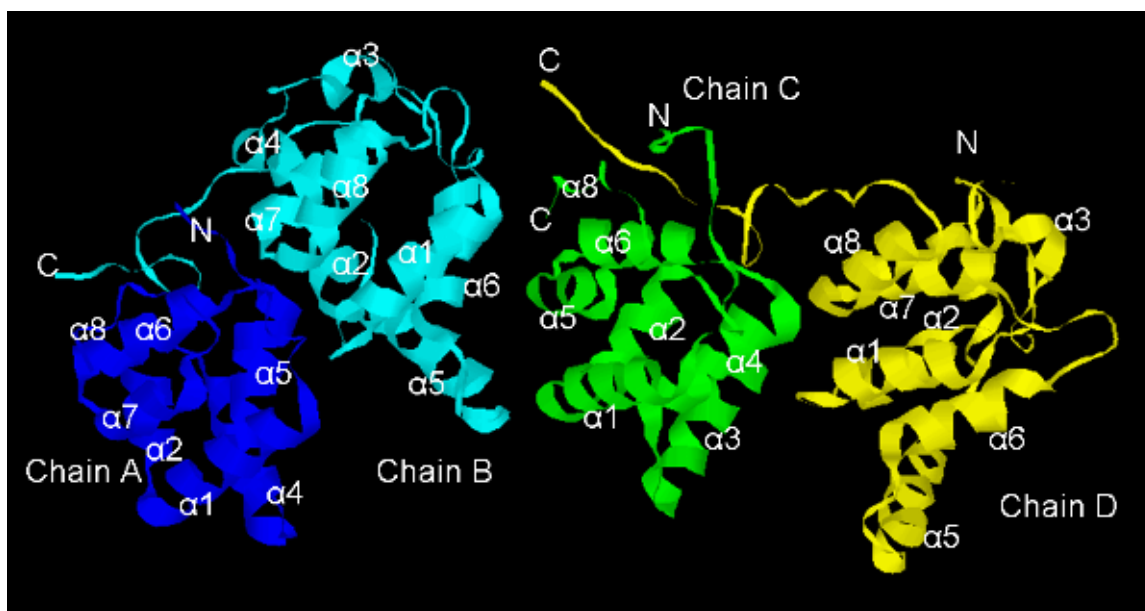

Figure 9: Three dimensional complex between the DDs of Pell and Tube proteins (Xiao et al., 1999). They are found in *D. melanogaster*. The complex is obtained from RCSB PDB database (1D2Z) and labeled. The complex shows DD of Pelle (chain A and C) and DD of Tube (chain B and D) with all visible α helices labeled.

Previous work showed that FAS, FADD, Pelle and Tube contain DD and bind to their interaction partner through DD homotypic interactions. FAS-FADD complex is involved in apoptosis induction whereas Pelle-Tube complex plays a role during *D. melanogaster* embryogenesis. The dimerization of Pelle and Tube (Figure 9) seems to rely on contacts between alpha-helices 4 and 5 of Pelle DD with alpha-helices 6 and the unique C-terminal tail of Tube DD (Xiao et al., 1999). It has also been found that the DD of FADD engages the DD of Fas with the loop surface, the inter-helical loop and adjacent 1 or 2 turns of helices 1 and 2 which

was first identified in Tube DD but it extends the surface into helices 2 and 3 on the same side of the motif (Hill et al., 2004). Furthermore, Fas and FADD use helices 2 and 3 and helices 3 and 4 respectively (type I) (Qin et al., 1999), helices 3 and 4 and loop connecting helices 4 and 5 (type II) (Xiao et al., 1999) and flexible helix 3 (type III) interactions in DISC (Weber and Vincenz, 2001). These interactions of Fas/FADD are also found in our models.

From these previous studies it is apparent that different parts in the DD play a role in different interactions. Taking into consideration the phylogenetic analysis, thus the possibility of presence of different interaction regions in DD is examined. The apparent absence of a conserved interaction surface suggests that DDs may associate by a variety of mechanisms. Interestingly the nature of the interactions also seems to be different between DD complexes. Electrostatic interactions are thought to be a key component in the interaction between FAS and FADD DDs (Huang et al., 1996). In contrast, van der Waals and hydrogen bond contacts have been shown to be involved in the complex between Pelle and Tube DD (Xiao et al., 1999).

5.5 Analysis of predicted interaction surfaces

Table 4: Residues involved in interactions obtained from 3D-Dock.

Name of protein	Residues important in interaction[1]			Position
Complex I				
P55TNFR1	EFVRRLGLSD(273-282)	VLRDMD (424-429)		Helix 2, first residue in helix 3/ helix 5 and residues in following loop
TRADD	SLAYEYEREGLYEQAFQLLRR (251-270)			Helix 3, 4 and loop in between
Complex II				
TRADD	LDSLAYEYEREG(252-263)			Helix 3 and following loop
FADD	GKDWRRLAR(109-117)	SDTK(122-125)	CQMN(168-171)	Helix 2 and preceding one

				residue, helix 3 initial residues, residue in the loop between helix 5 and 6.
Complex III				
TRADD	QRGC (238-241)	GRRA (277-280)	VEAL (286-289)	Loop between helix 4 and 5, 2 and 3, helix 5 (Interaction surface for NFκBrecruitment)
	SVGLKWRKVGR (225-235)		LVEA (285-288)	Loop between helix 1 and 2 , helix 2 (Interaction surface for CRADD recruitment)
RIP	DHDY (616-619)	EKVYQMLQKWVM (626-637)		Helix 3, helix 4 and following 3 residues (Interaction surface for NFκB recruitment)
	DKHL (584-587)		KEKV (625-628)	Residues before helix 1, loop between helix 3 & 4 (Interaction surface for CRADD recruitment)
Complex IV				
RIP	LAQA (649-652)	HQCSRIDLLSSLI (654-666)		Helix 5 and 6, loop in between them
	WKNCARKL (598-605)	GFTQ (606-609)	IDEI (612-615)	Loop between helix 2 and 3, helix 3, helix 2,
NFκβp105	LEIPDP (823-828)	QMGYTE (878-883)		Helix 1 and 6
RIP	QAIFDNTTSLTDKHL (573-587)	VMREGI (636-641)		Loop between helix 4 and 5, N terminal 15 residues
NFκβp100	ERLG (793-796)	LAGGDL (823-828)		Loop between helix 4 and 5, helix 2
Complex V				
RIP	DHDY (616-619)	KEKVYQMLQ (625-633)		Helix 3 and 4
CRADD	LSQTDI (140-145)	QRF (169-171)		Loop between helix 2 and 3, N terminal

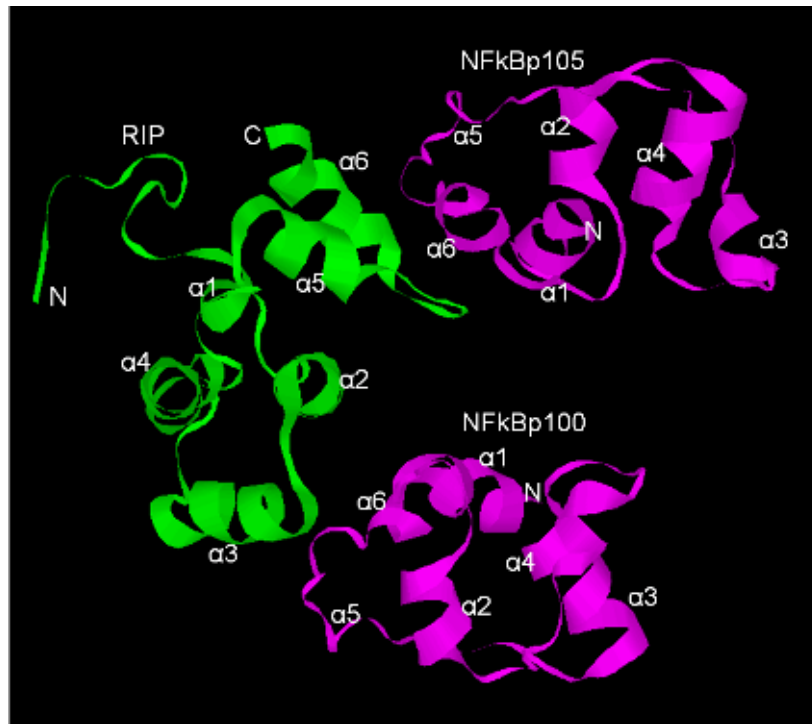|			of helix 3 and loop between helix 4 and 5

[1]Underlined: Residues playing key role in interaction, Red residues: conserved in all invested organisms.
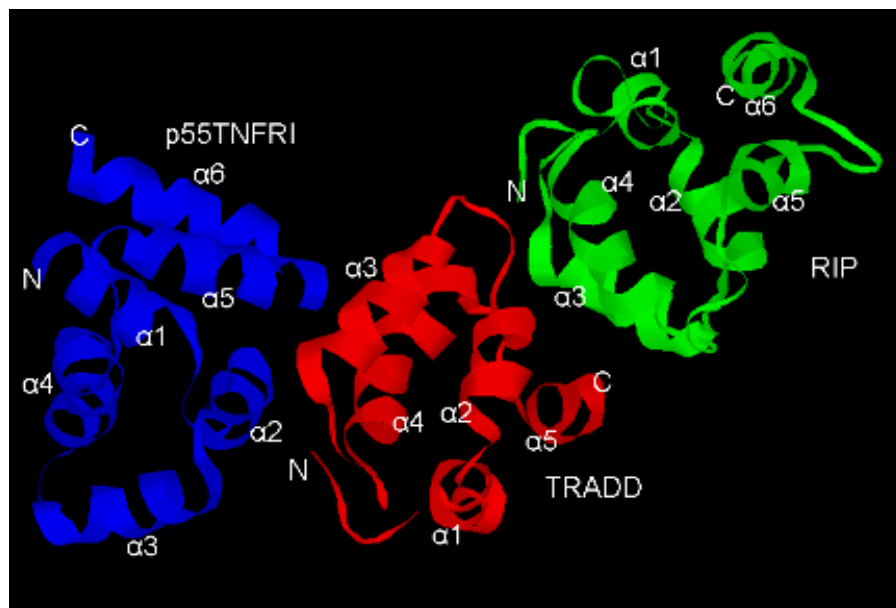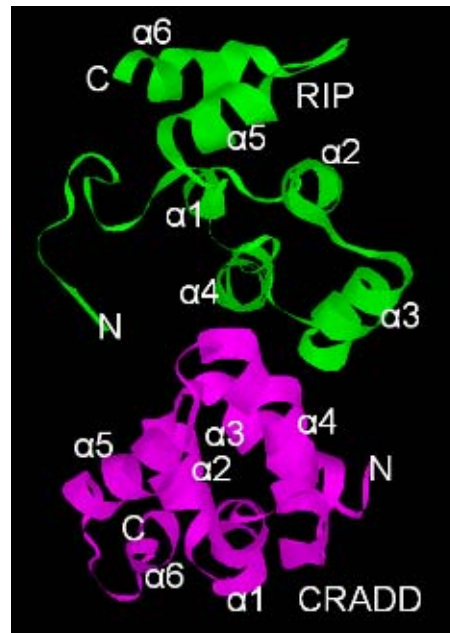

(A)
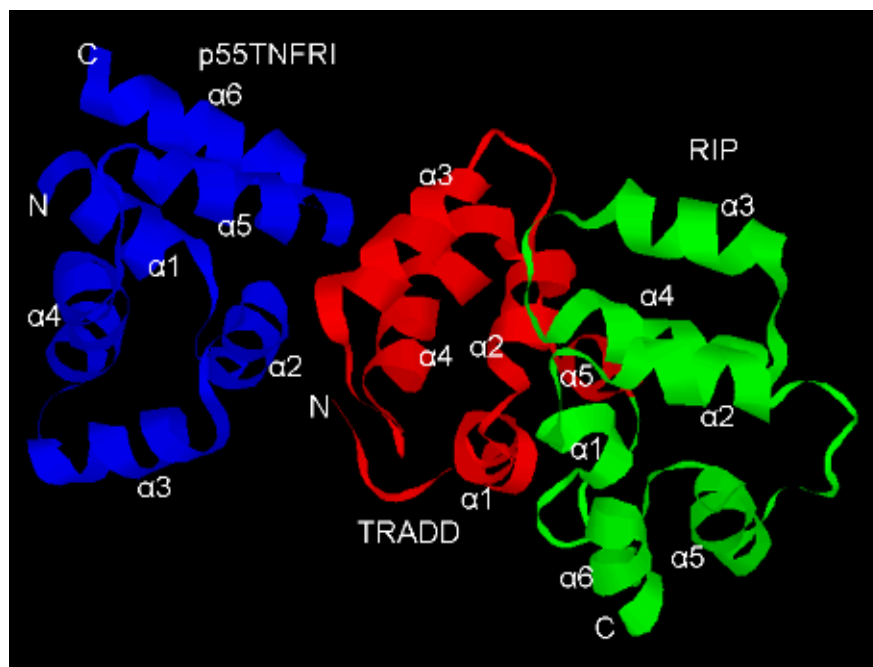
(B)

(C)

(D)

Figure 10: Using the 3D-Dock docking program the following complexes were modeled: A) The P55TNFR1-TRADD-RIP complex which could recruit NFκB p100 or NFκB p105; and B) the P55TNFR1-TRADD-RIP complex which could recruit CRADD. C) The RIP-NFκB complex. This complex uses an interaction surface different and not overlapping from D) the predicted RIP-CRADD complex. The structural elements of

the complexes are labeled and are shown as Ribbons. The picture was generated using Rasmol.
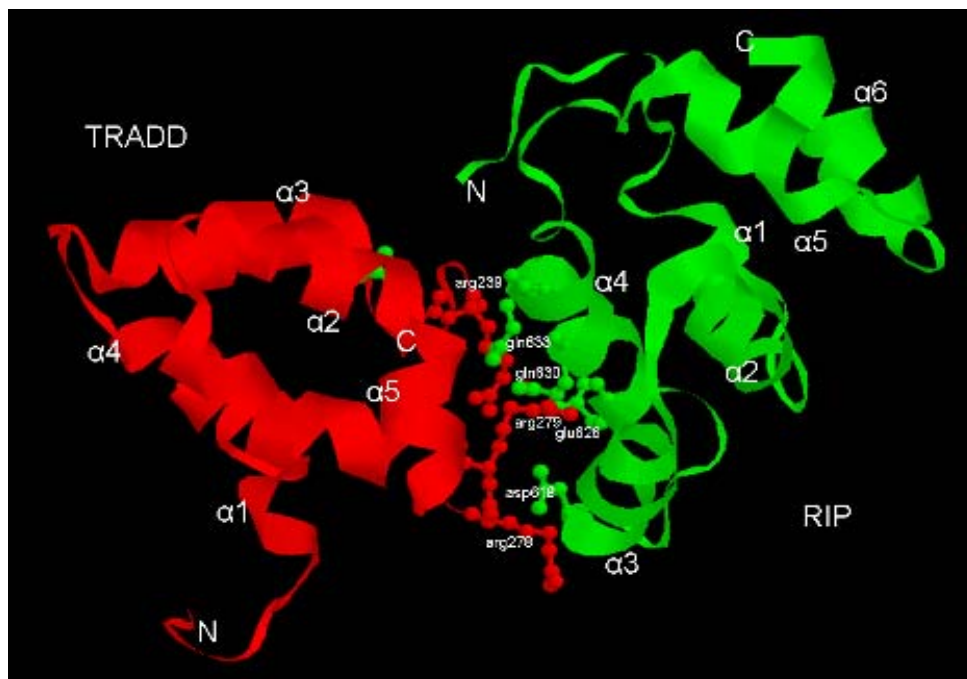
(A)
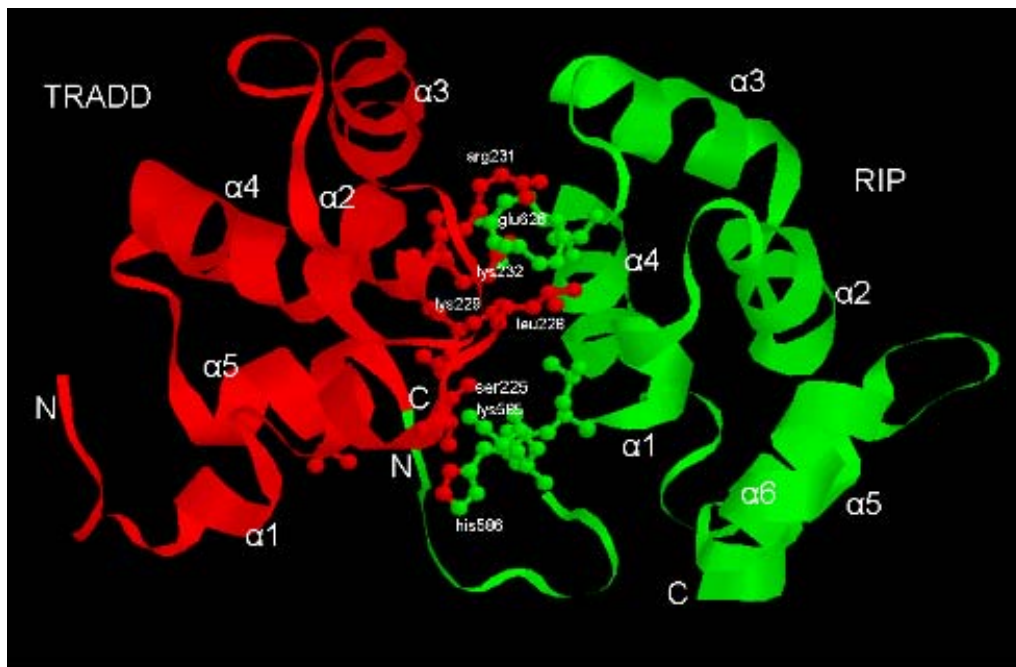
(B)

Figure 11: TRADD-RIP complexes obtained from docking program 3D-Dock and analyzed by Swiss Pdb-viewer. The figure shows structural details and interacting

residues in TRADD-RIP complex A: involved in recruitment of NFκB and B: involved in recruitment of CRADD.
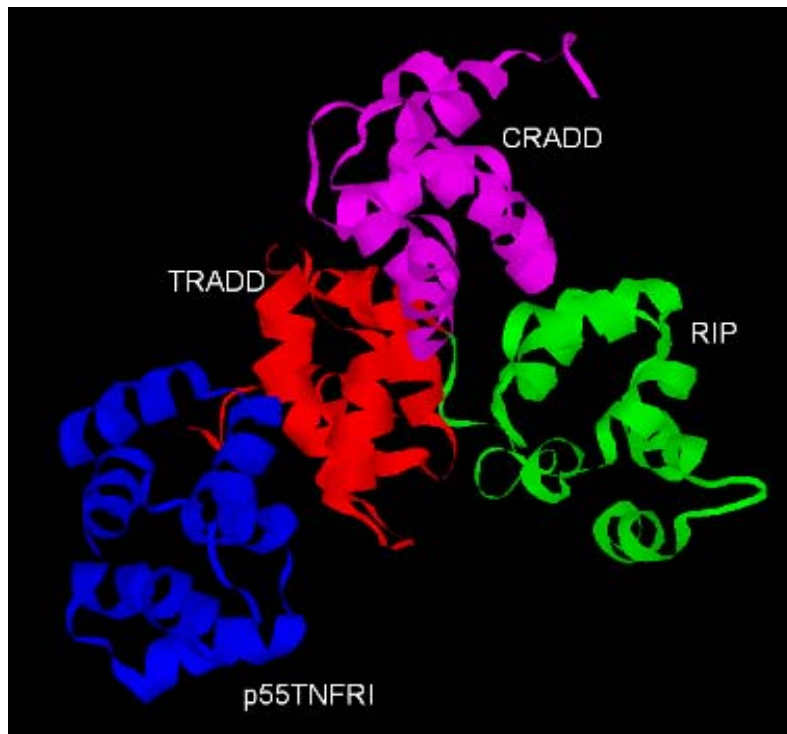
(A)
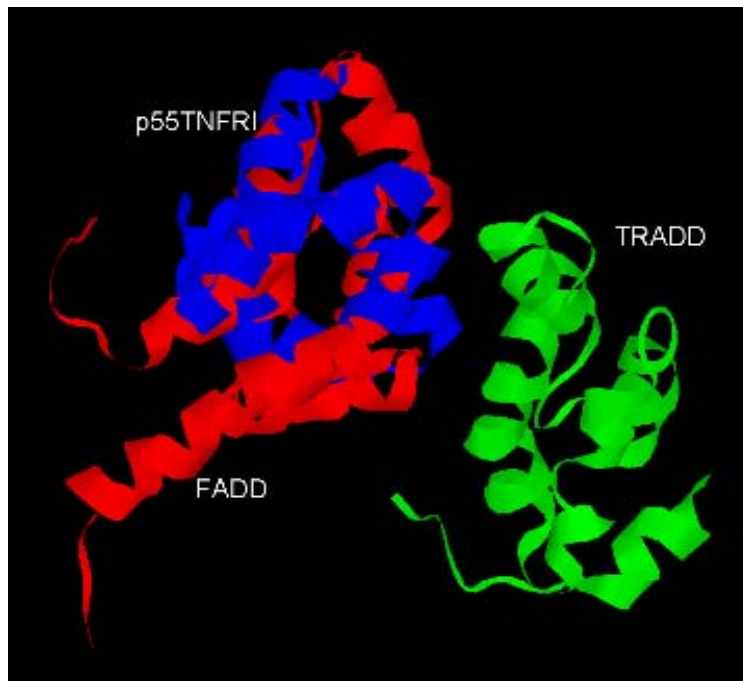
(B)

Figure 12: Complexes obtained from docking program 3D-Dock and analyzed by Swiss Pdb-viewer. A: Complex of p55TNFRI-TRADD-RIP-CRADD showing that recruitment of CRADD might play a role in stabilizing the whole complex, B: Complex of p55TNFRI-TRADD-FADD showing interacting surface of TRADD DD in TRADD-FADD complex overlapping with interaction surface of TRADD DD involved in the interaction with p55TNFRI DD. In the figure FADD is shown in red and p55TNFRI is shown in blue

To better understand how the p55TNFR1-induced pathway shifts between proliferation and apoptosis (Figure 5) we obtained (See Material and Methods section 4.4) high scoring complexes of p55TNFR1-TRADD (Figure 10A, 10B), TRADD-RIP (Figure 10A, 10B, 11A, 11B), RIP-CRADD (Figure 10D), RIP-NFκB (Figure 10C) and TRADD-FADD (Figure 12B) DDs from the 3D-Dock docking program (Table 4). The figure 10 and 11 describes the details of structural elements and interaction sites of complexes TRADD-RIP which can recruit NFκB or CRADD, RIP-NFκB and RIP-CRADD. The high scoring p55TNFR1 interacting surface with TRADD correctly identifies the experimentally known interaction surface (Telliez et al., 2000). Thus the method of prediction of the interacting surface of the first complex in the cascade is experimentally supported in this case. We assumed that the interaction surface in the binding of an upstream component of the cascade is less likely to play an important role in recognition and interaction with the next, downstream component. Thus for example, simultaneous interactions between p55TNFR1-TRADD and TRADD-RIP should happen at different interaction faces on TRADD (non overlapping interaction surfaces). These non overlapping interacting surfaces are studied in all above complexes and obtained key amino acids involved in the interaction by Swiss-Pdb-Viewer. Sequence analysis of these interacting surfaces produced residues conserved in all organisms and residues involved in the interaction but not conserved in the organisms. The conserved residues (Table 4) are probably important in general interactions. In contrast, non-conserved residues engaged in

the interaction should be responsible to maintain specificity. The extensive structural analysis of DD containing complexes led us to propose that sub-domains are present in DDs, as high scoring complexes often used different interacting surfaces. We cannot completely exclude the possibility of the use of the same interaction surface in different or successive steps of the cascade, but considering the high amount of cascade specificity and the variations observed in DDs involved in the apoptosis pathway, particularly in adaptor DDs, it seems unlikely that exactly the same interaction surface should be used for the interaction of the downstream components. Two TRADD-RIP complexes which use different DD interacting surfaces are obtained (Figure 10A, 11B, details of interacting residues in 11A, 11B). These TRADD DD surfaces do not overlap with the DD surface interacting with p55TNFR1 DD. The interaction of RIP DD with known downstream interactions partners is then examined. Two interesting interacting complexes between TRADD-RIP-CRADD DD and TRADD-RIP-NFκBp100/p105 DD are identified. The modeled complexes would thus suggest that recruitment of CRADD and NFκB is dependent on two different, exclusive DD complex conformations observed in the TRADD-RIP DD complex (Figure 10A, 10B, 11A, 11B). Furthermore, exclusive interaction surfaces identified in our study lead either to p55TNFR1-TRADD-RIP-NFκB or to the p55TNFR1-TRADD-RIP-CRADD complex. The TRADD-RIP-CRADD complex suggests that after recruitment, CRADD might play a role in stabilizing the whole complex (Figure 12A). TRADD DD is known to interact with FADD DD (Micheau and Tschopp, 2003; Varfolomeev et al., 1996), however, none of the structures has been solved. We examined the TRADD-FADD DD interaction as modeled to predict the mode of its interaction. The DD surface of TRADD interacting with FADD DD found in all high scoring complexes showed large overlap with the interacting surface of TRADD DD with p55TNFR1 DD (one of the interacting surface described in Table 4, Figure 12B). These data predict that for the FADD DD to interact with the TRADD DD, the TRADD DD has to be released from P55TNFR1. The latter

has experimentally been observed by Micheau et al. (Micheau and Tschopp, 2003). This suggests that when TRADD has bound p55TNFRI it induces a proliferation signal, and when released it can bind to FADD to induce apoptosis (Micheau and Tschopp, 2003). Re-examining the structural data in light of available mutation data (Table 5) shows that our models are well compatible with the available experimental data.

Table 5: Effect of mutations on death domain proteins

a) mutations in FAS and corresponding diseases (Gronbaek et al., 1998; Landowski et al., 1997). Molecular effect: Block of apoptosis		
Position (codon)	Mutation	Mutation observed in disease
244	Asp -> VAL	Diffuse large B cell lymphoma (DLCB)
248	ASN -> LYS	DLCB, Mucosa associated lymphoid tissue (MALT)
256	GLU -> LYS	Follicle center cell lymphoma
262	LYS -> PHE	DLCB
283	LYS -> ASN	DLCB
275	TYR -> SER	Multiple myeloma
253	ASP -> TYR	Multiple myeloma
235	LYS -> ARG	Multiple myeloma
264	ASN -> HIS	Multiple myeloma
b) hematological malignancies: Mutations observed in FAS and TRADD No mutations observed in FADD and RIP		
c) Detailed mutational analysis in TRADD (Park and Baichwal, 1996)		
Position alanine substitution	Effect due to substitution of alanine	
296-299 (extended DD[1])	Prevent induction of NFkB reporter	
219-225,245-251,269-271	No effect on binding of TRADD to P55TNFR1 but capable of inducing NFkB dependent reporter to normal extent	
240-243	Fail to activate NFkB reporter but could induce cell death	

[1]extended DD: We used DD defined by SMART (Letunic et al., 2004) (http://smart.embl-heidelberg.de/), the residues 296 to 299 do not belong to DD according to those databases.

Our models can provide an essential guideline and will be useful for experiments including mutagenesis tests on predicted interactions. The

modelling approach presented here for DD can be used to unravel further and different signalling pathways.

5.6 Conclusions

Death domain superfamily proteins bind through homotypic interactions. Structurally they are composed of an anti-parallel six helical bundle structure (Xiao et al., 2002; Xiao et al., 1999). Our sequence analysis of this superfamily extends previous data (Aravind et al., 1999; Bridgham et al., 2003) and shows that receptor DDs are more conserved than adaptor DDs. The latter are further subdivided into DDs of proteins that can activate or inhibit apoptosis. The analysis also points out that only the activator DD DAP (Death associated protein kinase) is grouped together with apoptosis inhibitors (Chen et al., 2004). Next, several interaction surfaces for DD containing proteins in the p55TNFRI pathway are modeled. Their specific forms and shapes are delineated in Figure 10. RIP's several interaction possibilities rely on the critical residues that are equally distributed in RIP DD and are not concentrated at specific sites.

Several interaction surfaces have been examined by detailed experiments in this superfamily; for example the complex between Apaf-1 and procaspase-9 (CARD-CARD) involves interactions between faces of proteins mainly formed by helices 2 and 3 and helices 3 and 4 respectively (Type I) (Qin et al., 1999). The complex (Figure 9) between Pelle and Tube (DD-DD) involves the loops between helices 1 and 2, and 5 and 6 as exemplified by the Tube DD. The second surface exemplified by Pelle DD, is formed by helices 3 and 4 and the loop connecting helices 4 and 5 (Type II) (Xiao et al., 1999). Remarkably, although the DD fold is highly conserved, characterization of the homologous domains found in the cell death proteins FADD (Bang et al., 2000; Jeong et al., 1999), Fas (Huang et al., 1996), and TRADD (Park and Baichwal, 1996) all suggested a binding surface for their partners that diverges from Pelle and Tube. Taking into consideration the available information and our structural modeling the validity of the identified

different interaction surfaces in DD is strengthened. In spite of such vigorous studies on DDs, the role of these proteins is still not clear in their interaction behavior to mediate either proliferation/survival or apoptosis. TRADD and FADD DDs are able to bind to each other effectively and both are capable of binding to the DD of RIP stronger than the DDs of FAS and TNFR1 (Varfolomeev et al., 1996). Unlike the FAS FADD interaction which always lead to apoptosis, induction of apoptosis through P55TNFR1 TRADD interaction depends on successful interaction between TRADD-FADD DD and inhibition of FLIP induced by complex I as described by Mischeau et al. (Micheau and Tschopp, 2003). Studies also demonstrate the role of these proteins in activating the proliferation pathway (Hsu et al., 1996; Hu et al., 2000; Kasof et al., 2000; Kataoka et al., 2000; Malinin et al., 1997).

Given the variable nature of DD and their portable co-adaptation with specific adaptors (Naismith and Sprang, 1998), We chose here to focus upon proteins containing DD that take part in a caspase dependent pathway. RIP overexpression results in NFκB translocation, JNK activation and apoptosis (Holler et al., 2000; Kasof et al., 2000; Kelliher et al., 1998; Meylan et al., 2002; Stanger et al., 1995, ; Thome et al., 1998; Yu et al., 1999) (see also Figure 5). Further, RIP is also known to interact with FADD, TRADD (Varfolomeev et al., 1996), CRADD (Ahmad et al., 1997) and can induce NFκB activation. We structurally modeled (Figure 10) all these interactions described in the literature. RAIDD/CRADD may also activate caspase 2 (Duan and Dixit, 1997) in a complex called the PIDDosome inducing stress induced apoptosis as the DD containing protein PIDD is induced by p53(Tinel and Tschopp, 2004). CRADD is constitutively expressed in many tissues and may take part in different pathways(Ahmad et al., 1997). Caspase 2 is further known to act as a positive or negative effector of apoptosis depending on the cell lineage and the stage of development (Bergeron et al., 1998).

It has been shown that NFκB p105 DD is absolutely required for TNFα induced serine 927 phosphorylation by the IKK (IκB kinase) complex and the subsequent p105 degradation (Beinke et al., 2002). Recent work also suggests the recruitment of NFκBp100 to P55TNFR1 or FAS receptors via DDs supporting the possible interaction between the DD of NFκB and DDs involved in the apoptosis pathway (Hacker and Karin, 2002; Wang et al., 2002). The DD of NFκBp105 is at the C-terminal half of the protein, which is N-terminal to the IKK phosphorylation. Further published data (Beinke et al., 2002) suggest that α helix 3 of NFκBp105 is involved in binding to the IKK complex. Our docking studies suggest the involvement of the opposite face in the interaction with RIP DD, that is alpha- helix 1 and 6 of NFκB p105 DD and the loop between helix 4 and 5 together with starting residues of helix 2 of NFκB p100 are involved.

Taking the natural limitations of modelling and docking into account, the present comparative structural modelling of six protein complexes in the TNF mediated pathway lead, however, to the delineation of important interacting surfaces in these modeled complexes. This helps to shed light on the mechanism by which p55TNFR1 induces formation of different complexes and in turn signaling through different cascades. The studied proteins are documented to interact with partner proteins (Ahmad et al., 1997; Holler et al., 2000; Kasof et al., 2000; Kelliher et al., 1998; Meylan et al., 2002; Micheau and Tschopp, 2003; Stanger et al., 1995; Thome et al., 1998; Varfolomeev et al., 1996; Yu et al., 1999). Scrutinizing their interactions with our models highlighted different possible interactions in the pathway such as recruitment of CRADD or NFκB by TRADD-RIP complex in two different conformations. Thus our bioinformatical models suggest that the RIP DD might act as a scaffold to bind to NFκB p105/p100 DD which can lead to an easier recruitment of the IKK complex leading to activation of the NFκB transcription factor when bound to TRADD DD in one conformation. In another conformation we predict that TRADD-RIP interacts with CRADD activating the Caspase 2 mediated signaling pathway.

6. Discrete time modeling of the apoptosis pathway

6.1 Introduction to modeling the apoptosis pathway

Programmed cell death or Apoptosis is a conserved mechanism for the elimination of unwanted cells from an organism. The core cell death pathway is present in nematodes, fruit flies, mice and human. Large scale genome analysis has led to the discovery of homologues in all these organisms. The mere presence of the homologues might not imply the existence of the same regulation. Thus differences in the topology of the network affect the final response. Here in this chapter we try to develop a model using ordinary differential equations (ODEs) to study differences in responses due to different topologies and complexities in the apoptosis pathway. We then used the model in discrete dynamic simulation.

Often mathematical representation and analytical solutions of signal transduction pathways are difficult to formulate due to the large number of unknown parameters such as rate constants, concentrations of components etc. But even before such data become available simulations can enhance our understanding of regulatory principles and pinpoint critical behavior and parameters for further experimental tests.

We try to analyze the effect of the length of the pathway, the topology of the pathway and how the stability is achieved between the pro- and anti-apoptotic components activated by identical receptors. Robust systems can maintain the functionality at different concentrations of the components (Kitano, 2004). Stable responses in spite of different concentrations can be achieved by a number of strategies such as regulating relative concentrations of activators, inhibitors, threshold concentrations (concentrations necessary to activate the next component in the pathway) and the amount of specific component necessary for activation. However, we show here how to conceptually develop a model for apoptosis in spite of unknown parameters such as exact concentrations and rate

constants to understand the evolution of complex cascades and their regulation. For a comparative qualitative analysis intended here one can actually neglect observed concentrations and concentrate on pathway topology and its regulation.

Modeling complex biological cascades by simulations is a powerful method in order to understand regulatory principles, complex dynamic phenomenon and particularly effects at the systems level. Modeling signal transduction pathways is complicated and is at an early stage. Several specific pathways and reaction schemes have been analyzed analytically (Brightman and Fell, 2000; Huang and Ferrell, 1996; Kholodenko et al., 1999). However, closed analytical solutions fail if the system is complex and particularly if one wants to integrate molecular and physiological aspects.

We compare the apoptosis pathways of *C. elegans*, *D. melanogaster* and *M. musculus*. The basic network of these pathways was reconstituted from sequence analysis, literature and data obtained from KEGG (Kyoto Encyclopedia of Genes and Genomes). Simulations for other pathways can be developed in a similar way to study different signal transduction pathways.

6.2 Model description

The initial components necessary for apoptosis pathway activation are triggered at each time step in the simulation. All components in the apoptosis pathway before activation are set to zero. The different parameters are summarized in Table 6.

Table 6: Established model parameters

Parameter description	Symbol	Value or range
Maximum concentration of components	MAX_UNIT	*For activators*: 10 *For inhibitors*: Sum over (all inhibited components)
Operative concentration of a	THRESHOLD	0.05

pathway components		
Factor affecting production of component	K	
	Caspase3/Ced3/Decay	5
	Caspase7/Dcp1	15
	Caspase 9	408
	Caspase 8/Dronc/Dredd	4
	All other components	10
Time steps	T	500

The specific regulatory components acting on elements of the apoptotic pathway are incorporated in the model. Other regulatory machinery (such as transcription, feed back regulation, effect of cytokines and growth factors) is difficult to explicitly include. To simplify this, the term maximum concentration (MAX_UNIT) was included as a limit for every component. It was set at 10 for all activators. The MAX_UNIT for inhibitors is the sum of the concentration of components that they inhibit at time t. Thus inhibitors are not abundantly available but present in an amount enough for effective inhibition, for example the equation for the inhibitor IAP is written as:

$$\text{dIAP/dt= (NFkB[t]*(casp3[t]+casp7[t]))/(K + NFkB[t])}$$
$$\text{IAP[t] = IAP[t-1]+dIAP/dt}$$
(1)

Thus at any time point IAP can not be produced more than the concentrations of caspase 3 and 7 together. Further, the previous component in the pathway has to be more than 0.05 standard units in order to activate the next component in the pathway. This threshold concentration is called THRESHOLD and is kept the same for all reactions. 0.05 is chosen for practical reasons to avoid activation at very small component concentrations. Bearing this in mind, the concentration of a compound (no matter whether activating or inhibiting) in the simulation was calculated according to the following equation (in essence the following is modeled by a Michaelis Menten type simplification and introduce further a threshold and a limit to concentrations to strongly simplify the complex cascade):

```
IF  (X₁[t]>THRESHOLD)
        dX₂/dt= (X₁[t]*MAX_UNIT)/( K + X₁[t])
ELSE
        dX₂/dt=0
```
$$\text{IF } (X_1[t] > \text{THRESHOLD})$$
$$dX_2/dt = (X_1[t] * \text{MAX\_UNIT})/(K + X_1[t])$$
$$\text{ELSE}$$
$$dX_2/dt = 0 \qquad (2)$$

$$X_2[t] = X_2[t-1] + dX_2/dt \qquad (3)$$

In the time step simulation, an increase of the component at time t depends on the concentration of the previous component in the cascade. The total concentration of the component at time t is the addition of its concentration at time t and its increase in the concentration at time t. The initial value of the first component in the pathway is set to one so that it can activate the next component at the first time step. Every component activates the next component. The apoptosis cascade is activated depending on the concentration of effector caspases. To simplify the model parameters every component activates the next one when it is more than 0.05, K is 10 for all components except for caspases whose K values are taken from the literature (Garcia-Calvo et al., 1999). The published K values were measured in *Homo sapiens*; we assumed them to be the same for corresponding caspases in all three organisms. Actual activation of the component in the cascade depends on the random probability of binding with previous components. For effector caspases this probability is one in the model as they are known to be auto-activating so the probability of effector caspases activating the next step is only dependend on its concentration at time t.

All reactions except proteolytic reactions are reversible, so that half of the previous component is formed back in the reaction. Inhibitory components reduce the concentration of the component proportional to its own concentration. Inhibitors act immediately on components reducing the concentration at that time t. Thus the net concentration of the component at time t is given by:

$$X_2[t] = X_2[t] - (\text{prob} * X_{2in}[t]) \qquad (4)$$

where X_{2in} is the inhibitor of X_2 and prob is the probability of binding the inhibitor to the component.

In the receptor ligand interaction the ligand concentration will increase as a function of time. When a concentration reaches the THRESHOLD it turns the receptor on, leading to activation of the receptor. Ligands bind to the receptor with random probability. The receptors that also activate apoptosis inhibitory components for example TNFAR and ILR activate surviving factor (SUR, includes TRADD, RIP1 and TRAF2) and MYD88 respectively with small probability 0.1.

This simplistic simulation (see following sections) allows not only testing the establishment of dynamic stability but also first insights how this is affected by different network topologies of the apoptosis cascade.

## 6.3 Comparison of the topology of apoptosis pathways

Alignment of apoptosis pathway in *C. elegans*, *D. melanogaster* and *M. musculus*: For the comparative analysis of the signaling cascade leading to apoptosis in *C. elegans*, *D. melanogaster* and *M. musculus* we aligned the cascade. The pathways of *C. elegans* and *D. melanogaster* were reconstituted from the known interactions in the literature. Most of the apoptosis cascade components in *M. musculus* were retrieved from the KEGG database and activation and inhibitory effects of components were assembled from the literature (Figure 13).
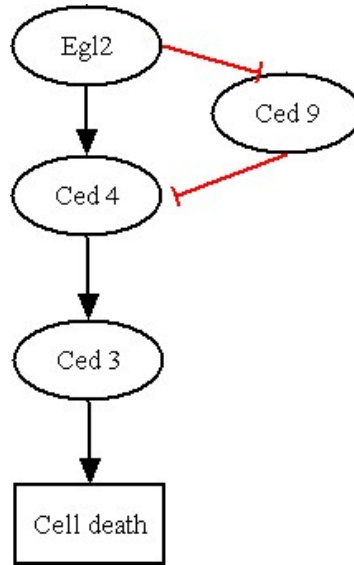
(A)
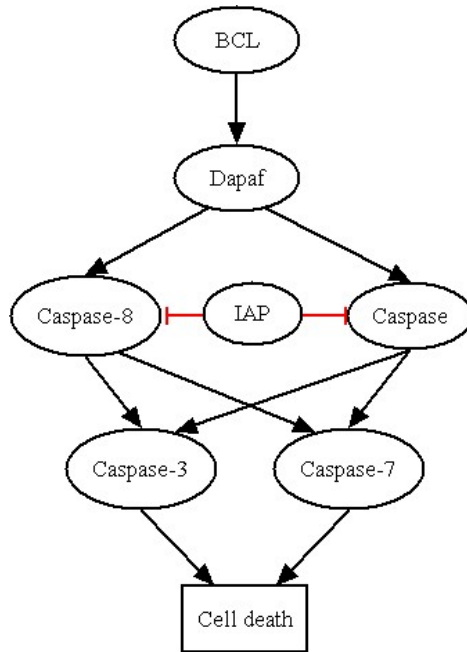
(B)
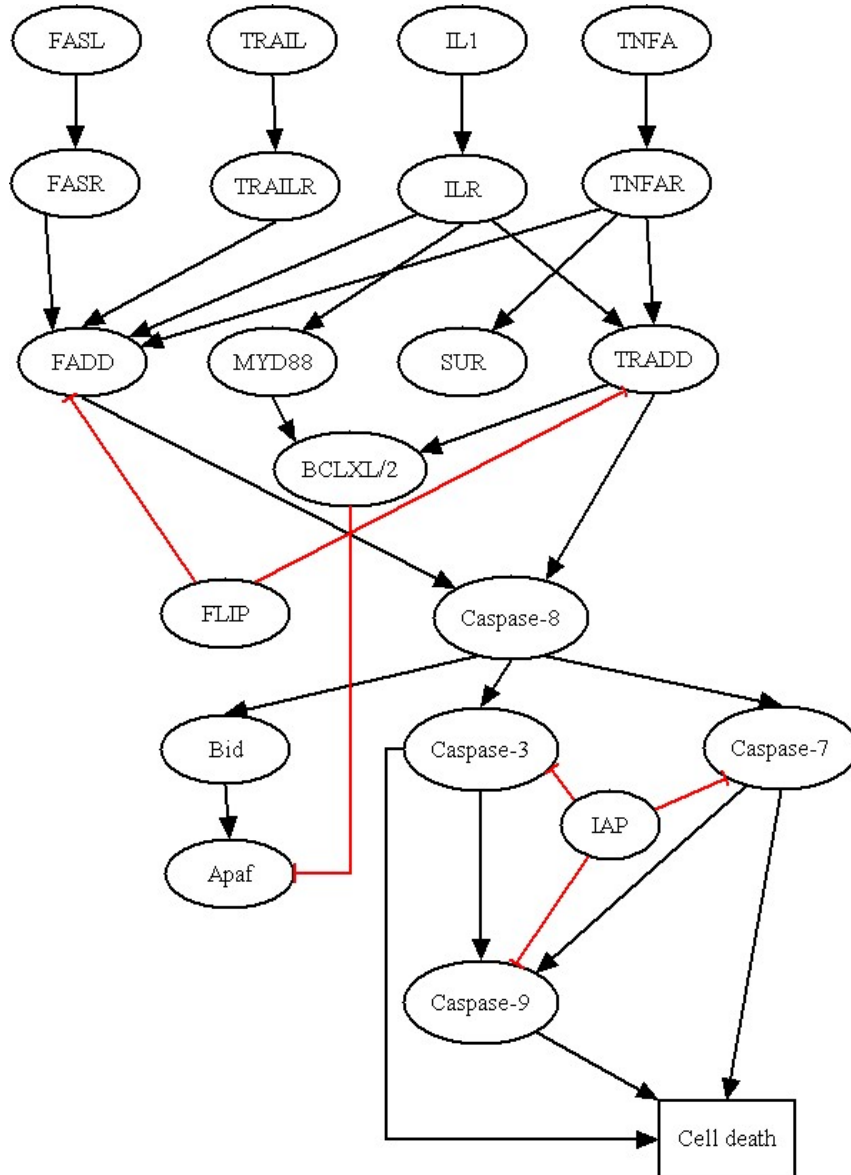
(C)

Figure 13: Scheme of components in apoptosis used in the model from C. elegans, *D. melanogaster* **and** *M. musculus***, showing increased complexity and network topology. The pathway was reconstituted from literature and KEGG database. The position of activators depicts the level at which components function. For example caspase-8 and caspase in** *D. melanogaster* **are activated at same time.**

In the figure 13, the complexity of the pathway increases from *C. elegans* to *M. musculus*. The numbers of components regulated are more in the evolved systems. In *M. musculus* depending on the cell type four ligands can activate the

cascade by interacting with receptor. FASR and TRAILR then activates only pro-apoptotic components whereas IL1R and TNFAR can also activate anti-apoptotic components (SUR and MYD88). SUR is used here for survival signal which is transmitted through TRADD, RIP and TRAF complex. Such ligand-receptor reaction is absent in *C. elegans* and *D. melanogaster*. FADD and TRADD then activate caspase-8. Caspase-8 also activates bid which turns on the intrinsic pathway by triggering apaf. Apaf then activates caspase-9 and BCLXL inhibits apaf. BCL family of proteins includes pro and anti apoptotic proteins. Proteins from this family are highly conserved across the species. One of BCL family protein activates apoptosis cascade in *D. melanogaster* by activating dapaf which has high sequence similarity to apaf in *M. musculus*. dapaf then activates caspase-8 in *D. melanogaster*. Caspase-8 then activates caspase-3 and 7 in *M. musculus* and *D. melanogaster*. Caspase-3, 7 and 9 are inhibited by IAP in *M. musculus* and *D. melanogaster*. Unless inhibited they execute the death of cell in both organisms.

The pathway alignment shows that in *M. musculus* and *D. melanogaster* effector components are regulated in contrast to *C. elegans*; the obvious question is, what is the effect of such a different topology? In *M. musculus*, some components are activated that do not only inhibit apoptosis activating components (for example IAP) but also activate components in the proliferation pathway (for example MYD88, BCLXL, SUR). Further, the proliferation pathway components MYD88, BCLXL and SUR are activated by the same receptor that activated apoptosis pathway. Then how apoptosis is successfully achieved? Is it because these inhibitors are activated later (in time scale) or they are not effective before?

Considering that the apoptosis signal is induced at time step one, two assumptions for inhibitor activation were used: (1) the inhibitors are also induced at a lower probability of 0.1 at t=0 that is along with apoptosis activators or (2) they are induced after apoptosis activators reach maximum concentration. These two hypotheses were checked in the present simulation.

The effects of topology of the overall pathway and in particular the topology of inhibitors and effector components were compared in our simulations. The Michaelis Menten formalism characterizes usually enzyme catalyzed reactions. The terms in the equations were efficiently re-modeled in our simulation to characterize the behavior of components in the signal transduction pathway. The components of highly regulated pathways are usually formed in high concentration after its induction and are feed back regulated efficiently. The pathway was verified for reachability of signals and its robustness.

The structure of the processes and parameters is the same in *C. elegans*, *D. melanogaster* and *M. musculus* so the differences observed in the results can be attributed to the differences in topology and complexity of apoptosis pathway. Please note that rate constants of caspases in *M. musculus* are known, they were used in *C. elegans* and *D. melanogaster*, as the purpose here was to see the effect of topology.

6.4 Signal processing through the apoptosis pathway in the three organisms
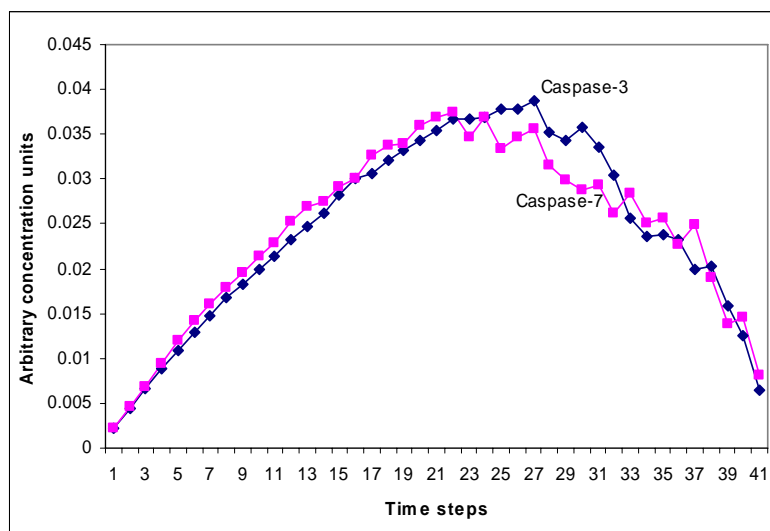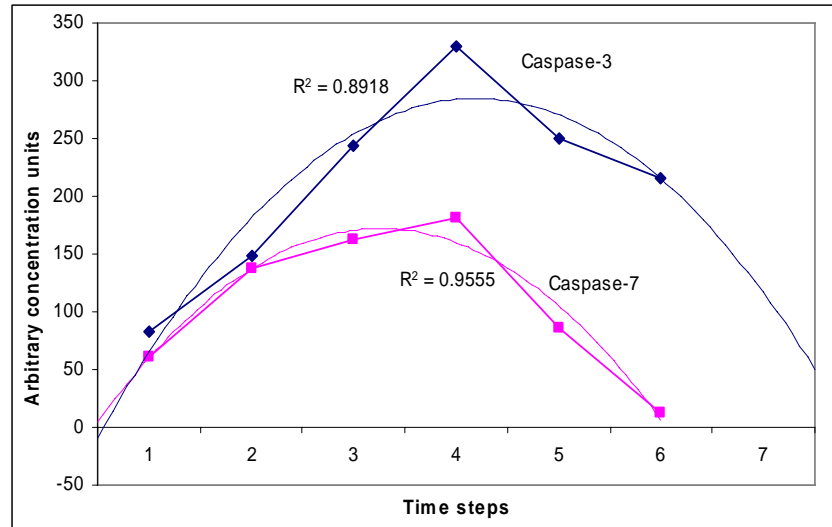
Figure 14: Effector caspase concentrations against time are plotted. The concentrations are increased giving a peak at time step 4 in *M. musculus* and at time step 24 in *D. melanogaster* followed by a decrease in the concentrations.

Simulations with parameters as detailed in section 6.3 model description were run for 10 time steps. In a set of simulation experiments, the positive apoptosis signal was given at each time step. In spite of continuous activation of the receptor the apoptosis could take place only for 6 time steps in *M. musculus* whereas in *D. melanogaster* for 40 time steps and in *C. elegans* for 140 time steps (at K=10). This can be attributed to the activation of apoptosis inhibitory processes by the same receptor signalling in *M. musculus* and in general better regulation of the pathway as complexity increases to avoid unwanted death. Please note that apoptosis is assumed to take place when the concentration of effector caspases is greater than 0.05. In reality apoptosis might take place only at optimal effector caspase concentrations. An increase in the concentrations of effector caspases in *M. musculus* and *D. melanogaster* mounting to a peak followed by a decrease in the concentration (Figure 14) is observed. Please note that *D. melanogaster* and *C.elegans* inhibitors are also activated with the same probability of 0.1 along with activating components. This keeps the topology of the inhibitors similar in all three organisms. Moreover, there is lack of exact information on the activation of inhibitors. In *M. musculus* it is known that

inhibitors of the pathway are activated due to IL1 and TNFA receptor signaling that also lead to stimulation of the pathway (Figure 13). In *C .elegance* the effector caspase ced-3 increases linearly with time as long as ced-4 (a regulator of ced-3) is present (Figure 15).
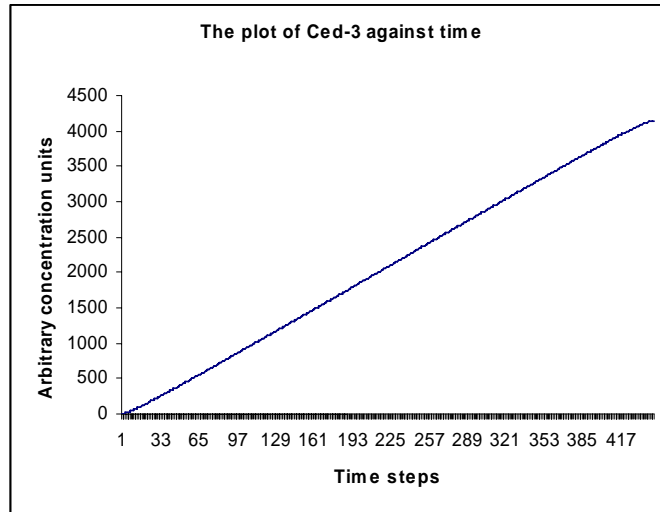

Figure 15: The plot shows that in *C .elegance* the effector caspase ced-3 increases linearly with time as long as ced-4 (a regulator of ced-3) is present.

A change in the value of K affects the number of time steps for which the apoptosis pathway remains active, increasing along with K and keeping the graph qualitatively same. The simulation was tested for robustness and sensitivity for a wide range of parameters (K: 10 to 100 and MAX_UNIT: 10 to 100). In all cases the differences in the three organisms were maintained, such as longer activation in *C.elegans*, effector curves (linear in case of *C. elegans* and activation peak in case of *M. musculus* and *D. melanogaster*), inhibitor curves (sigmoidal and saturation curves).
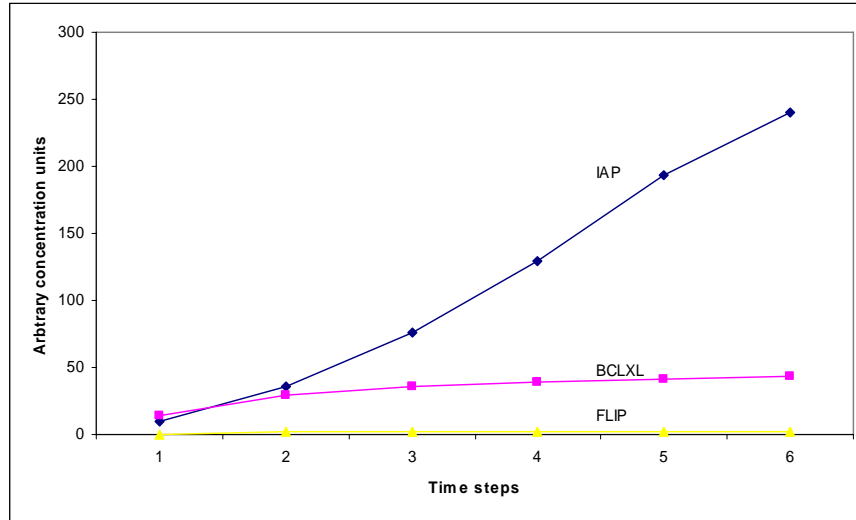
Figure 16: Inhibitors (FLIP, IAP and BCLXL) in *M. musculus* are plotted against time for which apoptosis is active. FLIP concentration is close to zero, increase in the FLIP concentration lead to inhibition of apoptosis after 6 time steps. IAP has the sigmoidal curve against time. And BCLXL (inhibitor of Apaf) increases till time step 2 and then remains stable for the period till apoptosis is active.
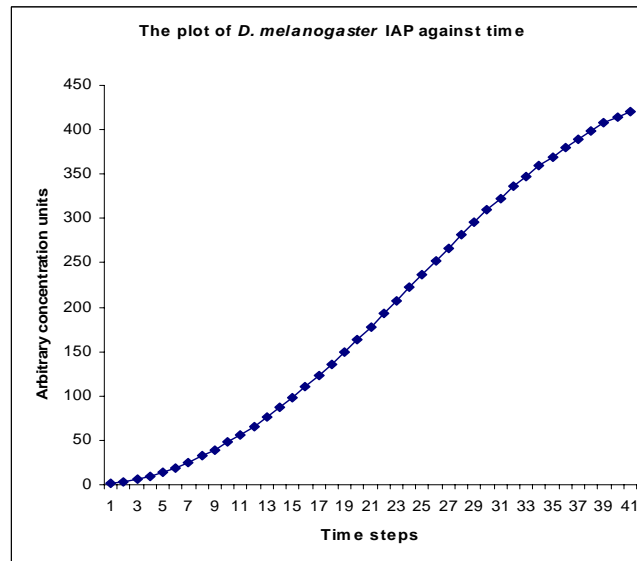

(A)
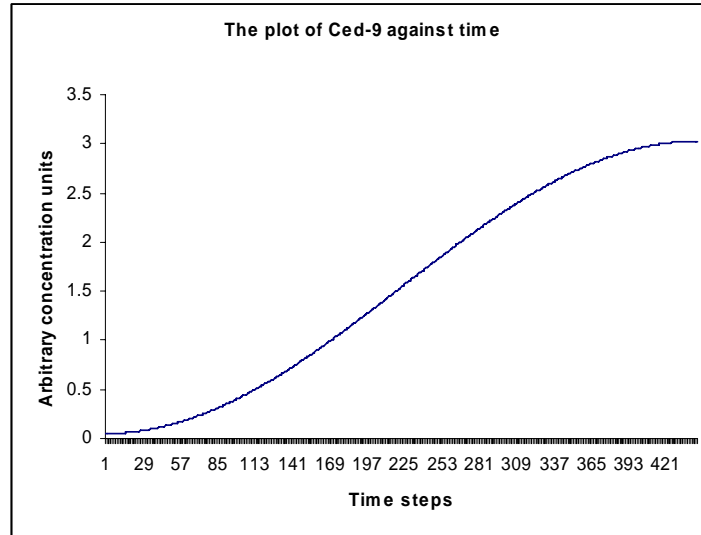
(B)

Figure 17: In the figure inhibitors of the apoptosis pathway in *D. melanogaster* and *C. elegans* are plotted against time. The figures A and B shows that inhibitors (IAP in *D. melanogaster* and Ced-9 *C. elegans*) follow sigmoidal curve when plotted against time in *D. melanogaster* and *C. elegans* respectively.

The curve of inhibitory IAP (in *M. musculus* (Figure 15) and *D. melanogaster* (Figure 17A)) and ced9 (in *C. elegans*) is sigmoidal when plotted against time (Figure 17B). In *M. musculus*, there are two more inhibitors with different topologies (Figure 16): FLIP remains close to zero as long as apoptosis takes place. Increased production of IAP compared to FLIP shows stronger regulatory control on effector components (end components of the pathway) (Figure 16). This might have evolved to regulate complex networks; as in *C.elegans* inhibition is not at the level of effector component (Ced9 inhibits Ced4 but not Ced3). Thus the topology of the pathway is critical and has important implications for the specific effect in the organism and it is adapted in this way also to different levels of multi-cellular complexity. BCL increases and then stabilizes so that apaf is not produced for long time. This also will lead to shut down of intrinsic pathway before extrinsic pathway.

6.5 Effect of deletion of the intrinsic apoptosis pathway in *M. musculus*
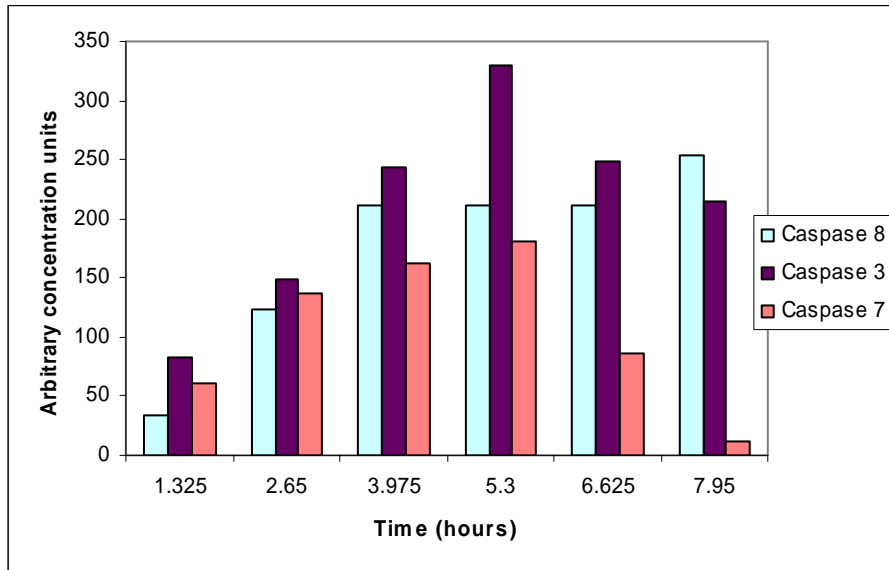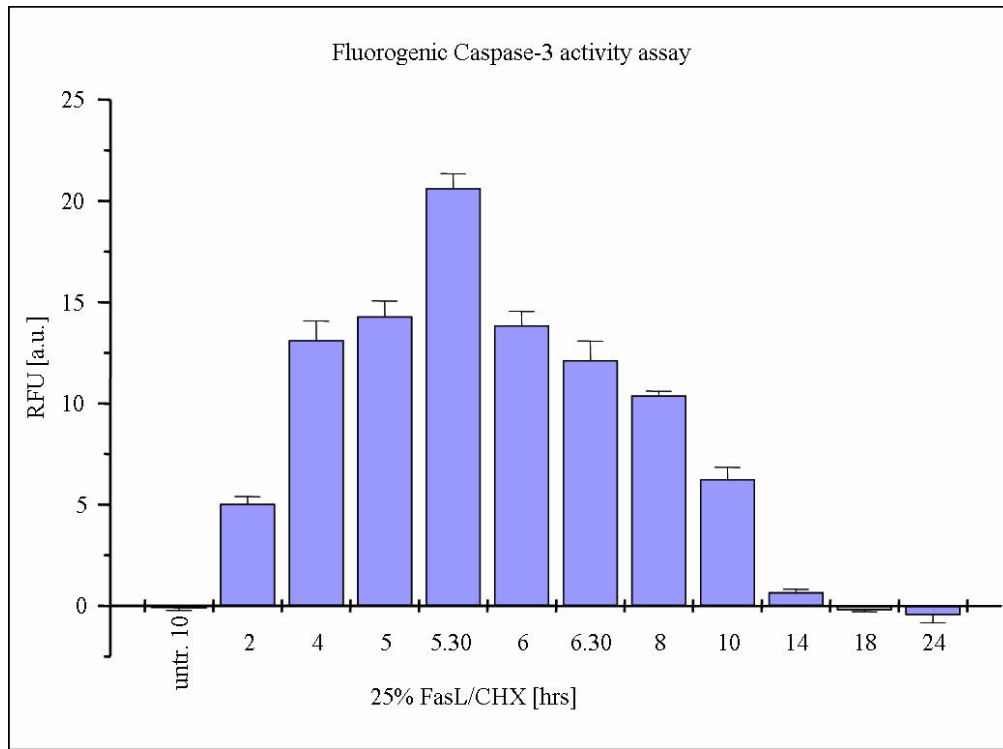

(A)
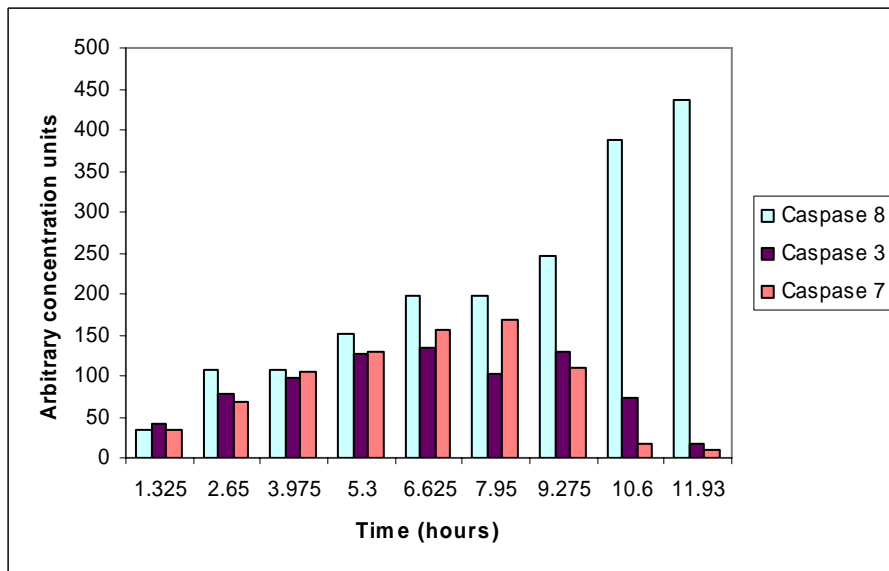
(B)

Figure 18: Model results for the concentration of caspase 8, 3 and 7 are plotted against time. (A): results in the presence of the intrinsic pathway. (B): in the absence of the intrinsic pathway. Note that concentration units are arbitrary and are used for the comparison.
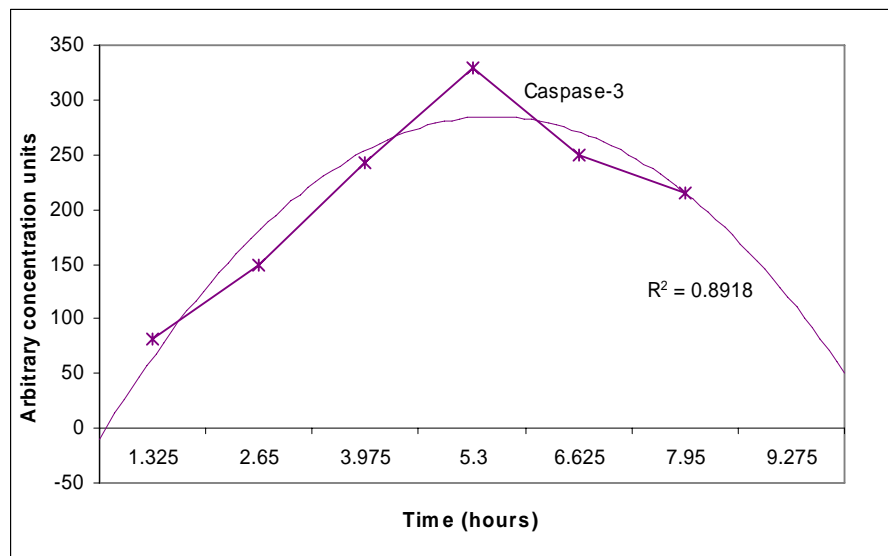
We consider in this section cell types where both intrinsic and extrinsic apoptosis pathway take place. Bid connects these two pathways activating caspase 9 and in turn caspase 3 and 7. Concentration of caspase 8, 3 and 7 is plotted against time in Figure 18A in presence of the intrinsic pathway and in Figure 18B in the absence of the intrinsic pathway. The comparison between both figures shows that the concentrations of effector caspases namely caspase 3 and 7 are much lower in the absence of the intrinsic pathway at complementary time steps. In contrast, the concentration of caspase 8 is unaffected (at time step 6 the concentration is 250 in both graphs). The apoptosis pathway is active for longer time (9 time steps) which can be explained by the reduction in concentration of effector caspases. An interesting observation is that the peak of caspase 3 and 7 is not at the same time step. Further caspase 7 concentration is greater than caspase 3 concentration at time steps 6 and 7. The pathway is predicted to be and the simulation is shown to be sensitive to changes in topology. The observed effect can be attributed to the differences in K values of caspase 3 (K=5) and 7 (K=15) and the fact that same inhibitor IAP controls the concentrations of both effector caspases. IAP concentration in the model depends on concentration of caspase 3 and 7 as explained before (See model description). Though the rate of caspase 3 formation is more than for caspase 7, it also leads to a higher activation of IAP at a given time reducing its net concentration. Note that when the intrinsic pathway is active, caspase3 is formed in large amounts because of its higher rate of production and more activating signal.

6.6 Model predictions and experimental validations

6.6.1 Caspase-3 activity

Fluorogenic Caspase-3 activity assay

(graph showing RFU [a.u.] vs 25% FasL/CHX [hrs])

(A)

(graph showing Arbitrary concentration units vs Time (hours), Caspase-3, $R^2 = 0.8918$)

(B)

Figure 19: Experimental test on the predicted levels of the executioner caspase 3. (A): Experimental data: Relative fluorescence units (RFU) measuring the activity of caspase-3 in response to FasL is plotted against time after incubation with 25% FasL/CHX. (B) Simulation predictions: The predicted values for caspase 3 are are plotted against time. Furthermore, polynomial fitting for the time course modeled yields the thin continuous line (polynomial fit given in the right corner together with correlation to the simulated data)

Whereas these general results at least suggest that our simulations capture and predict first features of organismic complexity in apoptosis regarding the topology of regulatory control, then to examine to what extent the concentrations and time evolvement of compounds simulated agreed qualitatively with experimental observations. As a first test we compare the, the caspase 3 activity, the major executing enzyme involved in apoptosis and its evolution during time with experimental data: fluorogenic caspase-3 activity of primary *M. musculus* hepatocytes (Figure 19A, 19B). Flurorogenic caspase-3 activity was measured after the treatment of primary *M. musculus* hepatocytes with 25% FasL plus 10 µg/ml CHX. Cytosolic extracts were made an aliquots were mixed with a fluoregenic caspase-3 substrate DEVD-AMC. Caspase-3 activity can already be observed after 2 hours of treatment with FasL/CHX. The maximum activity occurs at 5 hours and 30 minutes, after which the activity decreases in a time-dependent manner (Figure 19A). The simulation results reproduce the behavior of the caspase-3 similar to that observed experimentally when stimulated by FasL/CHX. The peak of caspase-3 is observed at 4.5 time steps followed by the decrease in the concentration (Figure 19B). This comparison demonstrates an experimental test of the predicted compound curves and time scales. Thus the time scale used in the model is in hours. The qualitative behavior of the end component caspase-3 in the murine apoptosis pathway is well-predicted. Note that the DEVD/AMC substrate used in these experiments can be used by both caspases 3 and 7. There is no specific substrate for caspase 8, as the caspase 8 substrate IETD-AMC is also cleaved by caspase 3. Thus experimentally it is only possible to estimate combined activity of caspase 3 and 7 as they share substrates. They also have same inhibitor and act at same level in apoptosis. Though time-scale and peak shape of the main executioner caspase under constant activation for the most complex cascade are well agreeing with observations, some other observations from experiments help us in scaling our parameters.

In vivo concentration of FAS ligand is estimated to be 10 to 50 ng/ml. In the model MAX_UNIT is adjusted to 10 which is close to the estimation after the asseignment of the unit ng/ml.

6.6.2 Survival of cells and experimental validation
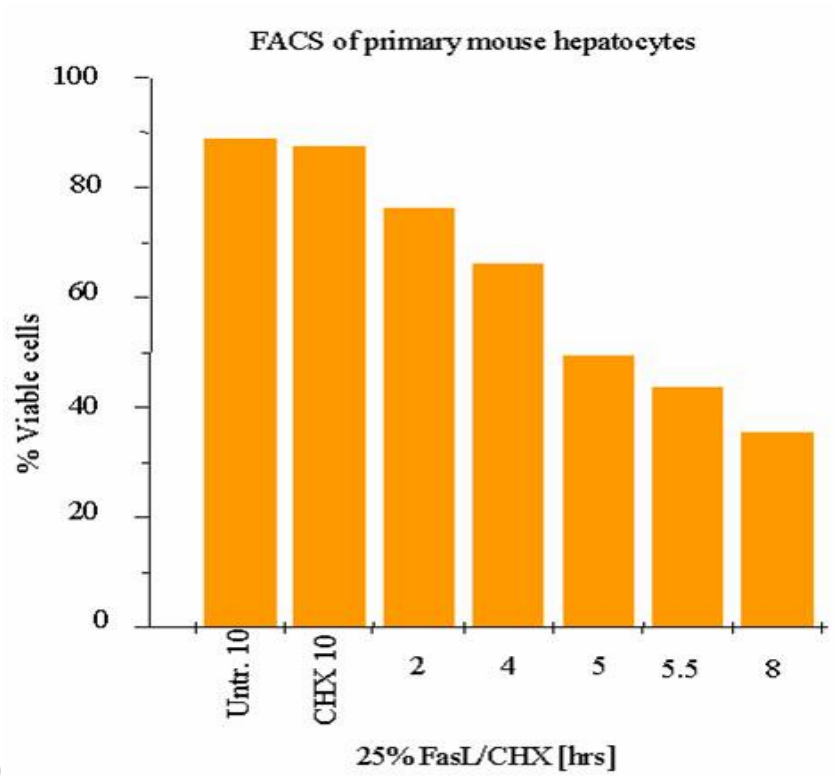
(A)
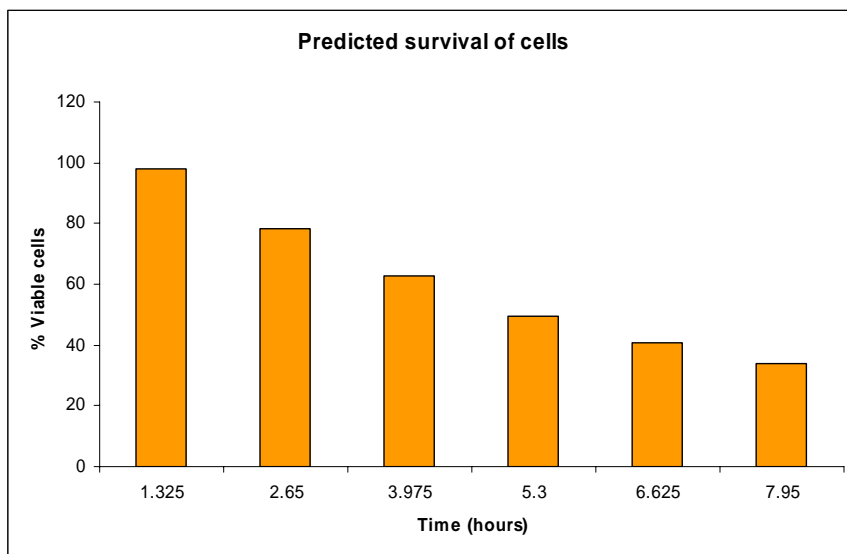
(B)

Figure 20: Experimental test on the predicted percentage of viable cells. (A) Experimental data: FACS assay described in material and methods was used to experimentally estimate percentage of viable cells. The percentage is plotted against time. The data shows viable cells when caspase-3 was until the caspase-3 is detectable. (B) Simulation prediction: The percentage of survival was assumed to be proportional to the concentration of Caspase-3. The percentage was calculated as described in results. The figure shows the accurate prediction of percent viable cells by the simulation.

We used this dynamic simulation to predict the viability of cells (Figure 20B). The number of cells killed is assumed to be proportional to the concentration of caspase-3. Fluorescence activated cell sorting assay was used to experimentally observe cell viability. Figure 20A shows the % viability of cells against time of incubation with 25% FasL/CHX in hours. This observation could be compared to % viability predicted by the simulation.

$$\%\text{viable cells } [t_i] = (100 \,/\, c3) * (\sum_{t=0}^{t_{max}} (\sum \text{cacspase-3/7}) - \sum \text{caspase-3/7})$$

(5)

$$\text{where c3 is a proportionality factor and } \sum \text{caspase-3/7} = \sum_{t=0}^{t_i} \text{caspase-3/7}.$$

The above formula was used to calculate % viable cells. The data fits exactly predicting 49.7% viable cells when highest concentration of caspase-3 is observed. Note that experimental studies take into consideration more number of time steps this explains why at 6th time step we still see 33.7% viability.

6.7. Activation of inhibitory components in light of experimental data

The model was developed with the two assumptions: (i) Apoptosis inhibitory components are activated along with apoptosis inducing/ activating components. (ii) Apoptosis inhibitors are activated after sensing the higher concentrations of the apoptosis inducing/ activating components. The good

approximation of the experimental results guided us to accept the first assumption. It has been found that in the TNFAR induced pathway the complex we is formed that activates NFKB only before TNFAR undergoes endocytosis (Micheau and Tschopp, 2003). Thus ILR and TNFAR are suggested to activate the inhibitor protein at a lower probability along with apoptosis activators probably as a sensor primarily to activators. Thus our fist assumption is also supported by experimental evidence.

6.8. Conclusion

Qualitative simulation is used in this paper to study the behavior of components in the apoptosis pathway. We could analyze the topological effects of the pathway due to the comparison between three organisms. Further the deletion studies (deletion of intrinsic apoptosis) showed that the simulation is sensitive to the component topology and produced logical outputs indicating the regulatory hot spots, namely: caspase regulation (see results) and separation between regulation of distal and proximal parts of the pathway. The co-relation between inhibitor time course and activator time course points to the efficiency due to regulation at the level of the effector component in complex networks (in *D. melanogaster* and *M. musculus* but not in *C. elegans*).

For a wide range of parameter settings the difference in response in the three organismic variations of the pathway is maintained: Long activation in *C.elegans*, short activation in *D. melanogaster* and only activation peak in *M. musculus*. In contrast, the inhibitory response builds up during evolution and is most stable in *M. musculus*. Thus the topology of the pathway is critical and has important implications for the specific effect in the organism. It can be speculated that it is adapted in this way also to different levels of multi-cellular complexity.

RESULTS PART II

Phagosome and Lysosome: Signalling and fusion

Results and chapter discussion

7. Modeling of the phospholipid network necessary for actin polymerization in the phagosomal membrane.

Phogosomes are highly dynamic vesicles that are formed *de novo* by the cell and subsequently mature (Griffiths, 1996). Particles inducing phagocytosis induce rapid and massive actin assembly via signal transduction in different cell types, allowing phagosome enclosing the particle to be formed (Allen and Aderem, 1995; Caron and Hall, 1998; Greenberg et al., 1991; Reaven and Axline, 1973), subsequently the phagosome fuse with the lysosome. The acquired acid hydrolases and vacuolar ATPases, acidify the phago-lysosome lumen and facilitate the digestion and removal of the pathogen. Live pathogens such as *Mycobcterium tuberculosis* secrete inhibitory lipids and/ or proteins that are released into the phagosome that can block phagosomal membrane function such as actin assembly and in turn fusion with lysosomes (Beatty and Russell, 2000; Clemens, 1997; Rhoades et al., 2003). Mycobacteria are serious causes of human disease. Over 3 million humans die every year from *Mycobacterial tuberculosis*. These microbes survive and grow inside phagosomes and block phagosomal membrane signaling processes (Russell, 2001). Many signaling molecules, in particular phosphoinositols, play a role in the processes of actin assembly and lysosomal fusion (Anes et al., 2003).

In vitro and *in vivo* phagosomes containing pathogenic or non-pathogenic mycobacterium can be studied using Latex Bead Phagosomes (LBP), due to the ease by which these organelles can be isolated in pure form from macrophages (Desjardins et al., 1994)' (Desjardins and Griffiths, 2003). They represent the simplest imaginable membrane system, a single bilayer around a (usually 1μm) bead. Thus the experimental observations were made using LBPs and were used to test the simulations.

7.1 Introduction to phospholipids network

The response of LBP and phagosomes containing non-pathogenic mycobacteria to a variety of lipids was very similar (Anes et al., 2003). When, however, the phagosomes enclose live pathogenic mycobacteria, the actin-polymerizing machinery is switched off, both *in vitro* and in macrophages (Anes et al., 2003). Seven of the lipids that activated LBP phagosome actin assembly could activate this process on live mycobacterial phagosomes. The same lipids stimulated the maturation of these phagosomes in cells, leading to pathogen killing (Anes et al., 2003). The analysis of a defined (and complex) membrane function (actin assembly) in the LBP system *in vitro* is thus likely to reveal general properties of membrane signaling networks, especially those relevant for host-pathogen interactions. Towards this goal, we compiled detailed experimental data on the effects of different lipids and soluble compounds on phagosome actin assembly and used these to construct the first network models of the signaling cascades operating in the phagosomal membrane.
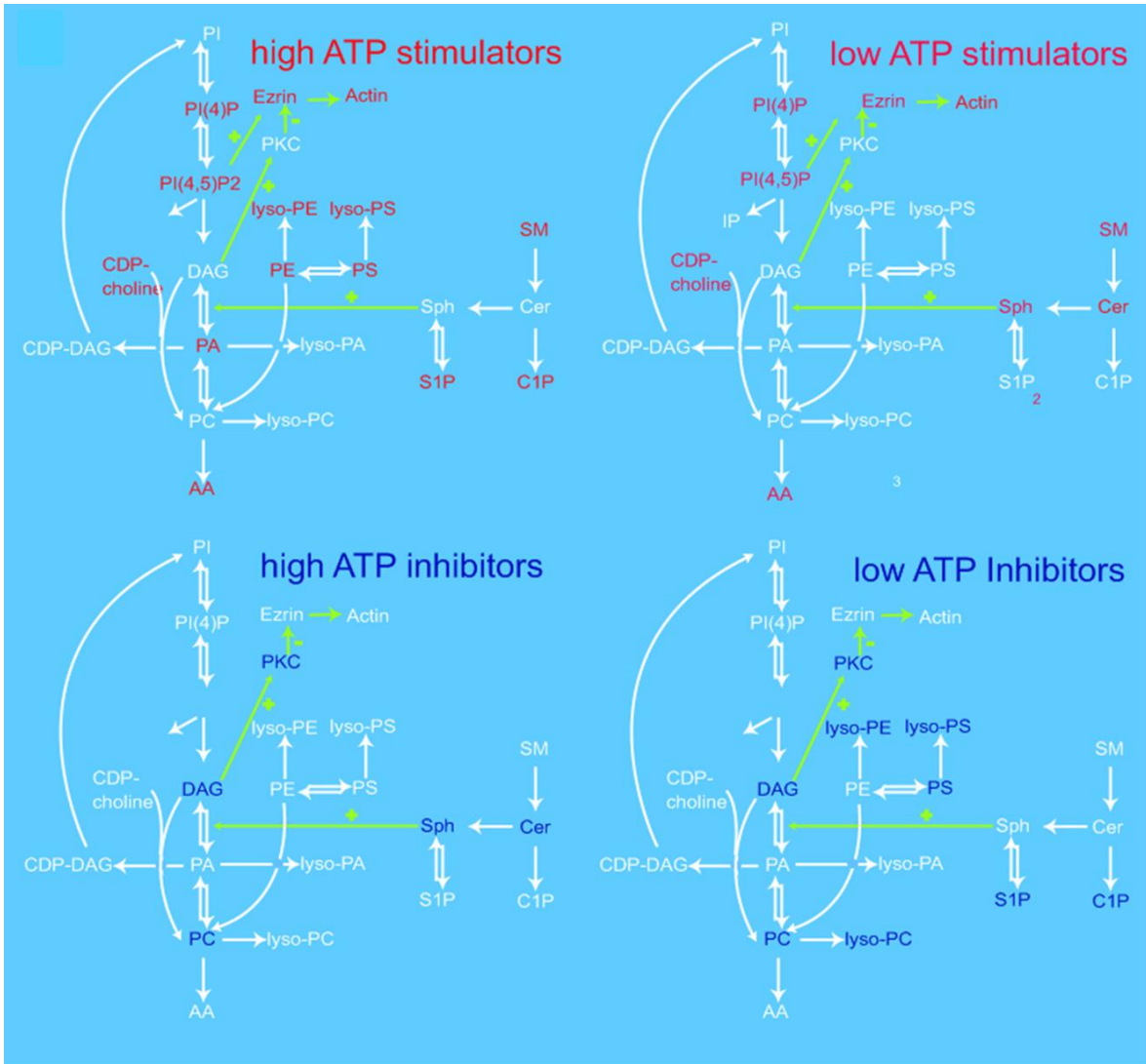
Figure 21: The figure shows the lipid and phospholipid network along with allosteric interactions affecting actin polymerization machinery on the phagosomal membrane. The red colored component activates actin polymerization at high or low ATP concentration. The blue colored components inhibit actin polymerization at high or low ATP concentrations.

The major experimental part of this study (the experimental part was done in EMBL by the group of Gareth Griffith) involved the addition of different compounds, mostly lipids, to the *in vitro* LBP actin nucleation assay (Defacque et al., 2000). The readout of interest was whether a compound stimulated (+), inhibited (-), or had no effect (0) on LBP actin assembly (Figure 21). In the previous study, positive and negative lipid effectors were identified, but the

response varied greatly depending on the concentration of ATP (Anes et al., 2003). The standard LBP assay operates using low (0.2 mM) ATP whereas physiological levels of ATP (5mM) inhibit the system. These two different responses appear to represent two different membrane signaling states or 'signatures' (Griffiths, 2004). For example, the addition of sphingosine stimulated actin assembly at low ATP but inhibited the process at high ATP, while its down-stream product, sphingosine-1-phosphate (S1P) behaved in the opposite manner (Figure 21; (Anes et al., 2003)).

Here we have extended this analysis to include a larger number of inter-connected lipids. Figure 21 shows the signaling network that is linked to the phagosome actin assembly process and provides a summary of the effects of the main lipids (and IP$_3$) that is modeled. The four different states of the system that emerged from our experimental data are shown in the four diagrams at high or low ATP, showing activation versus inhibition.

7.2 Dynamic simulation
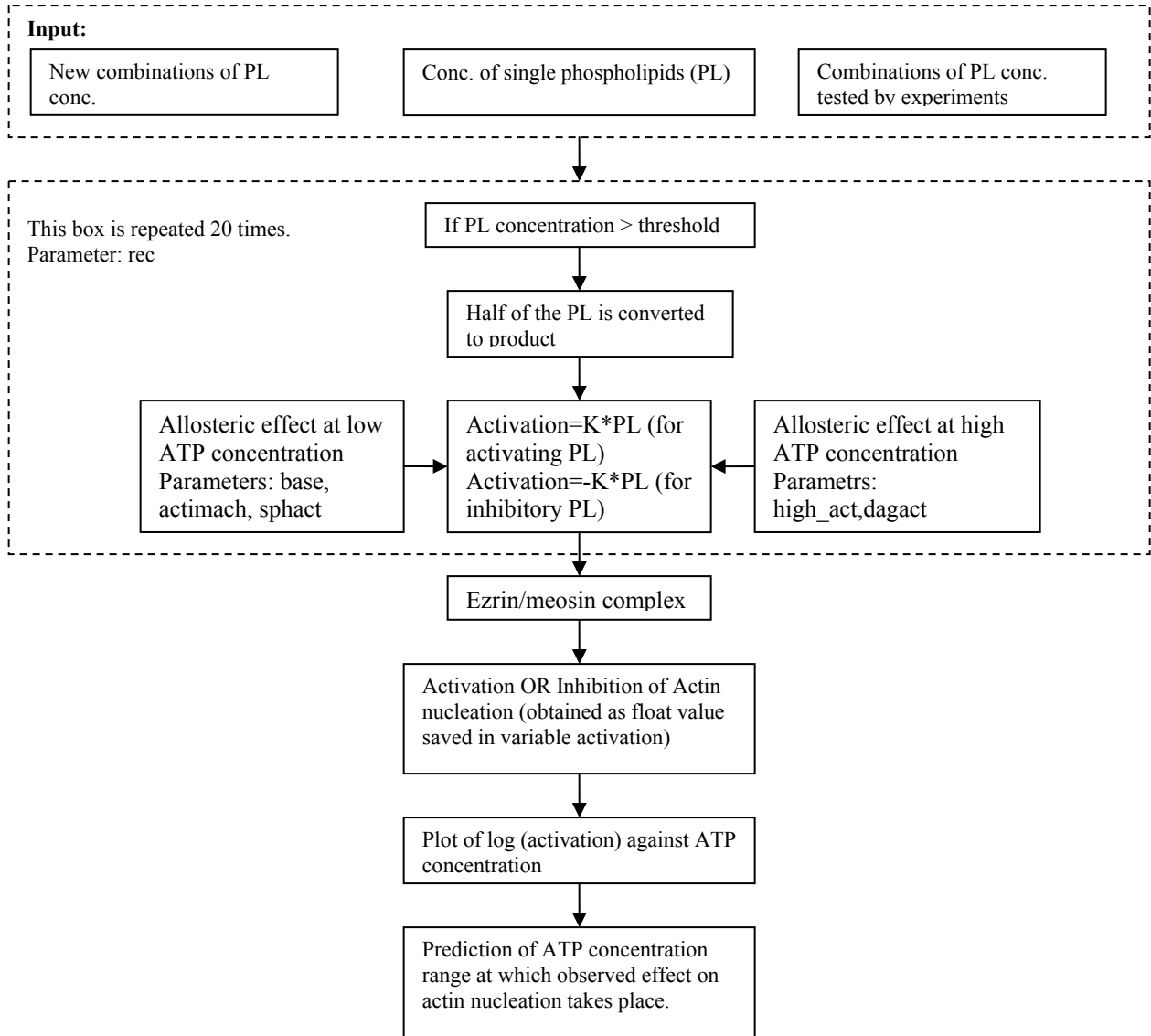
Figure 22: Dynamic modelling of phagosome signaling networks: Shows an overview of the algorithm used to model the lipid-based networks dynamically.

The links between phagosomal ATP synthesis and actin assembly can only be addressed comprehensively by considering the detailed network topology and dynamics of the membrane signaling networks. The elementary mode analysis (EMA) approach (Schuster et al., 2000) provided a good starting point in that it allowed to decipher the possible sets of inter-linked metabolic reactions that can occur between the 19 lipids that are modelled (Figure 21). The main compounds considered in experiments and modeling are lipids and the final

reaction achieved is the nucleation of G-actin to F-actin on the phagosomal membrane. As all relevant substances are primarily produced and consumed by metabolic conversions, a model of the metabolic fluxes involved provides a first approximation of this sigaling network. The principal pathways of the signalling cascade in the phagosome can be correctly described qualitatively by EMA.

A more detailed description considers additional concentration-dependent effects such as: (i) the dependence of reaction rates on substrate and product levels (ii) allosteric regulation (iii) indirect modulatory effects of interacting proteins and lipids. We have developed an extended model (Figure 22) that considers the quantitative experimental data on the ability of different lipids and other effectors to stimulate or inhibit LBP actin assembly relative to untreated controls. The model simulates, in discrete time steps the effects of adding a pulse of a single lipid, or a combination of lipids, and follows their subsequent conversion into further metabolites in the lipid network of the phagosomal membranes that regulate the actin assembly process. This model considers not only metabolic conversions between lipids but also direct interactions of lipids with the actin nucleation machinery and allosteric interactions (Shown in Figure 21).

Table 7: Model parameters and their effects

Name	Value	Effect
Type I parameters		
K	0.5	Translates phospholipids concentrations into actin activation or inhibition
Threshold	20	Minimum concentration of lipids required for any action
sphact	0.30	Stimulates PA formation, DAG kinase and PIP2 formation (by stimulating PI4P kinase)proportional to Sph concentration.
PAact	0.30	Stimulate Sph kinase leading to increase in S1P formation
Type II parameters		
dagact		Activation of PKC by DAG
High_act	1.3	Leads to differential effect of phospholipids at high ATP
actmach	1.5	Activation of CD44 and receptor by PIP2
F-actin	1	Activation of PLD

All model parameters (Table 7) were determined in many simulations to optimize prediction accuracy for single lipids, taking in to consideration the present experimental data on individual lipids and phospholipids to stimulate (+) or inhibit (-) phagosomal actin assembly. The rate constants and diffusion are only simplified modeled by factors to translate lipid concentrations into activation and thresholds to mimic diffusion barriers. It is described schematically Figure 22.

Two types of parameters operate on the lipids in the network. The first type considers the reactions (Figure 21) which are possible at either high or low ATP. Thus the parameter 'K' translates individual lipid and phospholipids concentrations (taken from the experimental data) into actin activation or inhibition at low and high ATP (set at 0.5 for all lipids). 'Threshold' (set at 20) is the minimum bulk concentration of lipid in micro moles necessary for a reaction to take place. From the experimental data activation of actin assembly at low ATP generally provides a signal (percentage of positive phagosomes) that is about 20% higher than signal at high ATP (which is considered as an inhibition). 'Base' (set at 0.20) simulates this effect in the model. The network topology regarding metabolic conversions and allosteric effects is taken into account. For example, sphingosine is known to activate the conversion of DAG to PA. Thus a factor 'sphact' (0.30) activates PA production depending on concentration of sphingosine. The weight of the factor (as done for the others given here) is optimized for prediction accuracy of network response (activating or inhibiting) based on the results of many simulations and using the experimental data on single lipids in phagosomal activation assays.

The second type of parameters is specific for high or low ATP. The effect of DAG on PKC activation at high ATP is simulated by the parameter 'dagact' (set at 2). Different states of the actin polymerization machinery (like ezrin/moesin/PIP2 complex which acts as a link between membrane and actin monomers) at high and low ATP are taken in to consideration by the parameters

'actmach' at low ATP (set to 1.5) and 'high_act' at high ATP concentration (set to 1.3).

This model also takes into consideration the direct interactions of PIP_2 with the actin nucleation machinery and specific allosteric interactions (Figure 21). This model (Figure 22) investigates the system out of equilibrium after a lipid has been added, using 20 simulation time steps (after which the system has reacted and is assumed to be in equilibrium again). It then models in a simplified way the complex and (incompletely known) enzyme fluxes. As in the real phagosomal membrane, the lipid or lipid combinations added to the phagosomal membrane in the model can be converted in several directions of the lipid network (Figure 21). If above the conversion threshold, in the subsequent time steps half of the resulting metabolite concentration is further converted evenly into all these possible directions (including the back-conversion in a reversible reaction), with each of the resulting lipids adding either 'activating' or 'inhibiting' input to the system. The ATP concentration (i.e "high ATP", 5 mM or "low ATP", 0.2 mM) was also an input into the model.

The final readout is a prediction, not only as to whether the overall system will inhibit or activate actin assembly, but also the magnitude of the effect. More complex effects such as facilitation of stimulatory or inhibitory effects of the lipids by additional interacting molecules, including allosteric effects, mediating kinases or phosphatases, and the proposed ATP synthesis, are only modelled in a simple, heuristic way in this study. The model still leaves out many further, identified, as well as unidentified proteins and lipids and the more complex regulatory networks. The analyses presented here can be used to give a more detailed model as more kinetic data become available. This would allow a more complete, concentration-dependent description in terms of a system of coupled differential equations (Heinrich and Schuster, 1996; Alves and Savageau, 2000).

7.3 Comparison of model results with experimental observations

Table 8: Combinations of phospholipids tested by the Model validating the above allosteric interactions

Level of activation (predicted)	Level of activation (experimentally tested)	ATP level
AA+PC> AA+DAG	AA+PC> AA+DAG	High ATP
SM+AA<=AA	SM+AA<=AA	Low ATP
SM+AA>AA	SM+AA>AA	High ATP
SM+PA<SM	SM+PA<SM	Low ATP
SM+PA<SM	SM+PA<SM	High ATP
PA+AA	PA+AA	Low ATP

Legend: Experimental tests involved the addition of various phospholipids and assaying the phagosomal activation by phogocytosis of latex beads by murine phagosomes and light microscopy. Abbreviations: AA: Arachidonic acid, PC: Phosphatidylcholine, DAG: Diacylglycerol, SM: Sphingomyelin, PA: Phosphatidic acid

The model can successfully predict the effects of different lipids in combination, with respect to inhibitory or activating effects, on phagosomal actin assembly (Table 8). Further, We can test and extend the network topology modeled and predict effects for different concentrations of lipids or ATP. Moreover the predictions for the effects of adding various combinations of lipids were in good agreement with the experimental data (Table 8).
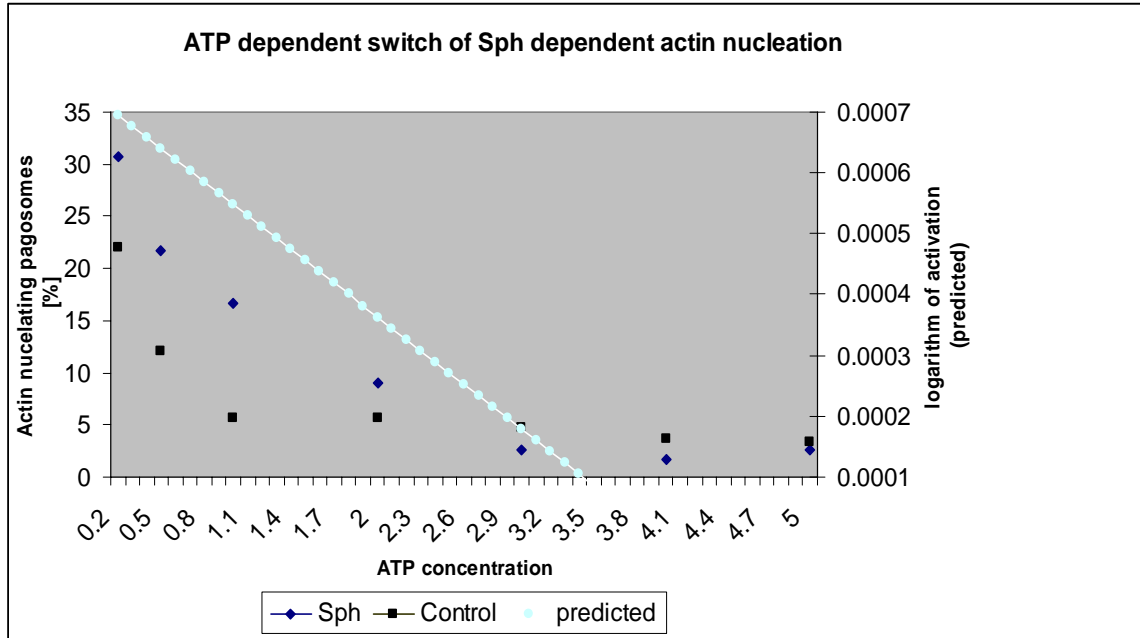
Figure 23: The figure shows the predicted and experimental ATP dependent switch of sphingosine dependent actin nucleation. The effect of sphingosine on actin nucleating phagosomes (%) is plotted against ATP concentration. Note that predicted activation is plotted in logarithmic scale and correctly estimates the switch at ATP concentration 3.05mM.

We extended the above model to predict activation/inhibition of actin assembly at any given ATP concentration. For a given lipid, the logarithm of the amount of activation/ inhibition) of actin nucleation is plotted against the ATP concentration and used to plot a graph, log (activation or inhibition by lipid y) = (slope* (concentration of ATP x)) + constant. The logarithm smoothes biases from extreme high or low values. This gives a reasonble prediction of the concentration of ATP (3.05mM) where sphingosine is neither activating nor inhibiting (Figure 23). The topology of the modelled network was also important; for example the allosteric reactions shown in Figure 23 were found to be necessary for reaching an agreement between predictions and the experimental data.

All model parameters (Table 7) were determined in many simulations to optimize the accuracy of prediction for single lipids, or combinations of lipids,

taking in to consideration the present experimental data, including the optimal concentration of individual phospholipids for their ability to stimulate (+) or inhibit (-) phagosomal actin assembly (Table 8). Further experimental data will help to model the different parameters more accurately.

Stepwise analysis of our program taking Sphingosine as an example:

Concentration of starting material phosphoinositide, sphingomyelin and PE is set to 200. Thus some amount (internal amount) of phospholipids is always formed. These phospholipids and concentrations were again chosen from different triple combinations of lipids and picked as they best simulated the effect of the internal lipids present in the network.

1. When 0.1mM of sphingosine (Sph) is put into the program the given concentration will be added to the internal pool of lipids present and increase the sphingosine concentration. The subsequent steps then follow for each reaction in the time step simulation:

2. Half of the Sph will be converted to sphingosine 1 phosphate (S1P) if the concentration of Sph is above the threshold level which is set to 20. The time step simulation thus models in a simplified, discrete way, the exponential decay of the metabolite given as a pulse to the lipid network. Similarly, the thresholds mimic in a simplified way a number of more complex effects such as limited diffusion and low enzymatic conversion rates at low concentrations

3. The reaction Sph to S1P is a reversible reaction. When S1P achieves the threshold concentration, half of the S1P will be converted again to Sph.

4. The concentration of specific lipids during the time step simulation will be influenced by additional network effects to simulate allosteric effects (e.g. from or on PKC). In the example, the effective lipid concentration of PA will rise (according to the concentration of Sph) starting from the existing

concentration of PA in the phagosomal membrane (bulk lipid concentrations-see above).

5. Corresponding concentrations of downstream and (in the case of reversible reactions) upstream lipids will be changed.

6. At each step the overall activation is calculated by summarizing all activating and inhibitory effects of the different lipids and adding this paramter to the total levels of activation or inhibition already calculated.

7. After the 20 time steps have been completed, the final value of activation is calculated by dividing the value for the total activation by the level of the control.

7.4 Topology tests: Allosteric interactions

Allosteric interactions were important in fine tuning of the outcome. Their importance was systematically tested in different simulations adding or removing specific allosteric interactions and testing how well the model could then predict the effect of adding individual lipids on the network. These tests gave the following results:

Allosteric interactions which play a role at high ATP are more important than those active at low ATP. PKC is included in the model and in accordance with experimental data collected so far, its interactions are more important at high ATP. Furthermore, the variables dagact and high_ act in the simulation play a role at high ATP. High_act (additional activation of PIP2 at high ATP) in particular seems to be more important as phospholipids PIP2, PA, PC and Sph (that is four out of 14 phospholipids) showed opposite effect on the system when high_act was set to 0. When *dagact* (stimulation of DAG kinase of PKC) was set to 0 the effect of DAG on the system was less and the lipid network behaviour was incorrectly predicted, in that it did not agree with the experimental data.

PartII: Modeling of the phospholipids network

7.5 Concluding Remarks: the relevance for *M.tuberculosis*

The analysis have provided sets the stage for an eventual understanding of how pathogens such as *M.tuberculosis* subvert the phagosomal signaling networks that regulate the key functions of phagosome actin assembly and the fusion with lysosomes, both of which are inhibited in infected macrophages; as a result of these inhibitions the pathogen grows within the phagosome. Although the experimental observations and the model have focused exclusively on the actin assembly process in their *in vitro* studies so far, in principle all phagosome functions for which one has an assay, including the fusion processes, can be subjected to the same approach that is used here for the actin assembly. Using these assays in conjunction with bioinformatic modeling, any 'virulent' factor isolated from a pathogen such as *M.tuberculosis* that could inhibit a particular phagosome function can be addressed with respect to how it affects the phagosomal membrane signaling networks.

8. Analytical and spatial model of phagosome lysosome fusion

8.1 Introduction to process of the phagosome lysosome fusion

De novo actin assembly on phagosome membrane is known to occur mainly on the cytoplasmic surface of membranes and as a requirement for its fusion with the lysosome (Kjeken et al., 2004). Identification of the mechanistic details of this crucial cell function has been hampered both by the complexity and rapidity of its action, and by the lack of an eukaryotic membrane model systems that are suitable for both *in vivo* and *in vitro* analyses. In all membrane systems examined so far, actin assembles on membranes in a manner that is quite different from the better understood microtubules. The later are nucleated within defined structures such as the perinuclear microtubule organizing center, and grow by addition of tubulin monomers to the end away from the nucleator. In contrast actin monomers are inserted at the membrane where the fast growing barbed or plus ends of the actin filaments are invariably located (Tilney, 1976), (Carlier, 1998). This type of formation might facilitate the transfer of organelle bound to actin binding protein (lysosomes) towards the actin nucleating organelle (phagosomes) (Kjeken et al., 2004).

Phogosomes are highly dynamic vesicles that are formed *de novo* by the cell and subsequently mature (Griffiths, 1996). Particles inducing phagocytosis induce rapid and massive actin assembly via signal transduction in different cell types, allowing phagosome enclosing the particle to be formed (Allen and Aderem, 1995; Caron and Hall, 1998; Greenberg et al., 1991; Reaven and Axline, 1973), subsequently the phagosome fuse with the lysosome. The acquired acid hydrolases and vacuolar ATPases, acidify the phago-lysosome lumen and facilitate the digestion and removal of the pathogen. Live pathogens such as *Mycobcterium tuberculosis* secrete inhibitory lipids and/ or proteins that are released into the phagosome that can block phagosomal membrane function

such as actin assembly and in turn fusion with lysosomes (Beatty and Russell, 2000; Clemens, 1997; Rhoades et al., 2003). Mycobacteria are serious causes of human disease. These microbes survive and grow inside phagosomes and block phagosomal membrane signalling processes (Russell, 2001). Many signalling molecules, in particular phosphoinositols, play a role in the processes of actin assembly and lysosomal fusion (Anes et al., 2003).The data has led to the proposal that one function of phagosomal actin filament assembly is to provide tracks for organelles such as lysosomes to move in a myosin dependent fashion towards the phagosome, thus facilitating fusion (Jahraus et al., 2001; Kjeken et al., 2004). Taking into consideration the above points, spatial modeling of actin polymerization and regulatory components involved in the process will be very interesting in order to understand the process of manipulation of the phagosome and its environment by pathogens.

Actin binding proteins can bind actin and phosphoinositides on the membrane simultaneously. This includes talin, vinculin and ezrin/radixin/meosin (ERM) proteins. They are candidates for involvement in actin nucleation on membranes (Bretscher, 1999; Gilmore and Burridge, 1996; Mangeat et al., 1999; Niggli et al., 1995). The ERM proteins are widely considered as mechanical linkers between the membrane and actin filaments (Algrain et al., 1993; Berryman et al., 1995; Bretscher, 1989; Hanzel et al., 1991). Ezrin/ meosin represent the minimal machinery that needs to be recruited by phagosomes from the cytoplasm in order for actin assembly to proceed (Defacque et al., 2000). The model simulates correctly the observed F-actin morphology on the phagosome membrane and a rapid searching behavior as an emergent phenomenon from the actin dynamics is represented in the model.

8.2 Description of the analytical model

Protein polymers in the cell assemble by different processes, here We discuss two (i) similar to dynamic instability (DI) (Mitchison and Kirschner,

1984a; Mitchison and Kirschner, 1984b) and (ii) Reversible polymerization (RP). RP is continuous competition of two processes, assembly and disassembly, where the monomer size controls the scale of the length fluctuations. In contrast, DI is, at the simplest level of description, a mechanism in which the polymer alternates between two distinct states of reversible polymerization. Though dynamic instability as defined in case of microtubules is not found in actin polymerization all actin binding proteins can (ABP) maintain two distinct states of polymerization and de-polymerization. Thus it is believed that both types of polymerization are observed in case of actin. Rapid cycles of actin polymerization are observed on phagosome membrane(Yam and Theriot, 2004). It is still not clear whether actin filaments play role in phagosome lysosome fusion and if it does is it an efficient way. To test its role in the fusion with the lysosome, here the effect of both (DI and RP) the possibilities of polymerization on the fusion in terms of time is tested. For both polymer types the average search time is computed.

Actin polymers are nucleated from the surface of spherical phagosome of radius R = 2 µm, they assemble and disassemble till they come into contact with a fix target (lysosome). The polymers are considered as rigid rods over distances of the order of the cell size, so the direction of the growth is radial and is fixed after the nucleation. For simplicity, the number of polymers is assumed to be constant, so that when one polymer shrinks to zero length, another re-nucleates and grows in a new (randomly chosen) direction. At the membrane RP will reflect instantaneously, while DI stops growing but waits until it has a catastrophe before shrinking. The average search time depends on the geometric parameters and on the polymerization parameters.

The F-actin polymerizes (p) and de-polymerizes (dp) on the surface of the phagosome with velocity 'v_p' µm/min and 'v_{dp}' µm/min for DI. The growing filament depolymerizes with the frequency 'f_{dp}' min^{-1} while growing and its rescue frequency is 'f_p' min^{-1}. The similar simple model for stiff, non interacting

polymers, growing in an infinite homogenous medium has been established for microtubules. The model makes use of only V_p μm/min, V_{dp} μm/min, f_p min^{-1}, and f_{dp} min^{-1} and does not require any assumption about the molecular mechanisms that determine them (Verde et al., 1992). As no molecular mechanisms are specified we could use the solution to actin polymerization found on phagosome membrane with modifications. The average velocity with which a given actin population grows, J is given by:

$$J= (f_p V_p - f_{dp} V_{dp}) / (f_{dp}+f_p) \text{---}(1)$$

It can be easily seen from equation (1) that when $f_p V_p > f_{dp} V_{dp}$ filament grows on average (refer to (Holy and Leibler, 1994) for more details). Whereas $f_p V_p < f_{dp} V_{dp}$ filaments do not grow on an average, they tend to disassemble all the way back to the phagosome. This gives rise to a steady state and has been shown to give a well defined distribution in the case of microtubule length (Verde et al., 1992). In the steady state length distribution is exponential with the average length d given by,

$$d = (V_p V_{dp)}/ (f_{dp} V_{dp} - f_p V_p) \text{---}(2)$$

Repeated cycles of actin assembly and disassembly are found on the phagosome membrane (this phenomenon will be addressed as flashing)(Yam and Theriot, 2004). Extending the model to our system of phagosome lysosome fusion with polymerization of actin on the phagosome membrane searching for the lysosome, we used the case when f_p tends to ($\rightarrow$) 0 as this gives the steady state. The filaments in this case do not grow on an average as $f_{dp} > f_p$ and will disassemble displaying flashing behavior. When $f_p \rightarrow$ 0, it follows from equation (2) d= da = V_p/f_{dp}.

RP evolve through the competition between assembly and disassembly; monomers are added at a rate r_p and are lost at a rate r_{dp}. The RP tip executes biased random walk, with a step size δ (0.004) equal to monomer size. Search time was found to be minimum at r_{off} = r_{on}, so the evolution of polymer is dominated by fluctuations rather than by drift.

To evaluate the role of actin polymerization and the significance of flashing on the fusion of lysosome with phagosome we calculated the search time and compared it to the time needed for the fusion of lysosome-phagosome (a) in the absence of actin assembly, (b) in constitutive presence of actin assembly and disassembly and (c) in the case of actin flashing. The search time is obtained as the sum of successful and unsuccessful events each with probability p and 1-p respectively. The probability i of signalling is 1 when actin assembly is constitutively (model b) present and otherwise i < 1 (model c).

$$T = pt_s + (1-p)p(t_s+t_u) + (1-p)^2p(t_s+2t_u) + \ldots\ldots\ldots$$

$$T = t_s + ((1-p)/p)t_u \text{ (Holy and Leibler, 1994) } \text{---------------------------}(3)$$

Where t_s is the time required for the successful events and t_u is the time required for unsuccessful events. If the target is small as in the present case then p<<1, so T~ t_u/p. Thus we need to estimate p and t_u. The probability p depends on two events, the polymer has to grow in the direction of the target and should become long enough to reach the target before it de-polymerizes completely. Thus p = qp*, where q is the probability of growing in the direction of the target and will be proportional to angular size of the target. As the phagosome is sphere and we assumed that 10 actin can polymerize in one degree. Thus q is calculated as 1/ 3600 for single polymer searching lysosome which is equal to 0.00028. p* is the probability of reaching length d_l before de-polymerizing completely. For DI, p* is clearly $e^{-dl/d}$ when fres → 0. For RP p* is δ/d_l when r_{on} = r_{off} = r. For n polymers searching for m lysosome the probability of successful events will be pnm. The duration of an unsuccessful search will be of an order of da/v for DI and R/rδ for RP. Thus

$$T_{DI} \sim (d_a e^{-dl/d}i)/ (qnmv) \text{ --}(4)$$

$$T_{RP} \sim (Rd_l)/(qr\delta) \text{ --}(5)$$

Though thee mathematical analysis of the system follows closely the approach of (Holy and Leibler, 1994) it turns out that the numeric simulations now applied to phagosomes now give new results.
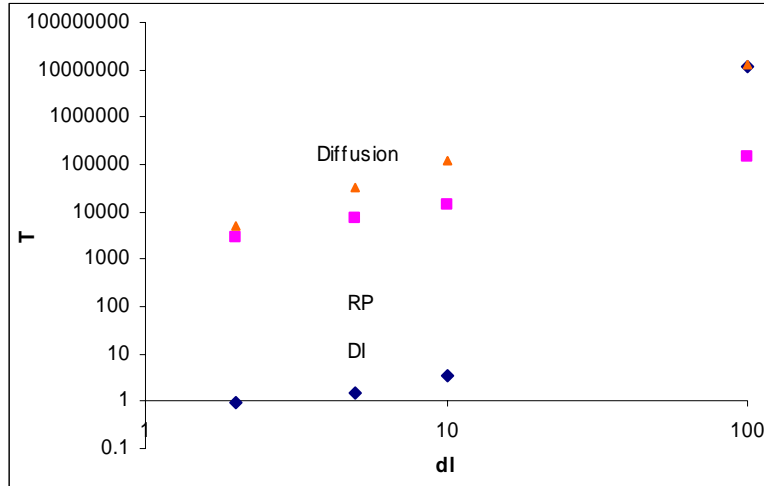
Figure 24: Average search time as a function of d_l to the (Nl=10) lysosomes for a search by 100 polymers. The search time required for RP are roughly 10^3 time more at i=0.5 than DI at lower d_l. Here we have f_{dp} = 2 min^{-1}, da=6 μm. For RP δ=0.004, r_{off} = r_{on}= $(v_p+v_{dp})/2δ$

The figure 24 shows that regarding phago-lysosome fusion as d_l, the distance between phagosome and lysosome increases the search time T increases too. Note that T_{DI} < T_{RP} roughly by the order of 10^3, for $d_l \sim d_a$. When d_l is large T_{DI} > T_{RP}. In the figure 24 the model c is depicted, the time difference between DI and RP are of the same order for model b, but the search time for model c (i<1) is less than model b (i=1). The phenomenon of flashing is clearly the characteristic of probability of signaling i and the frequency of de-polymerization f_{dp}.
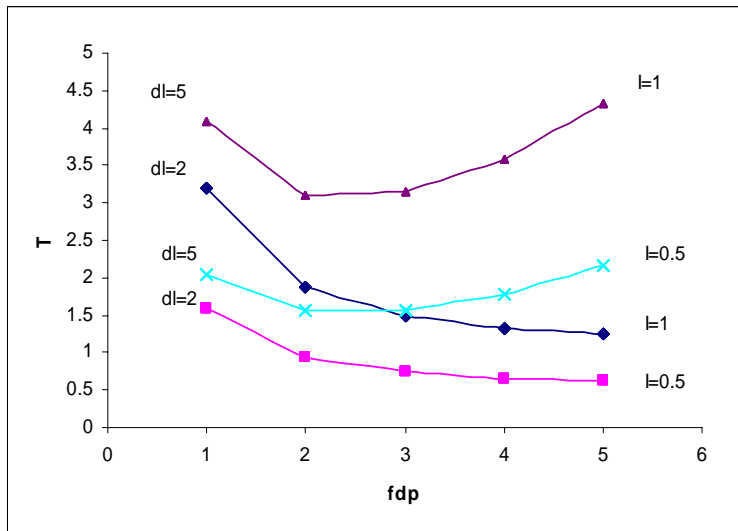
Figure 25: The plot of T_{DI} against f_{dp} shows that when i<1 the search time is reduced. Further at lower d_l search time T_{DI} reduces with f_{dp}.

The Figure 25 shows that as the frequency of de-polymerization increases the search time T decreases at lower d_l. f_{dp} corresponds to the frequency of flashing and at $d_l <= d_a$ search time decreases with f_{dp}. When d_l increases ($d_l > d_a$) the search time first decreases and then increases at higher f_{dp}. This is because at higher f_{dp} the probability p* of reaching the length d_l decreases. This leads to higher search times. This can be seen in following figure 24 where the average distances moved by the tip d_a, decreases as the function of f_{dp}.
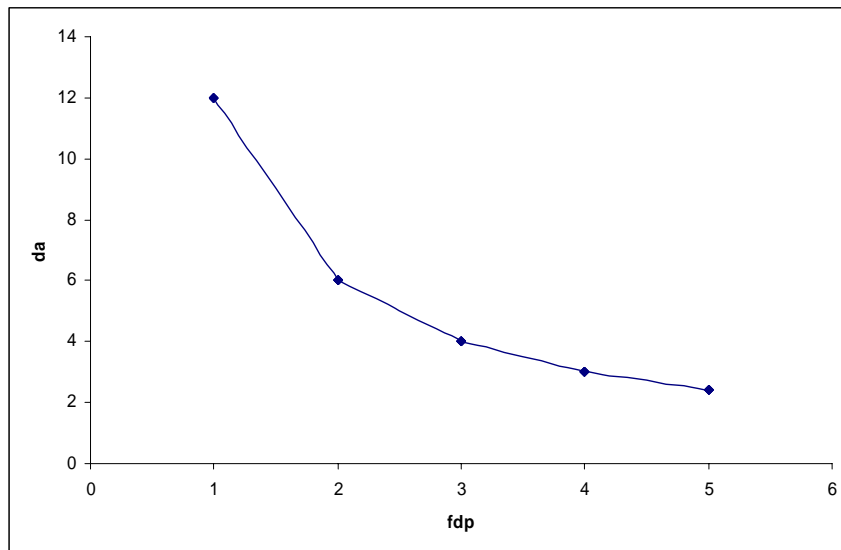

Figure 26: In the graph d_a is plotted against f_{dp} showing that as f_{dp} increases the average distance d_a moved by the tip decreases decreasing the probability of covering the distance d_l.

Thus as d_l increases search time T_{DI} also increases with increase in f_{dp} (Figure 25).
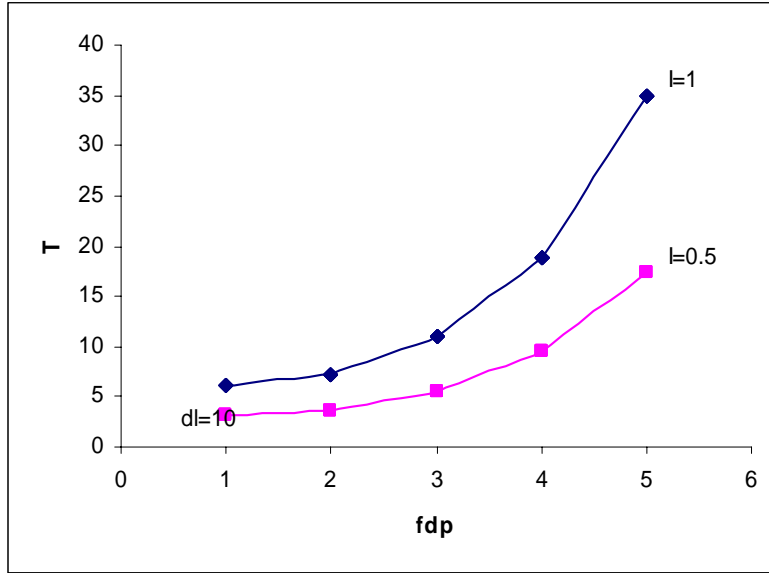
Figure 27: The plot of T_{DI} against f_{dp} at higher d_l shows that search time increases with the increase in the f_{dp} as the probability p^* of filament covering the distance d_l decreases.

We can then compare the time T_{DI} from the above results to the time necessary for the lysosome to diffuse to phagosome for fusion without actin (Figure 22). With the diffusion constant D = 0.01 $\mu m^2/min$, which is approximately greater by the order of 10^4 than the search time T_{DI} (when $d_l \sim d_a$) and by the order of 10^1 than the search time T_{RP}.

Thus actin dynamics on the phagosome membrane and intermittent signaling decreases the search time increasing the efficiency of the fusion. At an optimum DI parameters $d_a \sim d_l$ and $f_p \rightarrow 0$ the search time T_{DI} is less than in case of other two models. T_{RP} is less than time required to diffuse lysosome to phagosome. We can conclude that model b and c needs less search time than model a. Thus it is highly probable that the actin flashing observed on phagosome membrane is in search of lysosome in the cytosol and will definitely reduce the search time leading to quicker fusion.

8.3 Description of spatial model

The analytical model gave the concrete results on the general behavior, for example mechanism of actin polymerization, its importance in the fusion and optimum parameters ($da \sim dl$ and $f_p \rightarrow 0$) when search time is minimum. We next wanted to investigate dynamics of individual fusion events for this the spatial model was necessary.

Table 9: Parameters of the simulation.

Parameter description	Symbol	Value or range
Observation field		30 by 30 μm
Phagosome diameter		1 to 5 μm
Lysosome diameter		1 to 4 μm^2
Number of actin filaments	filno	2 to 8
Expected length of actin filament	Expactlen	4 to 25
Time steps for depolymerization	timesteps	4

The components of the model are positioned in a 30 by 30 μm square grid at the beginning of the simulation, which will be referred as the observation field that represents the cytosol. Actin monomers bound to ATP and profilin are distributed randomly in the observation field. The square dimensions are basically used to decide position of molecules at the beginning of simulation. The square dimensions do not inhibit any process, for example if lysosomes move outside the square they will appear on the other side. The position of actin monomers and all other components in the plane is decided by their co-ordinates. Thus for example the diameter of actin monomers is assumed to be 4 nm and its position is decided by the co-ordinates of the center of the circle. The sphere with diameter 4 μm represents the phagosome and is placed in the center. Four spheres with 2μm diameter represent lysosomes are placed randomly in the observation field. Thus this square mimics the part of the macrophage interior.

The position of the phagosome is fixed in the center. Lysosomes are constantly in Brownian motion.

The signal is generated randomly on the membrane of the phagosome. The signal can be generated by two ways: (i) by random generation and (ii) by continuous generation of the signal where the signal at a specific position increases the probability of the generation of a second signal closer to the first one. The analytical model lead us to select previous possibility explaining that in the cell a random generation of signals will be beneficial when the position of the lysosome in the cytosol is uncertain, thus it will increase the probability of finding the lysosome in the cytosol. The signal will decide the point at which polymerization of actin will start. One signal will lead to formation of only one F actin. However, actin monomers start accumulating from the neighboring area at the site of the signal induction. The actin length increases with velocity 0.2 µm/sec.

Actin tracker model implementation: F-actin grows randomly. If a F-actin filament hits the lysosome further polymerization of F actin and signal induction is stopped. The lysosome moves towards phagosomes in four steps along the F actin. F actin is depolymerized as the lysosome moves forward. If it does not find the lysosome till the filament length is equal to the optimum actin filament length, then they are depolymerized in four time steps. Depolymerized actin monomers are again distributed randomly in the square and are in turn bound to ATP and profilin. The time necessary to find certain number of lysosomes were analysed. New signals are formed if the lysosome is not found in the first cycle; actin nucleation is then initiated at a different place and in a different direction.

F actin can be formed from any point on spherical phagosome membrane upon signal induction. The direction of polymerization is also decided randomly. Interestingly, this increases the probability of finding the lysosome.

The main parameters that affect the probability of successful lysosome phagosome fusion are the actin length and number of F-actin filaments formed

(filno) divided by the number of signals. The actin filament length will be variable depending on the probability of binding to the lysosome (and myosin). The maximum length of F-actin that is formed before depolymerzation is a constant in the model and called as expected actin length (variable name expactlen). This decides the length achieved by F-actin in search of the lysosome, if the lysosome is not found when the length of F actin is equal to the expected actin length then the F actin is depolymerized. Biologically this is a critical parameter as actin polymerization is an energetically expensive process. It will be a waste of energy for the cells to form F actin in wrong direction with respect to lysosome position. The formation of an optimum number of F-actin filaments is also necessary for optimal conservation of energy.

8.4 Comparison of model results with experimental observations

Model considerations: The model is developed to simulate the formation of F-actin on the phagosome membrane and further to study its role in the fusion of phagosome and lysosome (Figure 28). The model and results were checked and developed in the progaming language C on the Windows workstation by Juilee Thakar. To actually visualize dynamics an openGL front end was written by Chunguang Liang, the output is shown in figure 28.
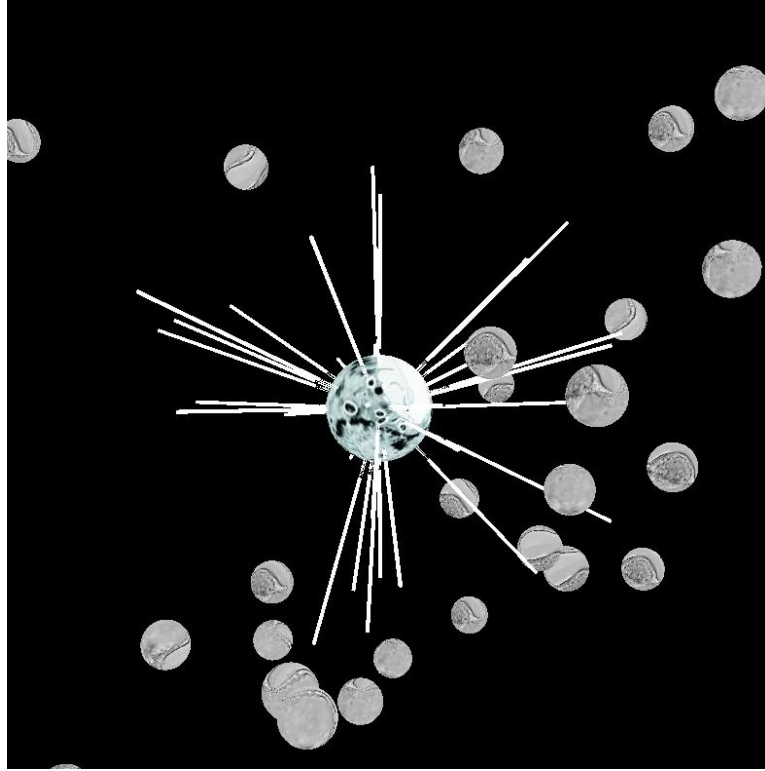
(A)
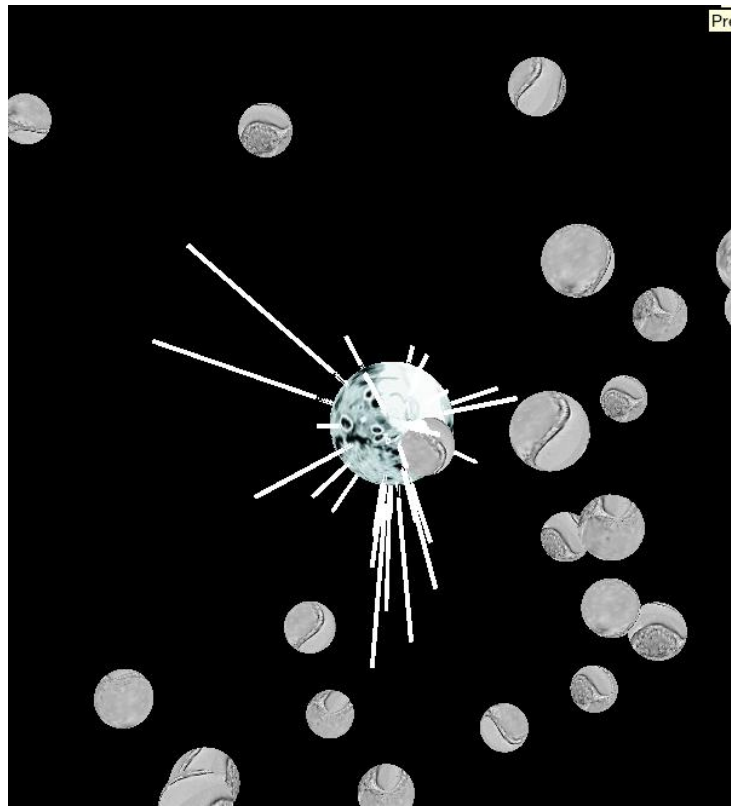
(B)

Figure 28: The figure A and B shows the actin polymers emanating from the phagosome (bigger sphere) which is positioned in the center. The smaller spheres are lysosomes distributed randomly in the space. In figure A we can see how F-actin searches for the lysosome and figure B shows the fusion process of phagosome and lysosome.

The simple model takes into consideration all fundamental steps in actin polymerization to generate the co-ordinates of lysosome, phagosome and F-actin. Actin is implicated in membrane fusion, but the precise mechanisms remain unclear. It has been shown using electron microscopy and biochemistry that membrane organelles catalyze the *de novo* assembly of F-actin that then facilitates the fusion between latex bead phagosome and a mixture of early and late endocytic organelles. Early endosomes fail to nucleate actin polymer on the membrane. Thus these experimental results leads us to build a hypothesis that actin assembled by the phagosome provide tracks for fusion with organelles such as the lysosome to move towards them via membrane bound myosins (Anes et al., 2003; Defacque et al., 2000; Jahraus et al., 2001; Kjeken et al., 2004). This is implemented as a sequential model. Studies have been performed to understand the role of actin in fusion. Actin nucleation takes place only on late endosomes/ phagosome which s dependent on membranes (Kjeken et al., 2004). Other evidence based assumptions listed below are made for simplicity of the model.

1. All lysosomes are bound to actin binding proteins such as myosin. Note that myosin inhibitors such as 2, 3-butanedione monoxine inhibit the fusion (Kjeken et al., 2004).

2. Depolymerization of F.actin takes place in four steps.

3. Signal induction represents the activation of the Ezrin/ moesin machinery that is the minimal requirement for actin assembly to proceed as mentioned above (Defacque et al., 2000).

4. Signal induction is random on the phagosome membrane and there is an optimum number of signals induced.

5. There is an optimum length of F-actin necessary for efficient fusion.

Parameter variation: All parameters tested are summarized in Table 9. The factors that affect phagosome-lysosome fusion are number of actin filaments, the length of actin filaments and the speed of the lysosome in the cytosol. Further Phagosomes and lysosome can be modeled in varying dimensions (Phagosome: 1 to 5 μm diameter, Lysosome: 1 to 4 μm diameter). These dimensions were approximated from experimental observations.
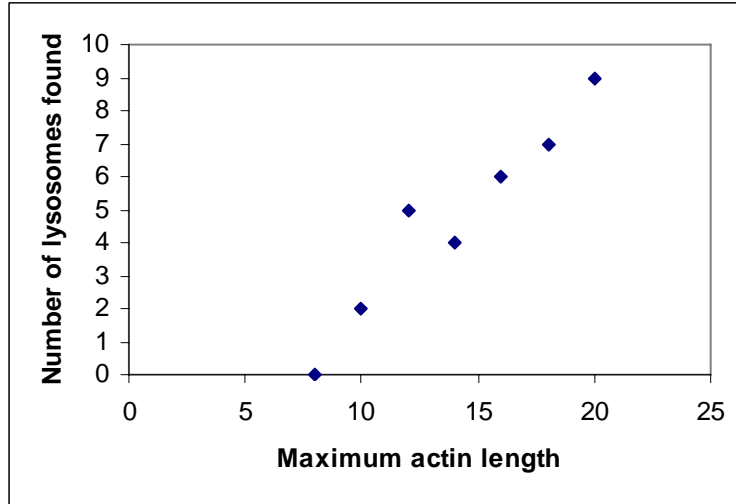
Figure 29: The plot shows that number of lysosomes found increases as expected actin length goes on increasing.

In the simulation we varied the values for the optimum length of the actin filament (4 μm to 25 μm), number of signals (actin filament number) and phagosome as well as lysosome dimensions. In each case we measured the time necessary for an actin filament to find the lysosome. At the beginning of the program the phagosome is placed in the center and lysosomes are placed randomly in the observation field. When the phagosome diameter was 4μm and the lysosome diameter was 2μm lysosome and phagosome fusion was achieved in minimum time. Thus these dimensions were used for further analysis. Signals were then randomly generated on the phagosome membrane. We then varied the number of signal and found that four signals are necessary to find the lysosome. Experimental observations show that around 50 or more actin polymers are

formed on phagosome membrane during active state (when signals are induced). Thus we used 50 actin polymers. The figure 29 shows that as expected actin length increases number of lysosomes found also increases. At the site of generation of signals nucleation of F-actin takes place, leading to polymerization. In reality, phagosomes have been observed to move, for the convenience of modeling we fixed our coordinate system within a phagosome.

The effect of the distance between lysosome and phagosome on the time required to find the ysosome was studied next keeping the actin length constant.
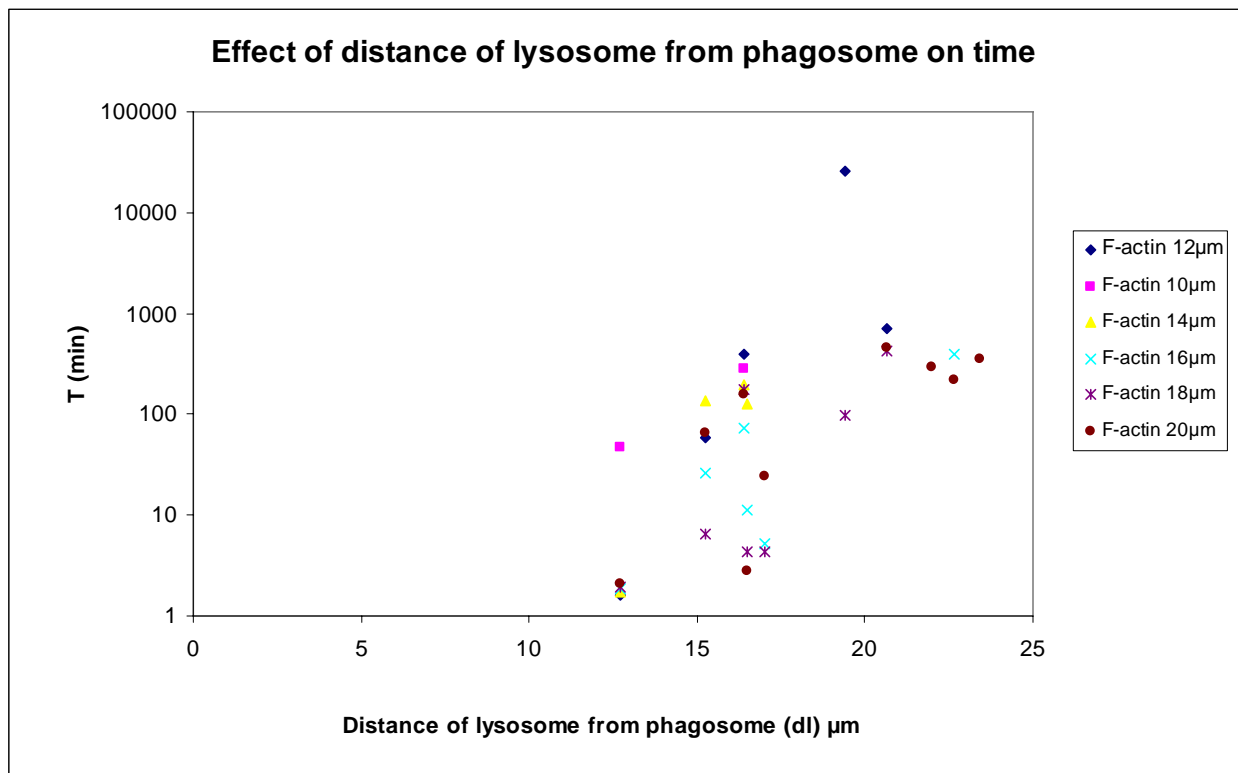
Figure 30: Effect of distance between phagosome and lysosome on the fusion time is plotted at different F-actin lengths. The plot shows that the relation is linear till F-actin length 12 and then follows the saturation curve.

The graph shows that the time increases as the distance between phagosome and lysosome increases. At an actin length 12 the time increases linearly with the distance between lysosome and phagosome. For an actin length 20, time increases linearly till the distance 20µm and then stabilizes.

It has been observed that within about 20 seconds there is the actin "blinking" of an actin plaque, and then it disappears again, next the plaque occurs within long time (minutes) at a completely different place(Yam and Theriot, 2004). However, the myosin tracking takes place within a second so that any phagosome-lysosome fusion process is difficult to observe. In our model the formation of actin polymers at random places followed by de-polymerization and re-polymerization at completely random (different) places agrees well with the observations.

8.5 Conclusions

Here in this chapter we have developed a model to study the collective behavior of lysosome, phagosome and actin in the cytosol. Although the situation studied is very simple compared with that in a cell, we take in to consideration fundamental characteristics of each component in the cytosol of a macrophage to develop a global model of lysosome-phagosome fusion. Further from these models emanate basic mechanisms followed by the cell to develop energetically less expensive means for the fusion of two organelles. We take into consideration the searching behavior of the actin filament necessary in order to find the lysosome in the cytosol, the thickness (bushy and individual morphology) and the length of the actin filaments.

Many processes in nature can be explained by continuous stochastic interactions at the molecular level. To describe and understand these processes in qualitative terms, there is a need for new tools allowing the analysis of collective behavior of organelles and molecules. The study of microtubule and actin filament dynamics is of central importance to the organization of cytoskeleton. Actin filaments have diverse functions, for example: cell motility, formation of contractile ring, stress fibers etc. The organization of actin filaments in all cases is varied, and plays a central role in its function.

In the analytical model three possibilities of actin polymerization are checked. The search time for the dynamic instability model (DI) is less by the order of 10^5 than in absence of actin polymers. The search time is calculated based on the probabilities. Similar approach has been successfully implemented in case of chriomosome searching by microtubules. This clearly shows that actin polymers play essential role in fusion of phagosome-lysosome. In DI the equilibrium is when fp$\rightarrow$ 0 (fp approaching zero) and the search time is minimum when da~dl (da approaximately equal to dl).

In vivo actin polymerization and fusion takes place in seconds, which make it highly impossible to understand the system. Analytical model strongly supported the importance of actin polymers during fusion. The model is developed based on probability hence we developed the simulation where we could actually change the actin length, phagosome dimentions, etc to see the effect of individual components on fusion. We found that the number of lysosomes found increases linearly with increasing actin length except for actin length 12 and 14. In the next plot (Figure 30) it is clear that the relation between time and the distance between lysosome-phagosome takes saturation curve as actin length increases above 12µm. Phagosome and lysosome dimensions also affected their fusion probability. The optimum diameter of the phagosome was found in the simulations to be 4µm and lysosomes were 2µm.

Some models are already published for the polymerization of actin monomers. These models take into consideration the role of actin dynamics in protrusion associated with cell motility or endocytosis (Bottino and Fauci, 1998; Carlier et al., 2003; Mogilner and Edelstein-Keshet, 2002). Often those parameters are dependent on diffusion, viscocity and velocity of protrusion of the cell. These are often difficult to estimate in living cells and tend to make predictions that differ substantially from *in vivo* systems (Mogilner and Edelstein-Keshet, 2002). Microscopic studies contribute to spatial and temporal organization of actin filaments and motility due to actin myosin complex formation (Nakayama et al.,

1998; Ponti et al., 2003; Verkhovsky et al., 2003). The theoretical model by Kruse and Julicher, 2003 (Kruse and Julicher, 2003) describe bundle formation due to cross linking molecules in polar filaments. Experimental evidence also proves the role of cross linking molecules in actin filament organisation, futher they also comment on persistence of membrane bound cross linked bundles (Tilney et al., 2003). Counter-ion is also shown to affect actin filament organization (Yu and Carlsson, 2003). We use here a system biology approach to study the behavior of many components of the cell.

Though the situation studied in this simulation model is simple the assumptions are testable. Further distinct steps in the fusion of phagosome and lysosome are described and modeled in the simulations. Inhibitors can be studied blocking particular steps. As a further extension, we can also estimate the percentage of signals inhibited by *M. tuberculosis,* and the percentage of signals necessary for efficient fusion of phagosome and lysosome.

Despite recent advances, there remain a number of puzzling questions about actin polymerization on phagosome membranes and its role in fusion with the lysosome. First, because the searching behavior is highly directional, actin filaments must be assembled in a directional manner and at a precise time and place. It is unclear whether an Arp2/3-like process drives F-actin assembly or if a completely separate mechanism is responsible. Whether filament turnover is due to a highly active actin-depolymerizing factor or to unusual polymerization kinetics is also uncertain. How myosins are anchored to the underlying cytoskeleton and how their motor activity is regulated are areas for further investigation. Here in this model we try to study some of these questions. We develop a completely new approach to study the phagosomal system in the light of the limited kinetic data available. In this model we have made for the first time an attempt to simulate searching behavior of actin filament and comment on the best strategy for the cell to get rid of an intracellular pathogen. Further we could also observe different patterns according to the intensity of the signal induction

and compare it with microscopic observations. The input parameters show specific effects, and the results are testable. The time step simulation established model specific parameters which can be correlated to observations.

Our analytical and spatial resolution model of the phagosome shows as emergent phenomena (i) an active searching for the lysosome based on an actin tracker model (ii) a stepwise process of actin polymerization and lysosome fusion. Blocking of critical steps will allow testing of the model and is predicted to be implicated in the survival of pathogens. Model step length, number of signals involved in actin polymerization and detailed parameters are given for further experimental testing. Experimental observations confirm predicted lengths of actin filaments, phagosome and lysosome size, velocity of actin polymerizations and time course (Defacque et al., 2000; Griffiths, 1996; Kjeken et al., 2004).

RESULTS PART III

Host pathogen interplay exemplified by Bordetella:
Heuristic approach

Results and chapter discussion

9. Immune responses to *Bordetellae* species.

9.1 Introduction to *Bordetellae* pathology

The two components of immune system 'innate' and 'adaptive' immunity are essential for the protection against infection. Invasion of pathogens activate innate immune responses, a response to foreign material that help in eliminating or slowing the spread of the pathogen. The effector mechanisms used by the host to control infection include production of pro-inflammatory cytokines and chemokines, recruitment of inflammatory cells to the site of infection and activation of lymphocytes and natural killer cells. If the pathogen persists, antigen-specific adaptive immune responses are activated. The adaptive immunity can be divided into humoral and cellular responses. Humoral immunity refers to the antibody-mediated responses against pathogen, while cellullar immunity involves activation of macrophages and NK cells and the production of various cytokines in response to antigen.

Bacteria have also evolved strategies to counteract host defense. These strategies include evasion of humoral and cellular immunity by antigenic variation, interference with antigen processing or presentation, and subversion of phagocytosis and killing by cells of the innate immune system (Mills and Boyd). Many pathogens achieve this by increasing the production of anti-inflammatory or immunosuppressive responses, which normally function to control or terminate the protective effector immune responses of the host (Mills, 2004). This interplay between pathogen and host results in a complex dynamical behavior whose ultimate outcome is persistent disease or recovery.

The Bordetellae are examples of pathogens which persist in mammals proving their successful strategies to overcome host defenses. Members of the *Bordetella* genus are small, gram-negative coccobacilli that colonize the respiratory tracts of their hosts, adhering to ciliated epithelia and spreading via

respiratory droplets. Three species *B. bronchiseptica*, *B. parapertussis* and *B. pertussis* are very closely related, but have different host ranges and cause different diseases in their host. *B. bronchiseptica* infects wild and domesticated animals including leopards, koala bears, cows, sheep, dogs, cats, rabbits, rats and mice. Symptoms of infection range from mild to severe, typified by atrophic rhinitis in pigs and kennel cough in dogs. *B. bronchiseptica* infections can be persistent and last for the life of the animal. *B. pertussis* is highly infectious in humans and is endemic in much of the world. The pertussis (whooping cough) disease is acute, with severe coughing illness that can progress to become spasmodic, and in some cases leads to death. *B. parapertussis* also infects humans and causes a coughing illness nearly indistinguishable from that of *B. pertussis* except for the lack of lymphocytosis associated with pertussis toxin that is expressed only by the latter.

It appears likely that *B. pertussis* and *B. parapertussis* independently adapted from *B. bronchiseptica*-like progenitors, perhaps present in domesticated animals, to become human pathogens (Preston et al., 2004). Although the human pathogens do not cause persistent infection, like *B. bronchiseptica*, the rapid spread of these organisms within relatively dense and mobile human populations is apparently sufficient to allow transient infections to circulate on an ongoing basis and to persist within a population. Here we study differences in these highly similar species in order to better understand the immune responses of the host to these organisms with the following questions in mind: What are the regulatory hot spots, the most important virulence factors and immune mechanisms that determine the dynamical outcome of the Bordetella infection? What are the common elements and differences in strategies used by different Bordetellae?

The genomes of *B. pertussis* and *B. parapertussis* are substantially smaller than those of *B. bronchiseptica*, due in part to the loss of numerous sizable multigenic regions. For example, *B. pertussis* has apparently lost a genomic

region of at least 22 Kb that is required for O-antigen assembly in both *B. bronchiseptica* and *B. parapertussis*. Interestingly, there appears to be a number of other genes that are present in all three but are expressed in only a subset of these species (see Table 10). These include genes expressed by only B. bronchiseptica, such as those encoding the type III secretion system (TTSS) and flagella, and those expressed by only B. pertussis, including those encoding pertussis toxin and its accessory genes as well as a number of genes designated vrg (virulence repressed genes) . The overwhelming majority of known virulence factors are similarly expressed by all of the bordetellae, including adhesins (filamentous hemagglutinin, pertactin and fimbria) or toxins (adenylate cyclase toxin, dermonecrotic toxin and tracheal cytotoxin).

Table 10: Virulence factor of three closely related Bordetella species:

	B. pertussis	*B. parapertussis*	*B. bronchiseptica*
Adhesins	P	P	P
Filamentous hemagglutinin	P	P	P
Pertactin	P	P	P
Fimbriae	P	P	P
Tracheal colonization factor	P	A	A
Serum resistance protein (Brk)	P	?	?
Toxins			
Pertussis toxin	**P**	**A**	**A**
Adenylate cyclase toxin	P	P	P
Dermonecrotic toxin	P	P	P
Tracheal cytotoxin (only non protein)	P	P	P
LPS/ Endotoxin	**P**	**P + O-Ag**	**P + O-Ag**
Secretion system			
TTSS	**A**	**?**	**P**

P: present A: absent

Bordetellae are mostly classified as external pathogens but some times they have been observed live in macrophages. Infection by any of the three

species induces innate and adaptive responses including cellular and humoral immunity. *M. musculus* infection models have been established with the bordetellae and used extensively in the analysis of various parameters of infection, reproducing those of human disease in most regards. Colonization is very efficient, and all three Bordetellae increase in numbers rapidly over the first few days postinoculation. The inflammatory infiltrate, leukocytosis, gradual generation of antibody and T cell responses and delayed bacterial clearance all mimic aspects of human disease. Cytokines produced during the course of infection and their regulation by bacterial virulence factors play an essential role in shaping the immune response. Thus cytokines, antibodies, inflammatory responses are important in pathology (Mattoo et al., 2001).

The immune responses to the pathogen include the sequence of processes that are activated directly by the sensing of bacteria or by a preceding signal. In the following study we started with the available data from the literature and experiments to construct a network model of these processes. The network is further developed by filling information by making educated guess in case of instances where the direct information is unavailable. The network then is used as a substrate for a discrete dynamic simulation. The results of the simulation are validated by comparison with experimental results and then used for predictions. As there is much less info on the infection time course in *B. parapertussis* we will focus on *B. bronchiseptica* and *B. pertussis*.

9.2 Network model of immune responses to *Bordetellae*

9.2.1 Comparison of immune responses to *B. bronchiseptica* and *B. pertussis*

The chief mode of Bordetella transmission is by aerosols. After entry, bacteria undergo a phase change to activate the BvgA/S two component system

and a set of virulence genes, leading to the expression of adhesins and toxins (Table 10).

The first immune mechanisms that respond to bacteria are Toll like receptor 4 (TLR4) mediated signaling and the alternative complement pathway. All three species express lipopolyssacharide (LPS) that is recognized by TLR4 receptors on macrophages and dendritic cells. TLR4 receptor mediated signaling in response to pathogen-associated-molecular-patterns activates transcription factors to induce formation of cytokines in different cells. Some of these cytokines, for example IL-1, 6, TNF-α, β are pro-inflammatory and recruit polymorphonuclear leukocytes (PMNs) at the site of infection (Mann et al., 2004). PMNs activated by sensing of complement-coated bacteria initiate phagocytosis. PMNs also produce cytokines which in turn recruit more PMNs. Naïve dendritic cells (DCs) present at the site of infection are also activated in response to bacteria.

DCs then present antigen to naïve T cells (these DCs are also called antigen presenting cells). APCs then produce set of cytokines which lead to differentiation of T0 cells into Th1 cells (for example IL12) or into Th2 cells (for example, IL 4, IL10). We will denote the cytokines inducing differentiation of T0 cells to Th1 (Th2) cells and cytokines produced in turn by Th1 (Th2) cells as Th1 (Th2) related cytokines. These cytokines are mutually inhibitory, i.e. Th1 (Th2) related cytokines inhibit the production and function of Th2 (Th1) related cytokines. Thus the balance between Th1 and Th2 related cytokines play an important role in the immune response.

Th2 cells activate B cells, which produce antibodies against those antigens presented by APCs. Opsonization by complement fixing antibodies produced by antigen-stimulated B cells leads to the activation of the classical complement pathway. Activated PMNs express Fc receptors which recognize the Fc region of antibodies bound to antigens. Thus adaptive immunity enables new mechanisms of PMN activation and phagocytosis (Pishko et al., 2004).

Th1 cells produce a set of cytokines, IFN-γ, TNF-β, IL2 which activate resident macrophages to phagocytose bacteria. Pro-inflammatory cytokines and Th1 related cytokines also attract more macrophages by chemotaxis, which then phagocytose bacteria. Indeed, both in *B. bronchiseptica* and *B. pertussis* recovery from the infection is associated with the development of pathogen specific Th1 cells (Mills et al., 1993; Ryan et al., 1997) and these cells play critical role in clearance of the bacteria (Mahon et al., 1997; Mills et al., 1993; Mills et al., 1998).

Bacteria

Pathogen sensing

Alternative complement pathway

Classical complement pathway

TLR4 signaling

Epithelial cells

Complement

Ag-Ab complex

Signaling to attract PMNs

Pro-inflammatory cytokines (IL-1,6, TNF-a,b)

Recruited PMNs

complement/ complement receptor signaling

Binding to antigen

FC receptor signaling

Production of more cytokines

Activated phagocytic cells

Other antibodies

Complement fixing antibodies IgG, IgM

IFN-g signaling

Macrophages

Inhibition by anti-inflammatory cytokines

Antibody production

T$_H$1 cells

T0 cells

T$_H$2 cells

B cell stimulation

B cells

IFN-g, TNF-b, IL2

Cytokines inducing differentiation of T0 cells to TH1 cells

Cytokines inducing differentiation of T0 cells to TH2 cells

IL-4,5,6,13

Clonal expansion

Th1 related cytokines

Th2 related cytokines

Active PMNs phagocytose bacteria

Recognition using MHC 2

IL-12

IL-4

Signaling to attract dendritic cells

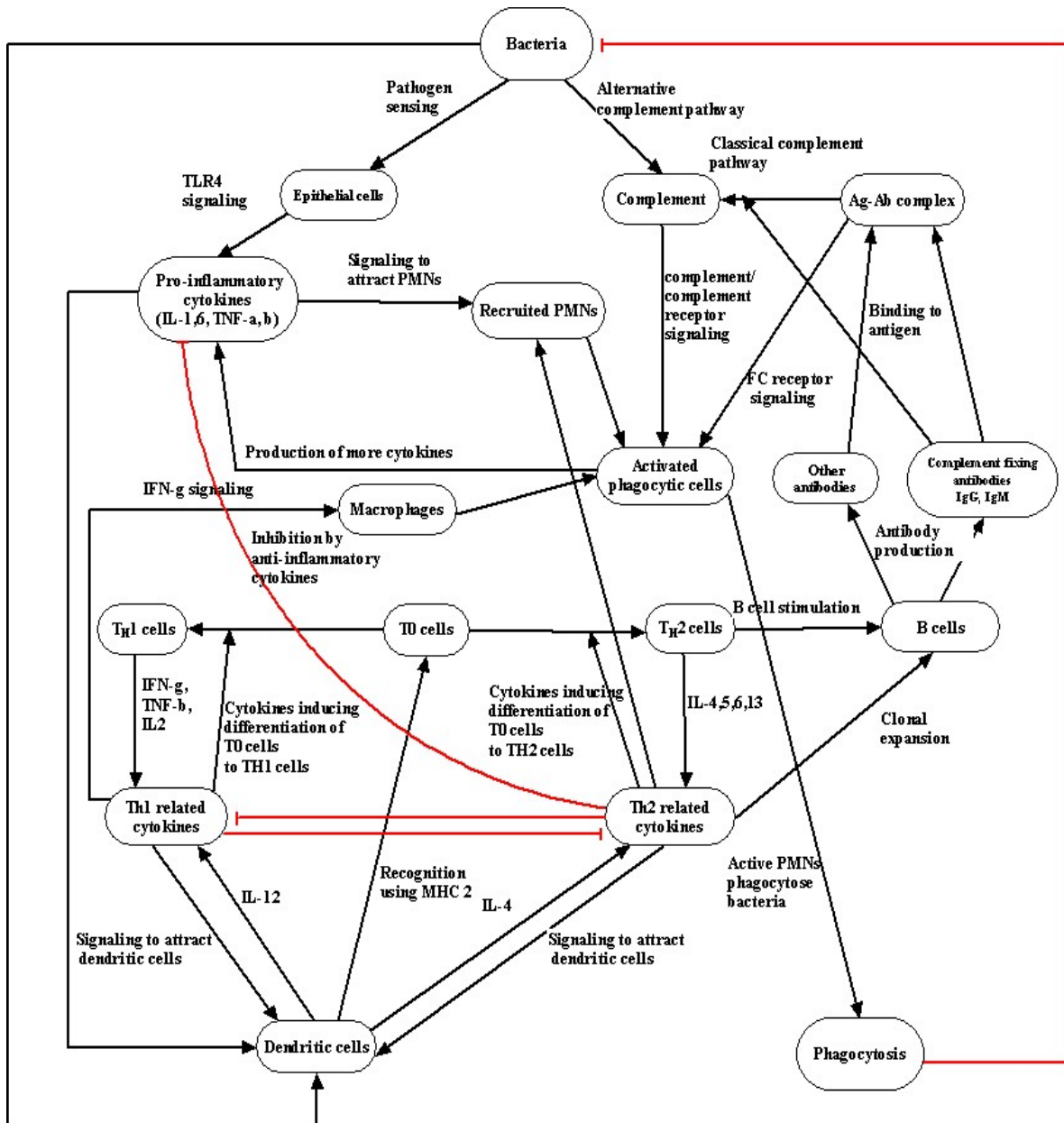Signaling to attract dendritic cells

Dendritic cells

Phagocytosis

Figure 31: The consensus network of immunological steps and processes activated upon invasion by Bordetella species. In the network nodes denote immunological steps connected by edges.

Not all interactions and processes shown in this consensus picture (Figure 31) are active at the same time, thus we need to complete this static picture with information on the time course of the infection.

The time course of immune responses can be divided into three stages: innate (*B. bronchiseptica*: 0 to 7 days, *B. pertussis*: 0 to 7 days), Th2 responses leading to the generation of antibodies (*B. bronchiseptica*: 7 to 28 days, *B. pertussis*: 7 to 14 days) and Th1 responses leading to clearance (*B. bronchiseptica* : 28 – 70 days, *B. pertussis*: 15 to 28 days) (Figure 32).
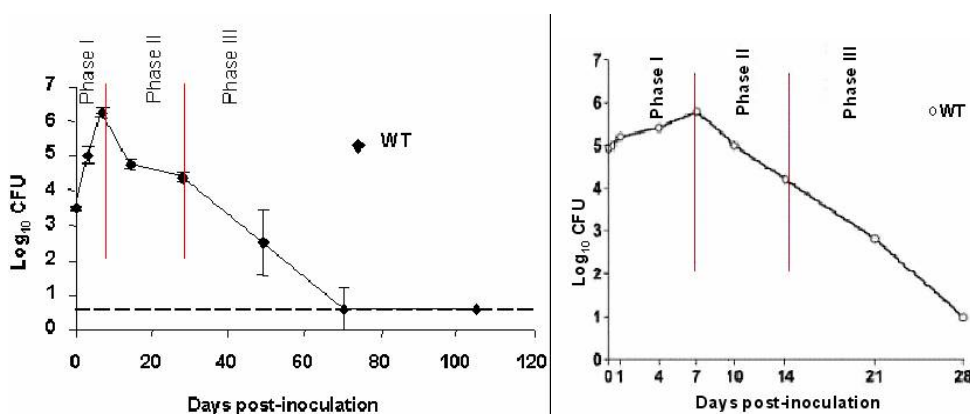

Figure 32: Time course of the infection showing three phases in the course of infection of (A) B. bronchiseptica (B) B. pertussis(Byrne et al., 2004). phase I: Innate immune responses, phase II: Activation of Th2 related responses and inhibition of Th1 related responses and phase III: Commencement of Th1 related responses and clearance.

9.2.2 Specific virulence mechanisms of *B. bronchiseptica* and *B. pertussis*

B. bronchiseptica and *B. pertussis* share high degree of genotypic and phenotypic relatedness which facilitates comparative studies of pathogenesis. In BALB/c mice unlike *B. pertussis* infections of humans, *B. bronchiseptica* typically

persists in upper respiratory tracts of its hosts. *B. bronchiseptica* infections are often asymptomatic whereas *B. pertussis* causes acute disease. The comparative studies of two strains *B. bronchiseptica* RB50 and *B. pertussis* Tohoma I show that RB50 grows to higher numbers in the nasal cavity and persists there indefinitely. Tohama I, in contrast, grows to higher numbers in lungs but is cleared from all sites by day 50. Histological examination of respiratory tract tissue shows that RB50 induces considerably greater lung pathology than Tohama I, mostly due to infiltration of neutrophils. Vigorous antibody response to RB50 has been observed compared to Tohama I (Harvill et al., 1999). Thus these and many more differences can be attributed to following specific virulence mechanisms.

During the early innate responses, LPS is recognized by host receptors. The structure of LPS is different in these species, containing a complex trissacharide in *B. pertussis*, a trissacharide plus an O-Ag in *B. bronchiseptica* and altered trissacharide plus O-Ag in *B. parapertussis*. O-Ag of *B. bronchiseptica* causes the inhibition (or significantly reduced activation) of alternate complement pathway (Burns et al., 2003). BrkA protein confers resistance to classical complement dependent killing in *B. pertussis*, however they are sensitive to alternative complement dependent killing (Harvill et al., 1999). Early recruitment of PMNs is inhibited in the presence of pertussis toxin and thus PMNs activation and antibody mediated phagocytosis is delayed.*B. bronchiseptica* has a type III secretion apparatus (TTSS). TTSS has also been observed to induce apoptosis in PMNs (Yuk et al., 2000), dead PMNs further produce more pro-inflammatory cytokines giving positive feedback.

Both pathogens have evolved a number of strategies to circumvent adaptive immune responses (Mills, 2001) leading to severe suppression of antigen specific Th1 responses during the acute phase of infection (McGuirk et al., 1998).

TTSS inhibits NFkB, a transcription factor with essential role in cytokine production, affecting Th1 /Th2 ratio. TTSS specifically inhibits the generation of

IFN-g by splenocytes on day 7, thus inhibits the differentiation of naïve T cells into Th1 cells. IFN-g is shown to facilitate clearance unlike IL-10 which is necessary for activation of Th2 responses. TTSS leads to the shift in the balance towards Th2 cells as IL-10 producing splenocytes are generated before IFN-g producing splenocytes

B. pertussis also has developed similar but more subtle mechanisms for the suppression of Th1 related responses. IL-10 is produced in early stages through TLR4 signalling giving peak at 24 hours (Higgins et al., 2003). Filamentous hemagglutinin (FHA) (McGuirk et al., 2002) (figure 33) and Adenylate Cyclase toxin (Ross et al., 2004) in association with LPS stimulates IL-10 production by dendritic cells and macrophages and promotes development of Tr1 and Th2 cells. Thus earlier peak of IL-10 transiently inhibits IL-12 and Th1 responses and promotes development of Tr1 and Th2 cells (Higgins et al., 2003). Tr1 cells have been shown to suppress *B. pertussis* specific Th1 responses *in vitro* and *in vivo*, thus Tr1 cells may represent invasion strategy by pathogen to subvert Th1 responses. They might also play a role in limiting immunopathology in the lungs (McGuirk et al., 2002). Later increased recruitment of Natural killer (NK) is observed which might be because of presence of persistent pathogen. NK cells stimulate IFN-g secretion by activating IL-12 and IL-23 production by dendritic cells, this shifts the balance from Th2 responses to Th1 responses(Byrne et al., 2004).

9.2.3 Specific time course of the infection and immune responses in *B. bronchiseptica* and *B. pertussis*

The network consists of nodes and two types of directed edges. Nodes represent immunologically significant steps in the cascade and the edges describe the relation between nodes. Incoming arrows describe the activation (⟶) / inhibition (⊣) of the node. In some cases the relation described by the arrows/edges are the immunological processes activating the next step for

example the incoming edge to the node TH2 cells from T0 cells describes the process of differentiation from T0 cells to Th2 cells. The arrow anchoring the edge describes that such process is induced by the node from which this arrow leaves.

After the bacterial invasion due to recognition of the virulence factors innate immune responses are activated in first 7 days. On 7th day the bacterial number reach the peak in both species, followed by the decline. Epithelial cells lining the lungs are the first cells to sense pathogens leading to TLR4 signaling inducing pro-inflammatory cytokines this takes place in first 24 hours. Neutrophil infiltration then reaches its peak between 10 to 14 days in *B. pertussis* whereas in *B. bronchiseptic*, earlier recruitment is observed during first 7 days starting at 12 hours. As mentioned previously TTSS induces apoptosis of PMNs inducing higher amounts of PICs and in turn increase PMNs recruitment till 3rd day (Figure 33A,B). Two times DC infiltration is observed in *B. pertussis* during 4 to 7 days and 15 to 21 days. TH2 cells are observed in *B. bronchiseptica* between 7 to 28 days (Figure 34A), because of the inhibition of Th1RC production by TTSS. As Th1RCs are also inhibited till 14 days by FHA/ACT (Figure 34B), first DC infiltrate leads to differentiation to TH2 cells during 7 to 14 days. TH2RC inhibits the recruitment of PMNs in *B. bronchiseptica* resulting in delayed phagocytosis. TH2 cells activated B cells followed by antigen specific antibody production. These responses lead to the decrease in the bacterial number thus the concentrations of virulence factors is decreased. We also assumed that the virulence factors undergo chemical decay. This leads to the shift in balance from TH2 cells to Th1 cells during 15 to 35 days in 28 to 70 (Figure 37A) and *B. pertussis* (Figure 37B) days in *B. bronchiseptica* . NK cells are known to reach a peak on 15th day in *B. pertussis* , which produce large amount of IFNg assisting the shift in T cell subtypes. Th1RC signaling further recruits more macrophages and PMNs leading to Ab/ complement mediated phagocytosis and clearance.

B. bronchiseptica usually grows to higher numbers in nasal cavity and lungs (Harvill et al., 1999). TLR4 signalling is necessary to limit growth of *B. bronchiseptica* but not of *B. pertussis* . LPS of *B. bronchiseptica* is more stimulatory than *B. pertussis* LPS, resulting in higher cytokines and greater pathology due to large number of neutrophil recruitment in case of *B. bronchiseptica* (Harvill et al., 2000). Thus in phase I of *B. bronchiseptica* greater pathology and higher concentration of bacteria is observed whereas in phase II the PMNs recruitment is inhibited by Th2RC which will result in maintaining the higher number of bacteria, this can be the reason for extended phase II and phase III in *B. bronchiseptica* .

(A)
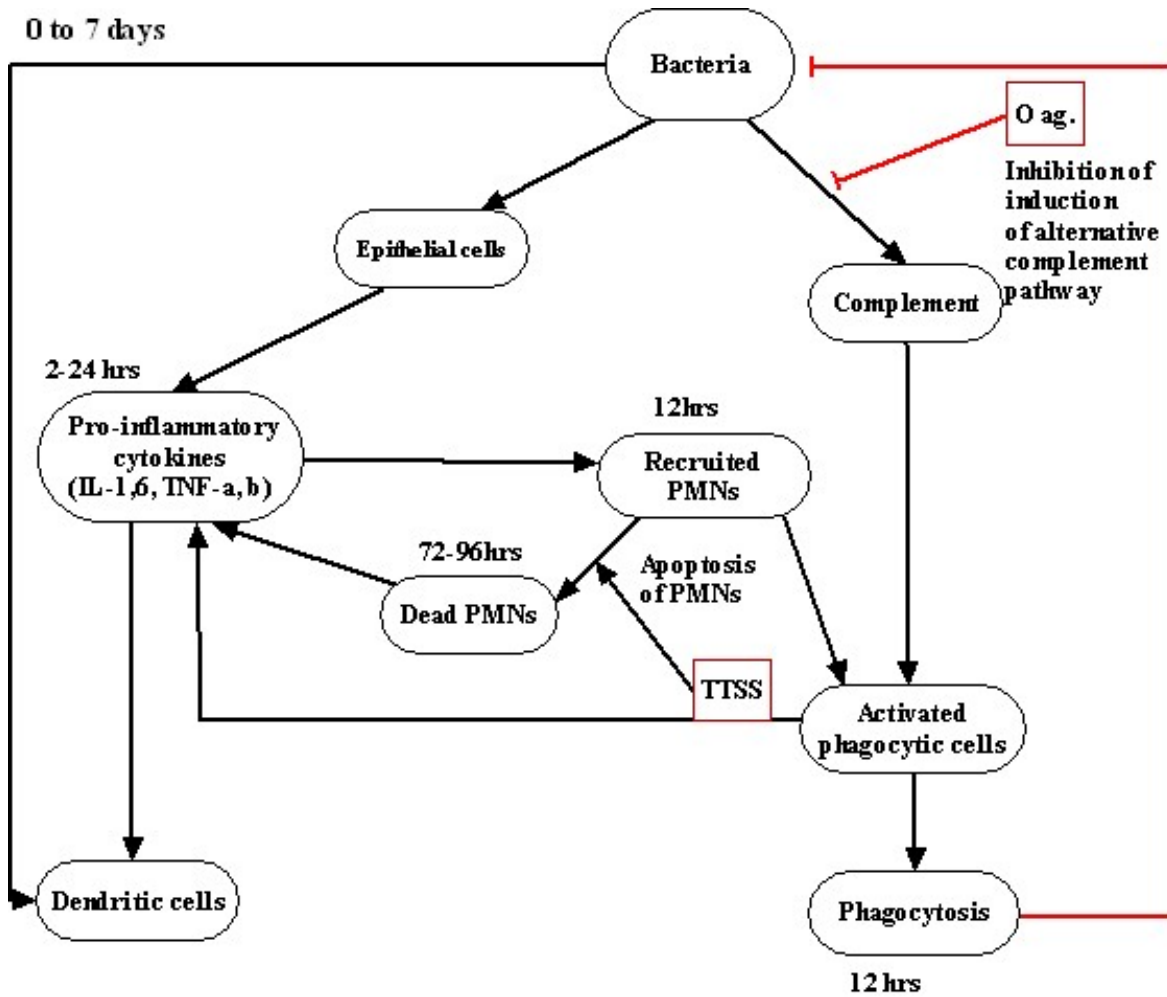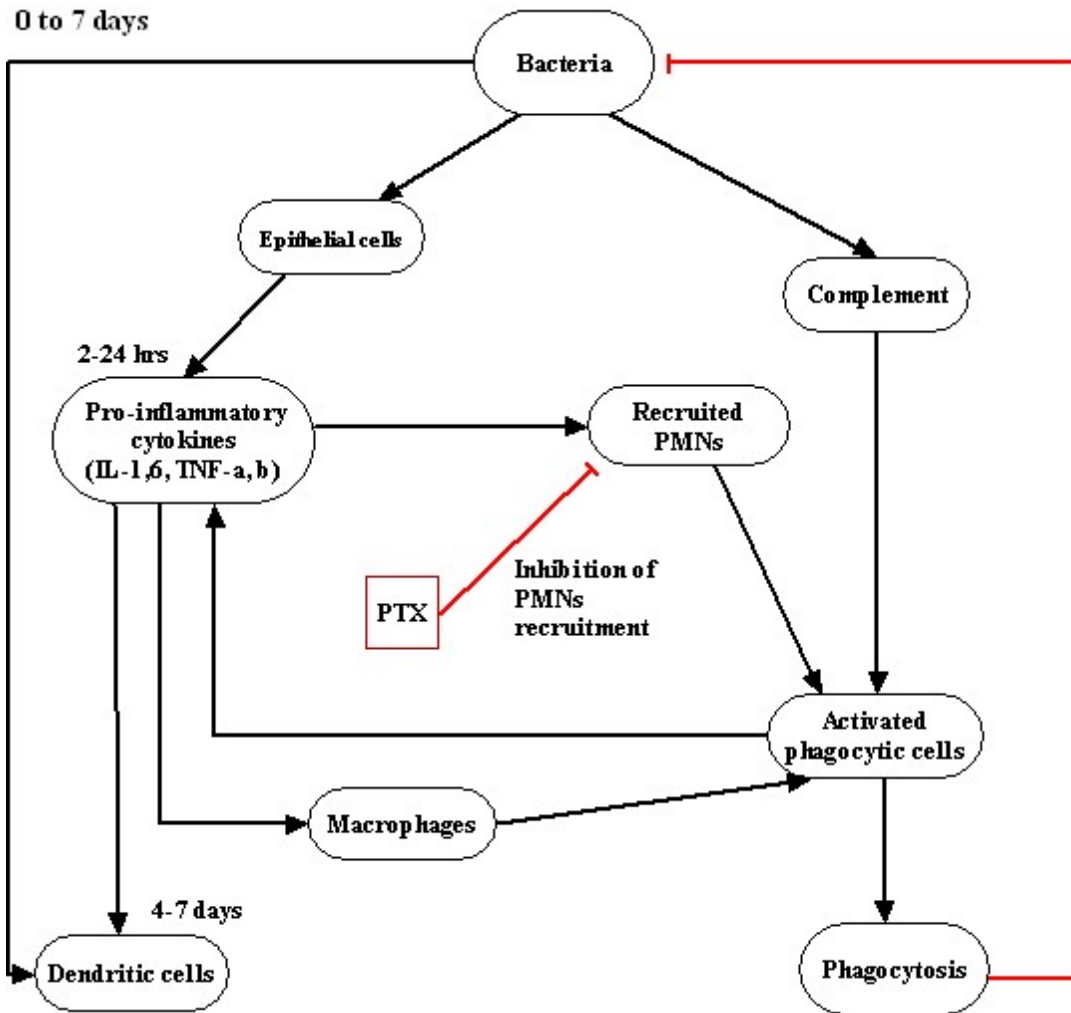
(B)

Figure 35: Innate immune responses leading to activation of dendritic cells, phagocytic cells and pro-inflammatory cytokines. (0 to 7 days in B. bronchiseptica and B. pertussis) A) Phase I of B. bronchiseptica B) Phase I of B. pertussis depicting innate immune responses to the bacterial invasion.

7 to 28 days

(A)
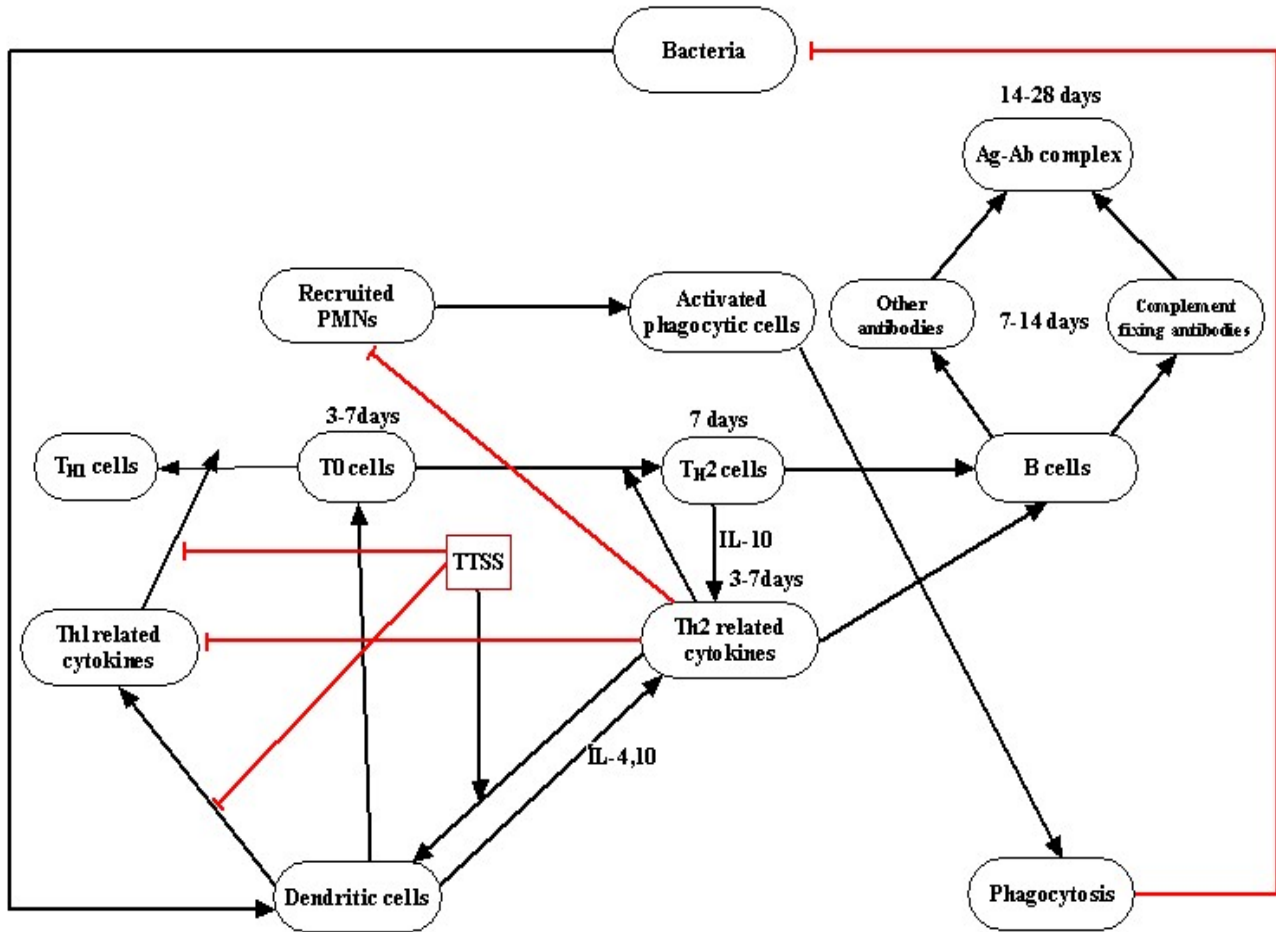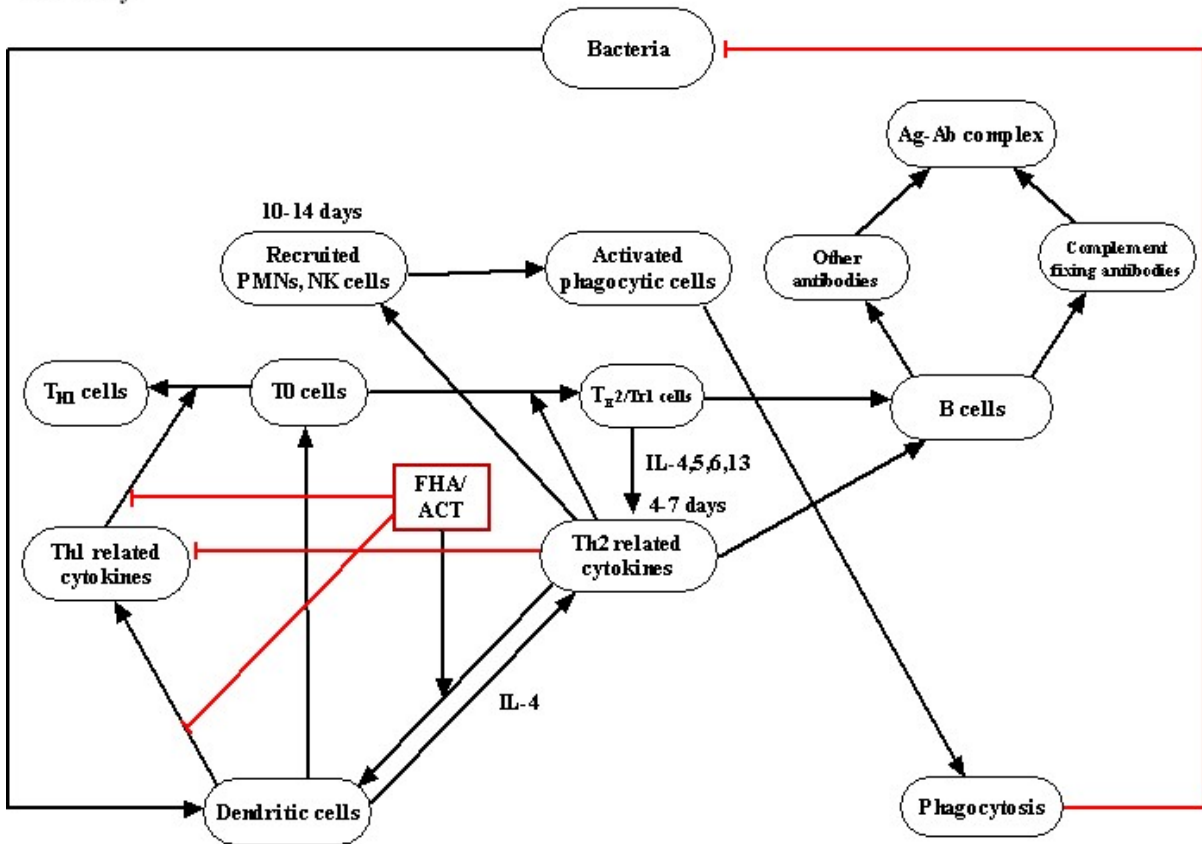
(B)

Figure 36: A) Phase II of B. bronchiseptica B) Phase II of B. pertussis depicting Th2 related responses.

28-70 days
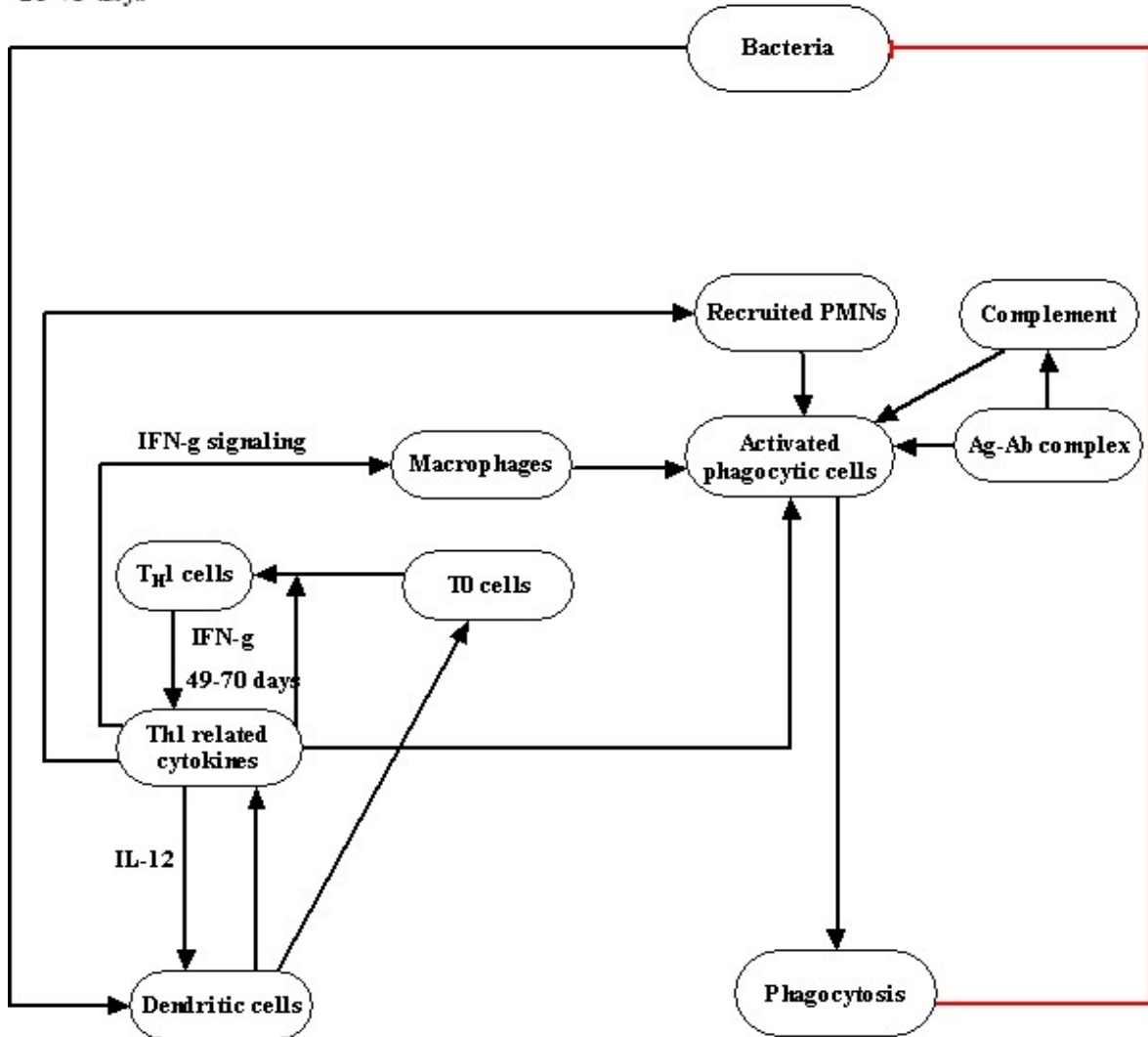
(A)
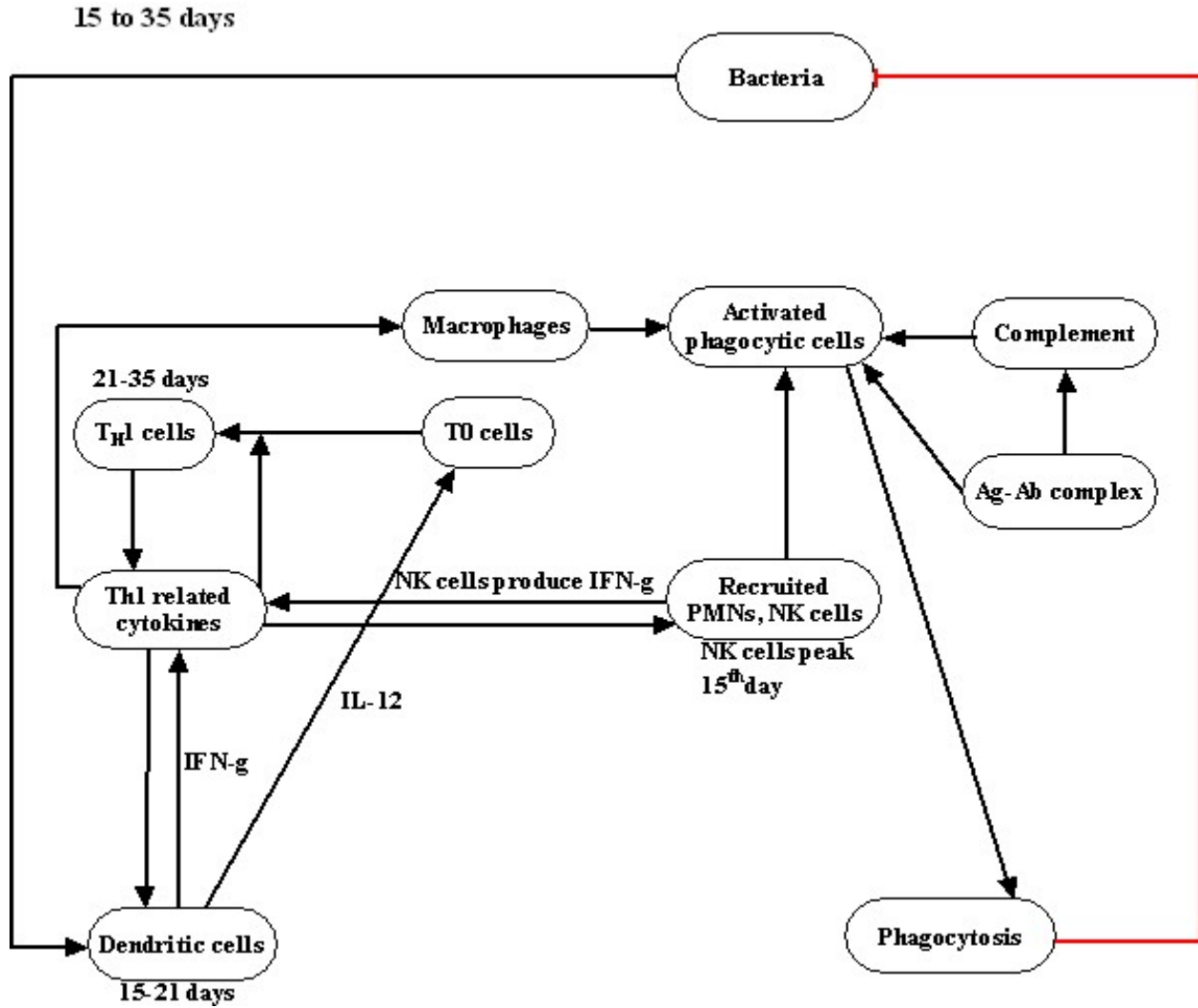
(B)

Figure 37: A) Phase III of B. bronchiseptica B) Phase III of B. pertussis depicting Th1 related responses.

9.3 Dynamic model

Each node has two states 1 and 0. The states of the node can change in time according to the Boolean function that describes the node. The Boolean function of the node is written as a statement with logical operators "AND","OR","NOT" which describe the inputs to the node.

There are total 18 nodes common in *B. bronchiseptica* and *B. pertussis*; 2 species specific nodes in *B. bronchiseptica* (O Ag and TTSS) and 1 (Pertussis Toxin (PTX) and filamentous hemagluttinin, Adenylate cyclase toxin (FHA/ACT)) in *B.*

pertussis. The Boolean interaction functions are constructed from interactions in nodes described in the network (Figure 35, 36 and 37). The main network (Figure 31) was divided into figure 35, 36 and 37 according to time course described in section 9.2.2.

All processes are described here by a step function so that each node has a specific activator and inhibitor. One node can activate or inhibit another node only if they are connected by an edge and have value 1 or 0 respectively. The inhibitors are assumed to be dominant over the activators.

The states of the nodes evolve in discrete time steps. The state of next time step of a node is decided by the Boolean function F of the nodes that are connected by edges to the node under examination. If X and X1 are connected by an edge and X1[t-1] is the state of the node X1 at time t-1, then the state of X at time t in most of the cases is written as X[t]=F(X[t-1]). In remaining cases this time delay was removed to mimic the results from literature, such possibilities are described in detail later. This defines a discrete dynamical system whose iteration determines the evolution of the state of nodes. For example, antigen-antibody complexes are formed by antibodies (either complement-fixing or complement-independent) bind to the surface of bacteria, thus

Ag-Ab complex[t] =Bacteria[t-1] AND (Other Ab[t-1] OR Complement fixing Ab[t-1])

Similarly relation between all nodes is written using Boolean function (Table 11).

Table 11: Boolean functions used in the model

Node	Boolean Function
(Common in *B. bronchiseptica* and *B. pertussis*)	

Bacteria	Bacteria $[t]=NOT \sum_{i=0}^{4}$ AND Phagocytosis[t-i] AND Bacteria[t-1]
Epithelial cells	Epithelial cells[t] =bacteria[t-1]
Complement	Complement[t] =Bacteria[t-1] OR (Ag-Ab complex[t-1] AND Complement fixing Ab[t-1])
Ag-Ab complex	Ag-Ab complex[t] =Bacteria[t-1] AND (Other Ab[t-1] OR Complement fixing Ab[t-1])
Complement fixing Ab	Complement fixing Ab[t] = B cells[t-1] OR Complement fixing Ab[t-1]
Other Ab	Other Ab[t] =B cells[t-1] or Other Ab[t-1]
B cells (Antibody producing)	B cells[t] =TH2 Cells[t-1]
Pro-inflamatory cytokines (PIC)	PIC[t] =Bacteria[t-1] OR ActPhagCells [t-1] AND NOT Th2RC [t-1] AND NOT PIC[t-decayt]
Th1 related cytokines (Th1RC)	Th1RC[t] =(TH1 cells[t-1] OR (DC[t-1] AND T0cells[t-1])) AND NOT Th2RC [t-1] AND NOT Th1RC[t-decayt]
Th2 related cytokines (Th2RC)	Th2RC [t]=(TH2 cells[t-1] OR (DC[t-1] AND T0cells[t-1])) AND NOT Th1RC [t-1] AND NOT Th2RC [t-decayt]
Recruited PMNs	Recruited PMNs[t] = PIC [t-1]
Activated phagocytic cells (ActPhagCells)	ActPhagCells[t] = (Recruited PMNs[t] AND (Complement[t-1] OR Ag-Ab complex[t-1])) OR macrophages[t-1]
Macrophages	Macrophages[t] =PIC [t-1] OR Th1RC[t-1]
T0 cells	T0 cells[t] =DC[t-1]
TH1 cells	TH1 cells[t] =DC[t-1] AND T0cells[t-1] AND Th1RC [t-1]
TH2 cells	TH2 cells[t] =DC[t-1] AND T0cells[t-1] AND Th2RC [t-1]
Dentritic cells (DC)	DC [t]= Th1RC[t-1] OR Th2RC[t-1] OR PIC[t-1] OR bacteria[t-1]
Phgocytosis	Phgocytosis[t] = (ActPhagCells [t] OR Macrophages[t-1]) and Bacteria[t-1]
(B. bronchiseptica specific description)	
TTSS	TTSS[t]=Bacteria[t] AND NOT TTSS[t-decayt]

OAg	OAg[t]= Bacteria[t] AND NOT OAg[t-decayt]
Dead PMNs	Dead PMNs[t]= Recruited PMNs[t-1] AND TTSS[t-1]
TH1 cells	TH1 cells[t-1]= DC[t-1] AND (T0cells[t-1] AND Th1RC[t-1]) AND NOT TTSS[t-1]
Th1 related cytokines (Th1RC)	Th1RC[t] =(TH1 cells[t-1] OR (DC[t-1] AND T0cells[t-1])) AND NOT Th2RC [t-1] AND NOT TTSS[t-1] AND NOT Th1RC[t-decayt]
Th2 related cytokines (Th2RC)	Th2RC [t]=(TH2 cells[t-1] OR (DC[t-1] AND T0cells[t-1]) OR TTSS[t-1]) AND NOT Th1RC [t-1] AND NOT Th2RC[t-decayt]
Complement	Complement[t-1] =Bacteria[t-1] OR (Ag-Ab complex[t-1] AND Complement fixing Ab[t-1]) AND NOT OAg[t-1]
(B. pertussis specific description)	
Pertussis toxin (PTX)	PTX[t]= Bacteria[t] AND NOT PTX[t-decayt]
FHA/ACT	FHA/ACT[t]= Bacteria[t] AND NOT FHA/ACT[t-decayt]
Recruited PMNs	Recruited PMNs[t] = PIC [t-1] AND NOT PTX[t-1]
TH1 cells	TH1 cells[t-1]= DC[t-1] AND (T0cells[t-1] AND Th1RC[t-1]) AND NOT FHA/ACT[t-1]
Th1 related cytokines (Th1RC)	Th1RC[t] =(TH1 cells[t-1] OR (DC[t-1] AND T0cells[t-1])) AND NOT Th2RC [t-1] AND NOT FHA/ACT [t-1] AND NOT Th1RC[t-decayt]
Th2 related cytokines (Th2RC)	Th2RC [t]=(TH2 cells[t-1] OR (DC[t-1] AND T0cells[t-1]) OR FHA/ACT [t-1]) AND NOT Th1RC [t-1] AND NOT Th2RC[t-decayt]

In *B. bronchiseptica* and in *B. pertussis*, based on the experimental results we included two more conditions that control the states of cytokines and toxins: As cytokines and toxins are not everlasting components we included decay of these components. Cytokines node in the model is divided in to Th1 related cytokines (Th1RC), Th2 related cytokines (Th2RC) and Pro-inflammatory cytokines (PIC). Anti-inflammatory cytokines is the subset of Th2 related cytokines. Considering the time scale for which cytokines are detectable during the infection PIC decay

rate (decayt=3 time steps) is greater than Th1 and Th2 related cytokines. In other words PIC will be removed (degraded) if it is present for 3 continuous time steps and its reappearance will depend on the next activation signal. Dynamic simulation of this system guided us to another condition: Th1RC decay rate (decayt=7 time steps) should be greater than Th2RC (decayt=12 time steps) resulting in the tight association between clearance of bacteria and activation of antigen specific Th1 responses as observed during the course of infection. Thus the resulting conditions are,

PIC[t] =Bacteria[t-1] OR ActPhagCells [t-1] AND NOT Th2RC [t-1] AND NOT PIC[t-decayt]

Th1RC[t] =(TH1 cells[t-1] OR (DC[t-1] AND T0cells[t-1])) AND NOT Th2RC [t-1] AND NOT Th1RC[t-decayt]

Th2RC [t]=(TH2 cells[t-1] OR (DC[t-1] AND T0cells[t-1])) AND NOT Th1RC [t-1] AND NOT Th2RC [t-decayt]

Similarly antigens 'O Ag' (decayt = 3 time steps), 'TTSS' (decayt = 12 time steps), 'PTX' (decayt = 3 time steps) and 'FHA/ACT' (decayt = 12 time steps) also decay after continuous presence of antigen for specified number of time steps. These time intervals were decided according to the known role of antigens from literature in the particular phase and the time interval of the phase in the simulation. We will correlate the time intervals to the days of infection by analyzing the time required for the each immunological process.Thus the resulting conditions are,

OAg[t]= Bacteria[t] AND NOT OAg[t-decayt]
TTSS[t]=Bacteria[t] AND NOT TTSS[t-decayt]
PTX[t]= Bacteria[t] AND NOT PTX[t-decayt]
FHA/ACT[t]= Bacteria[t] AND NOT FHA/ACT[t-decayt]

As phagocytosis in the first phase (during innate immunity) is not sufficient for the clearance of bacteria (that is why adaptive immunity is

activated and clearance of *Bordetellae* needs three phases) we modified the condition so that the phagocytosis is effective in clearing only when it takes place

$$\text{Bacteria } [t] = (\text{NOT} \sum_{i=0}^{4} \text{AND Phagocytosis}[t\text{-}i]) \text{AND Bacteria}[t\text{-}1]$$

continuously for five time steps. Thus the resulting condition is,

The $\sum\limits_{i=0}^{4}$ depicts that the present (i=0) as well as past four (i>0) states of

phagocytosis decides the present state (presence (1) or absence (0)) of Bacteria at time t.

In the presence of antibodies and/ or complement recruited PMNs are activated instantaneously which then phygocytose the bacteria. Thus there is no time delay between recruitment of PMNs, its activation and phagocytosis by PMNs (table 11).

9.4 Systemic effects of deletions

The initial states of all nodes are 0, except the state of node "Bacteria".

Wild type

The resulting model succeeded in reproducing a time course similar to that is observed (see section 9.2.2 and figure 32) during the infection in the dynamic simulation,

- Innate immune responses leading to activation of dendritic cells, phagocytic cells and pro-inflammatory cytokines. (two time steps)
- Activation of antigen specific Th2 responses and inhibition Th1 responses. (12 time steps)

- Activation of antigen specific Th1 responses leading to recovery of the infection and clearance of bacteria. (9 time steps in *B. pertussis* and 11 time steps in *B. bronchiseptica*)

When bacteria are present pro-inflammatory cytokines are produced and alternative complementary pathway is activated in *B. pertussis*. O antigen of *B. bronchiseptica* inhibits alternative complementary pathway. Pertussis toxin inhibits recruitment of PMNs in response to PIC. At third time step Th2 related cytokines are produced, TTSS in *B. bronchiseptica* and FHA/ACT in *B. pertussis* inhibits Th1 related cytokines. Thus presence of Th2RC activates differentiation of naïve T cells to Th2 cells which in turn activate antibody production by B cells. At time step 10 in *B. pertussis* and 12 in *B. bronchiseptica* Th1RC is produced leading to activation of macrophages, released inhibition of PIC leading to clearance of bacteria at time step 24 and 23 respectively (Figure 38A(I) ,B(I)). We have to note that the time scale of the dynamic model does not correspond to the one in experimentations. Specific processes will need different duration in different hosts. Comparison with the experimentally observed time course (Figure 32) also shows that observed quantitative differences can not be reproduced in present qualitative model.

For the evaluation of the model we deleted some components and analyzed the outcome. Comparison of these deletions with experimentally studied mutants (references are given at respective places) proved the reliability of the model regarding its topology.

9.4.1 Systemic effects of deletions and comparison with experimental observations

(A)   (B)

Figure 38: Comparison of patterns of key nodes in (A) B. bronchiseptica and (B) B. pertussis in following cases i) Wild type ii) O Ag deletion / pertussis toxin deletion iii) TTSS deletion / FHA/ACT deletion iv) B cell deletion v) naïve T cell deletion vi) treatment with antibodies prior to infection.

Effect of individual components was tested by deletion of the component in the simulation. We compared the following responses,

1. The Time step at which bacteria were cleared which can be correlated to the number of days infection persists in the host.

147

2. Length and the shape of the plateau of recruited PMNs as sign of lethality or virulence of the infection.

3. Complement activation

Deletion of virulence factor O antigen:

The membrane distal repeated carbohydrate structure of LPS is O-Ag. The genes of wbm locus are required for the assembly of O-Ag in *B. bronchiseptica*. *B. pertussis* lacks these genes and thus a number of characteristics associated with O-Ag in other organisms. The O antigen mutant (Δwbm) in *B. bronchiseptica* is sensitive to complement mediated killing. The mutant has shown no defect in colonization of trachea and lung. It is interesting that Δwbm mutation does not cause significant change in the course of infection in *B. bronchiseptica* and *B. pertussis* naturally lacks this gene(Burns et al., 2003). Deletion of O Ag in our dynamic simulation (Figure 38A(II)) shows alternative complement pathway activation. It also otherwise has no effect on course of infection in *B. bronchiseptica*. The bacteria are cleared at 23rd time step similar to the wild type infection. Although O-Ag is likely to be most prevalent antigenic structure on the bacterial surface, it does not affect generation of anti- *B. bronchiseptica* antibodies since wild type and Δwbm mutant strains of *B. bronchiseptica* induced similar antibody titers. Thus observed normal course of infection in case of mutant can be justified.

Deletion of pertussis toxin (PTX):

Pertussis toxin plays its role in phase I, it inhibits neutrophil recruitment by modulating cytokine production by epithelial cells and macrophages or directly interfering with receptor signaling. This inhibition can be the reason for delayed response to antibodies observed in *B. pertussis* , by a mechanism that involves neutrophils and Fc receptors, suggesting that neutrophils phagocytose antibody opsonized bacteria via Fc receptors. PTX deletion (Figure 38B(II)) does

not lead to the earlier clearance (clearance 24th time step) in our simulation. PMNs are recruited earlier and there are more peaks of recruited PMNs. The plateau of peak of recruited PMNs is larger in the absence of PTX, thus the infection pathology is severe. This can be an evolutionary strategy to reduce host defense allowing the pathogen to persist. The data also proves (unpublished data from Eric Harvill' group in Pennsylvania state university USA) that higher proportion of recruited PMNs are observed in lungs in case of *B. pertussis* Δptx mutants.

Deletion of virulence factors TTSS and FHA/ACT:

TTSS in *B. bronchiseptica* and FHA/ACT in *B. pertussis* inhibit production of Th1RC; switching the balance between Th1 and Th2 cells leading to differentiation of naïve T cells to Th2 cells. This ability of FHA(McGuirk et al., 2002) and ACT(Ross et al., 2004) can be attributed to their ability of binding to CD11b/CD18 expressed on DCs. LPS of *B. pertussis* is also shown to enhance this function of ACT(Ross et al., 2004). TTSS is absent in *B. pertussis* , whereas in *B. bronchiseptica* TTSS mediates cytotoxicity, disrupts cell signaling and is required for persistence in the trachea. TTSS inhibits IFN-g shifting the balance between T cell subtypes and is also responsible for decreased antibody mediated clearance in *B. bronchiseptica* . Th2 cells though activate clonal expansion of B cells both processes are not sufficient for the clearance. Deletion of TTSS (Figure 38A(III)) leads to the clearance of bacteria at 7th time step and FHA/ACT (Figure 38B(III)) leads to the clearance of bacteria at 13th time step. Deletion of TTSS leads to earlier activation of phase III components followed by increased activated phagocytic cells and macrophages. In case of *B. pertussis* delayed clearance is due to inhibited recruitment of PMNs by PTX. Thus earlier production of Th1RC has less effect in *B. pertussis* due to presence of PTX.

Deletion of Bcells:

B cells deletion that leads to absence of antibody production does not lead to difference in the clearance timescales in *B. bronchiseptica* (Figure 38A(IV)) and *B. pertussis* (Figure 38B(IV)). Experimentally it has been shown that in B cell deficient MuMT mice that are defective in B cells shows persistent presence of bacteria in nasal cavity, trachea and lungs(Kirimanjeswara et al., 2003). In case of *B. pertussis*, though the bacterial number decrease, no clearance is observed(Kirimanjeswara et al., 2003). Closer look to these results and course of infection proves that antibodies are important for the decrease in bacterial number around day 7. As this discrete model can not take in to account this relative decrease we failed to show the effect of B cell deletion in the model. These results also proves that a decrease in the bacterial number at the same time results in a decrease in the concentration of bacterial virulence factors at day 7 is essential step in the bacterial clearance. Thus the assumption that the concentration of bacterial virulence factors decreases is supported.

Absence of adaptive immunity:

Deletion of naïve T cells (Figure 38A(V), B(V)) in the model leads to the absence of Th1 and Th2 cells. This leads to persistent bacterial number. Experiments with SCID and Rag$^{-/-}$ mice indicated that adaptive immunity is required to clear both organisms from the lower respiratory tract(Harvill et al., 1999). Though there are no T and B cells, the immune system remains active. Complement is activated in *B. pertussis* constitutively, but it is intermittently active (with period of 6) in *B. bronchiseptics* due to inhibition by O antigen. PIC, recruited PMNs, activated phagocytic cells and macrophages are produced with period 6. DCs are constitutively present. Phagocytosis also takes place with period of 6. Thus though innate immunity components are responsive to the presence of bacteria at all time steps, they are not sufficient for the bacterial clearance.

Treatment with antibodies prior to infection:

Antibody treatment prior to infection can be a profilaxis, hence we studied its effect. When the initial value of the node 'antibodies' was 1 and 'bacteria' node was turned ON at t equal to 3 bacteria were cleared on 8th time step in case of *B. bronchiseptica*. But similar study in *B. pertussis* leads to no early clearance. In experimental study, adoptive transfer of serum antibodies has shown to clear *B. bronchiseptica* (Figure 38A(VI)) but not *B. pertussis* ((Figure 38B(VI))) (Kirimanjeswara et al., 2003). The earlier treatment with antibodies results in opsonization of bacteria as soon as they invade the host. This will lead to increased phagocytosis of antibody opsonized bacteria through Fc receptors in *B. bronchiseptica* . PTX in *B. pertussis* inhibits the recruitment of PMNS, thus though Ag-Ab complexes are present they can not be phagocytosed due to absence of activated phagocytic cells.

9.4.2   Miscellaneous systemic effects of deletions

Epithelial cells are necessary for production of PIC in phase I. Deletion of epithelial cells delays PIC production till phase III where Th1RC signaling recruits PMNs and macrophages. The bacteria are sensed by DCs which activates adaptive immunity. The deletion of epithelial cells leads to one step delay in clearance of *B. bronchiseptica* , but *B. pertussis* are cleared at 24th time step as in wild type. It has been shown that initial epithelial TLR4 signaling is essential in limiting the growth of *B. bronchiseptica* but not of *B. pertussis.* Recruitment of PMNs is inhibited by PTX in *B. pertussis* but epithelial TLR4 signaling and resulting higher amounts f cytokines is necessary for recruitment of PMNs in *B. bronchiseptica* .

Deletion of other components delineated individual components that are an essential for the clearance and other components that assist in the clearance. Macrophages are essential in clearance of *B. bronchiseptica* and *B. pertussis* , as there is no clearance in the the absence of macrophages.The plateau of the peak

of activated phagocytic cells is not sufficient to keep phagocytosis active for essential number of time steps. Absence of PMNs or PIC lead to one step later clearance in *B. bronchiseptica*, as described in section 2 PMNs plays less role in *B. pertussis* clearance in concurrence there is no early clearance in *B. pertussis*. Single deletion of complement and antibodies does not lead early clearance, as they may assist in decrease in the bacterial number in transition from phase I to phase II and this effect can not be shown in this qualitative model. *B. bronchiseptica* actually inhibits complement in phase I so it may not be very essential in the clearance. Double removal of complement and antibodies delays the *B. bronchiseptica* clearance by one time step, thus as mentioned in section 2 limiting *B. bronchiseptica* numbers in phase I is essential step towards clearance. Deletion of PMNs, antibodies and complement decreases the plateau of activated phagocytic cells in phase I and III in *B. bronchiseptica* compared to wild type.

Deletion of DCs gives similar results as the deletion of adaptive immunity as they are essential for maturation and differentiation of naive T cells. The node Th1RC is essential for the clearance of *B. pertussis* whereas deletion of nodes TH1 cells and Th1RC extends phase II in *B. bronchiseptica* resulting in the clearance on 23rd time step. In case of *B. pertussis* sufficient activated phagocytic cells can not be formed in the absence of Th1RC. Absence of TH1 cells and TH2 cells though lead to clearance at time step similar to wild type the plateaus of Th1RC and Th2RC are reduced respective cases. Thus though it does not affect clearance in case of single invasion, under multiple invasions of pathogen TH1 cells will be essential to enhance the production of Th1RC , in turn to increase the plateau of recruited PMNs and macrophages in phase III. In the absence of Th2RC species are cleared on 21st time step as phase III is activated earlier. In the double deletion of PIC and Th1RC both species can not be cleared suggesting the importance of these cytokines in the bacterial clearance.

9.5   Conclusion

The recent *Bordetella* genome project shows that *B. bronchiseptica* has larger gene repertoire, and probably colonizes more habitats than the other two species (Preston et al., 2004). Scrutinizing the question why *B. bronchiseptica* rarely found associated with humans raises the possibility of *B. pertussis* having essential genes and/or mechanisms for infecting humans. The genome project identified 23 genes that are present in *B. pertussis* but are absent in *B. bronchiseptica*. However preliminary analysis of microarray mediated genotyping data (Cummings et al., 2004) indicates that all of these genes might be present in other strains of *B. bronchiseptica* . Apart from the genetic regulation that will affect the expression the data strengthens the possibility of differences at the level of immunological regulation.

In the present heuristic study we have modeled the differences in the host immunological regulation and virulence mechanisms of *B. bronchiseptica* and *B. pertussis*. In the simulation we could reproduce basic time course of the infection including activation of components in specific phases of the infection. Further it is easily possible to delete certain components and observe the effect of deletion on the bacterial clearance and/or activation or inhibition of immunological components. The results were counterchecked by experiments stongly support the success of the simulation. The simulation uses logical operators to describe the interactions between immunological components and bacterial virulence factors.

The exact time scale of processes in the dynamic model does not correspond to the one in experimentations. Phase II and III are approximately of same time scale in dynamic model where as of larger duration in *B. bronchiseptica* experiments. Specific processes need different duration in different hosts. Further experiments are performed usually on mice; mice are the natural hosts of *B. bronchiseptica* but not of *B. pertussis*. It is hence essential to identify these differences from the inherent differences in the pathogenic strategies of these

species. Comparison with the experimentally observed time course (sections 2.2 and 2.3) also shows bacterial numbers are usually higher in *B. bronchiseptica*, the pathological effects observed are also greater as compared to *B. pertussis*. Further LPS of *B. bronchiseptica* induce higher cytokines production than *B. pertussis*. These species specific quantitative differences can not be reproduced in the present time step model.

Virulence factors change the course of innate and adaptive immune responses. O-Ag and PTX inhibits early immune responses allowing the bacterial multiplication and survival. The shift from Bvg$^-$ to Bvg$^+$ phase results in either a decrease in O-Ag substitution or a decrease in O-Ag chain length (van den Akker, 1998). It has been speculated(Burns et al., 2003) that decreasing the proportion of LPS molecules containing long O-Ag repeats increases the accessibility to host tissues of other Bvg$^+$ phase factors, such as adhesions, or facilitates secretion oth toxins or immunomodulatory proteins while allowing bacteria to express a basal level of O-Ag for the protection against host defenses such as complement mediated killing. *B. pertussis* whereas naturally lacks the O-Ag which then can increase the accessibility to host tissues. On the other hand inhibitory effect of PTX on neutrophil recruitment is two fold; it allows *B. pertussis* to evade innate immunity early in colonization and also provides a means to resist the effect of serum antibodies in the lungs.

Filamentous hemaglutinin (FHA) and adenylate cyclase toxin (ACT) is present in both species(Preston et al., 2004). There are some differences in the length of proteins and number of repeats in FHA and ACT. The antibodies against ACT and the treatment with purified ACT in *B. bronchiseptica* and *B. pertussis* shows differences in the course of infection (Novotny et al., 1985). With this little knowledge about these two virulence factors it is not known how these both factors are responsible for the differences observed. Though *B. pertussis* does not secrete TTSS as *B. bronchiseptica*, *B. pertussis* has evolved with mechanisms to

modulate adaptive immunity possibly with lesser activation of immune components (see section 9.2).

It is apparent that adaptive immunity is essential for bacterial clearance. Though antibody production is not sufficient for clearance it is necessary to reduce the number. Deletion of adaptive immunity can not clear bacteria and all other components of the immune system remains active in the simulation. Prior treatment with antibodies in the simulation and the adoptive transfer of covalescent-phase serum is sufficient to rapidly clear *B. bronchiseptica* but not human pathogen *B. pertussis*. These results are compatible with human clinical trials, in which serum antibody titers could not be correlated with against *B. pertussis* (Giuliano et al., 1998; Morris and McDonald, 1957). It is also well established that *B. bronchiseptica* induces higher serum antibody titers than *B. pertussis* in the *M. musculus* model (Harvill et al., 1999).

The model is mainly developed by using the logical description of the system (Table 10) and does not use many parameters thus it is highly robust. We define only qualitative relations for the decay of toxins ans cytokins (see section 9.3). Further non-trvivial deletions did not give early clearance, for example deletion of Th1 cells but not Th2 cells in the model lead to early clearance of the pathogen.

Some of the observations lead to early clearance of human pathogen *B. pertussis* in the simulation. When PIC was ON at t=0 leads to earlier clearance (22nd time step) in ΔPTX. The inhibition of Th2RC and deletion of FHA/ACT lead to early clearance, thus these observations can help in directing the study of drugs against the disease and identify important parts of the network studied.

10. General Discussion

10.1. Exploring network data and creating network models

The first part of this general discussion explores the implications of pathway analysis and its use in drug discovery, followed by a more specific discussion on the different modeling strategies used in the thesis in the second part.

10.1.1 Biological implications of analyzing pathways

A wide range of modeling techniques have been developed that use pathway data of varying detail to answer specific biological questions. Qualitative and quantitative modeling of biological systems facilitates addressing questions outside of the direct capacity of the human brain, using software on powerful computers as exemplified in this thesis.

Questions such as 'What are the fundamental design patterns in the system?', 'What are the key relationships between system components?' and 'What are the physiological effects of system perturbation?' can be answered using quantitative and qualitative modeling. Quantitative modeling, such as representing a dynamic chemical process using a system of differential rate equations, requires highly detailed pathway information, such as kinetic constants, initial concentrations and clear connectivity of reactions (Bhalla et al., 2002).

Qualitative models (Li et al., 2004) can discover system properties not apparent in static pathway data as exemplified by the simulation of phagosome and lyosome. The effect of many different parameters could be analysed in such a simulation.
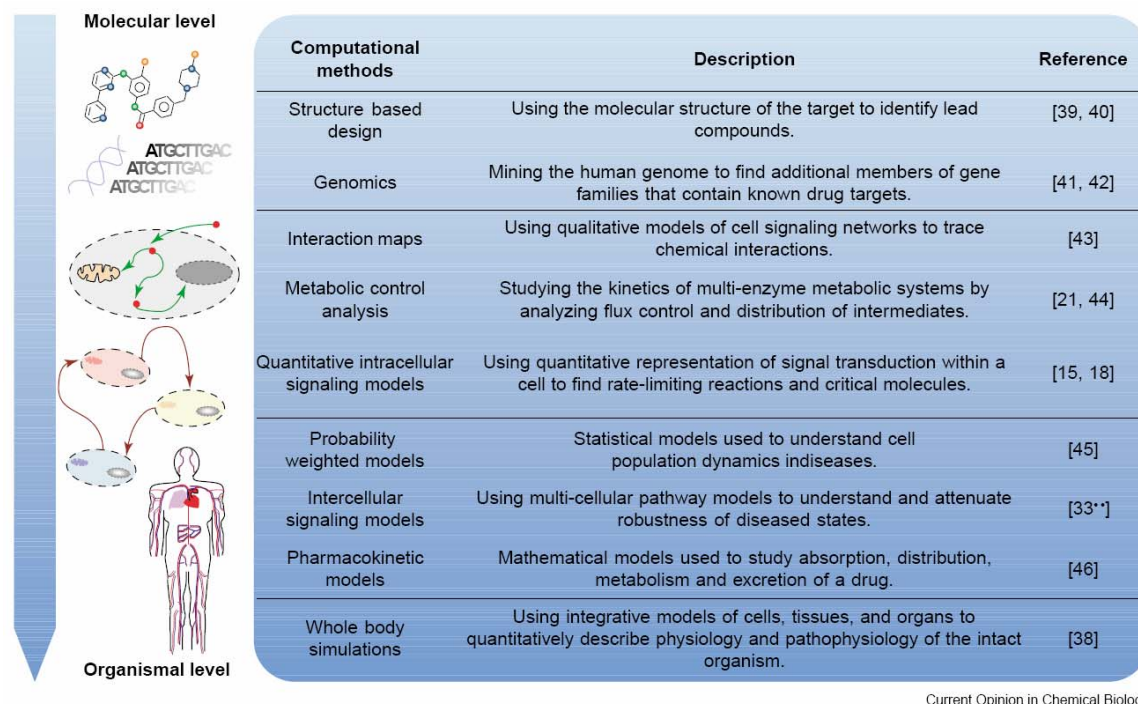
Evolution-focused questions, such as 'Which biological processes are homologous?' can be answered using techniques that identify common

functional motifs and design principles, for example, through species comparison performed in the study of apoptosis cascade.

Basic questions, such as 'What are the functions of some genes?' are still vitally important, since the majority of genes in most genomes have no known function. Examining genes in the network context can help answer this question. For example, a protein of unknown function connected to a set of proteins involved in the same biological process is likely to function in that process as well (Lee et al., 2004; Schwikowski et al., 2000). Less-detailed pathway data, such as proteomics-based protein– protein interactions, can be used to answer questions like 'What network patterns allow prediction of new interactions?' For example, structural and sequence analysis of DDs have been used to hypothesize that certain DD containing proteins mediate proliferative signals and to predict new interactions (Thakar et al., 2005).

Finally, questions such as, "what biologically relevant patterns are found in normal and disease state?" The patterns of immunological responses similar to figure 38 in response to normal and disease state can be formed. They will be vitally important for clinical health research. Similarly transcriptionally active regions in an integrated pathway network that correlate with disease state have been used to predict active pathway components that play a role in disease progression (Ideker et al., 2002; Pradines et al., 2004).

10.1.2. Systems modeling applied to drug discovery

Figure 40: Computational methods in Therapeutics. A listing of in silico methods used to complement and advance conventional drug discovery. Further details can be in references mentioned in the figure (Rajasethupathy et al., 2005).

There are some noteworthy challenges facing the pharmaceutical industry today where modeling might play a key role. Firstly, modeling enables systematic integration of the overwhelming amount of relevant information that has accumulated from high throughput screening methods. Further, models help in establishing a mechanistic understanding of the disease and of drug action, which is a marked shift from traditional 'black-box' approach to drug discovery. Finally systems modeling help in predicting probable side effects, and finding optimal dosages and treatment schedules.

Three levels of cellular responses can serve as possible nodes for drug targeting: signal reception, intracellular responses, and intercellular communication.

Signal reception: Cells receive inputs from different signaling molecules, which are often recognized by receptor proteins. At least 70% of drugs in development today target such receptors(Lundstrom, 2005). Cell-signal modeling can help elucidate the mechanisms of receptor responses to pharmacological interventions. Signaling models such as apoptosis activation through various receptors are being used to understand the mechanism of many other receptor–ligand interactions with therapeutic importance. For instance, exploring different possibilities of signal processing followed by p55TNFRI receptor can be useful in cancer therapy to explore the ways to induce apoptosis in malignant cells (Thakar et al., 2005). Preliminary success of apoptosis cascade modeling also opens new doors to study the side effects of different drugs (Thakar et al.). Similar modeling techniques have been used to explore how dimerization of G-protein-coupled receptors affects receptor localization, signaling and internalization in diseased states (Woolf and Linderman, 2004).

Intracellular responses: Once an external stimulus has been communicated to the cell interior, it is amplified and diversified through the activation of various signaling and metabolic pathways. Here, we see the beginnings of signaling complexity and the need to have a systems-level understanding of information processing and convergence. Cross-talk amongst the various pathways may yield switching, oscillations and other emergent properties that are not characteristic of the individual pathways themselves (Bhalla and Iyengar, 1999; Kitano, 2002). In the phospholipids network studied here a cross-talk between sphingosine and DAG activated PA show activating or inhibitory effect on actin polymerization depending weather sphingosine is phosphorylated or not (Figure 21) (Kühnel et al.). In a therapeutic context, modeling this cross-talk can reveal non-intuitive drug targets and show possible side effects. Haugh et al. (Haugh et al., 2000) have developed a model of the phospholipase C (PLC) pathway, a key signaling pathway shown to be essential

for cell motility and directionality (Wells, 2000). It has been implicated in cancer growth and metastasis and is a prospective target for cancer therapeutics.

Further a qualitative characterization of signaling networks can be very useful in addressing toxicity issues and side effects. For instance, it has been suggested that the toxic effects of pyrazinamide, a drug used for treating tuberculosis, could have been predicted using pathway analysis based on the literature available at the time of approval (Bugrim et al., 2004).

Intercellular communication: Cells do not function in isolation. Many physiological effects and diseases arise from synergistic interactions between multiple cells. For instance interaction between phagosome and lysosome is crucial in the removal of pathogens. This interaction is inhibited by *M. tuberculosis* and thus they successfully survive in phagosomes. Experimental study of this interaction is not possible as it takes place in a fraction of second *in vivo*. Modeling approach has been successfully used which points out important factors in this interaction (Thakar et al., b). It can be useful in targeting new drugs.

The model is developed to study intercellular communication during Bordetellae infection. Its validation by experimental observations opens the possibility to use this model in drug targeting (Thakar et al., c). Similar model for Asthama has been developed (Musante et al., 2002) which describes the complex interactions of airway physiology with the inflammatory response. This model simulated asthmatic symptoms in response to exposure to an allergen. Contrary to what animal studies had shown, the model predicted that anti-interleukin-5 (IL-5) treatment would be ineffective in treating airway obstruction observed in asthma. Results of anti-IL-5 clinical trials lent credence to the model (Leckie et al., 2000).

Conclusion: Qualitative and quantitative modeling strategies have been successful in modeling. Qualitative models help trace non-linear flow of information, and in so doing, can predict counter-intuitive effects of perturbing a

system. Detailed quantitative models can additionally provide a mechanistic basis for the failure of certain treatment paradigms, and explore alternative drug targets. The extent to which a model can be predictive increases as one tightens the kinetic constraints on a system.

10.2 Specific strategies used for modeling in this thesis

In the 21st century the study and analysis of systems at a global level becomes important with large amounts of data that is constantly collected with new experimental and computational techniques. It is impossibile to discuss here all research activities in these important directions of bioinformatic modeling. Some of them which are related to the work presented here in a broad context are:

- Postgenomic bioinformatics (Heinrich and Schuster, 1996; Hofestad, 2000)
- Prediction and analysis of pathways (Heinrich et al., 2002; Robubi et al., 2005a; Robubi et al., 2005b)
- Modelling cellular processes (Kitano, 2002; Tomita et al., 1997)
- Systems biology (Stelling et al., 2002)

Instead the following discussion puts emphasis on selected examples from other work which we consider particularly near to our approaches detailed in the results.

We used different methods to study biological networks (protein interactions, interactions between components of the pathways, organelle interactions and interactions between components of the system). For studying protein interactions sequence analysis depicting conserved and non-conserved residues which is further extended into structural analysis was used. The present comparative structural modeling in chapter 5 of six protein complexes in the TNF mediated pathway leads to the delineation of important interacting surfaces in these modeled complexes. This helps to shed light on the mechanism by which p55TNFR1 induces formation of different complexes and in turn signaling

through different cascades. Our models highlight different possible interactions in the pathway such as recruitment of CRADD or NFκB by TRADD-RIP complex in two different conformations.

A similar docking approach was also used to model the FAS-FADD DD interaction by (Weber and Vincenz, 2001). The arrangement of FAS and FADD was determined by them using the interaction modes of Pelle-Tube and Apaf-1-Procaspase-9. The proposed model reveals that both interactions can be accommodated in a single multimeric complex. The Weber model is built with the preconception that interacting surfaces in FAS-FADD are similar either to Pelle-Tube or Apaf-1-Procaspase-9. Our docking models are developed without any preconceptions. In contrast, we used multiple sequence alignment and phylogenetic analysis to build our hypothesis.

We then used a new model and approach applying ODE (Ordinary Differential Equations) in the qualitative analysis in chapter 6. The model could reproduce the caspase-3 shape of response curve and the percentage of viable cells across time. ODEs are often used for modeling kinetics of pathway. To address the complexity of CD95 induced apoptotic signaling sensitivity analysis within the mathematical model has been performed by Bentele, *et al* (Bentele et al., 2004) for the identification of critical system parameters. The mathematical model is based on biochemical reaction equations and the temporal behavior is described by a system of ODE. The approach based on biochemical reactions requires large amounts of kinetic data, as such information was unavailable they used sensitivity analysis to reduce the parameters. On the contrary our novel mathematical formlism is based on the Michaelis Menten assumption and requires as a consequence only few parameters. This approach assumes a saturation curve for all component concentrations. However, this is indeed observed in most of the signaling pathways, yet with different slopes of the curves.

A simple qualitative approach based on Boolean functions and additive rules was used for analyzing phospholipid networks essential for activation or inhibition of actin polymerization on phagosome membranes. Interestingly, we could also use this simulation for prediction of ATP concentration at which a switch takes place (see chapter 7). An analytical model based on probability allowed us to test the hypothesis about the role of F-actin in phagosome-lysosome fusion. This was further developed into a simulation to test specific effects in chapter 8. The first approach has already been used in case of the interaction of chromosome and microtubules (Holy and Leibler, 1994). These both approaches are more theoretical and are best used for systems where *in vivo* observations are difficult to make. Such models can be developed on known data to predict unknown processes. Though similar analytical and spatial modeling approaches have been used in case of microtubule polymerizations (Verde et al., 1992), centrosome formation (Mitchison and Kirschner, 1984b) and chromosome searching (Holy and Leibler, 1994), their exploration in actin function is highly limited. Goshima, *et al* (Goshima et al., 2005) have used a similar approach to explain self assembly of microtubules and the role of dynein in the assembly.

The analytical model used by us is probabilistic and does not allow to analyze individual parameters. It explains nicely the system at equilibrium but fails to give an explanation otherwise. In the spatial model we could analyse i) the effect of the distance between lysosome-phagosome, ii) dimensions of organelles and iii) the effect of F-actin length if f_{res} does not tend to 0 (or when d is not equal to d_a).

Last but not least we used a Boolean formalism (Rene and Richard, 1990) which was then developed into dynamic simulation for immune responses to *Bordetellae*. The network constructed by data mining allowed us to put all known information into the time frame of the progression of infection. The model could correctly predict much mutation data observed by experiments.

The approach used for modeling phospholipid networks in chapter 7 and interactions between *Bordetellae* and host immunity in chapter 9 is based on logical modeling of the systems. Both models use Boolean rules for the description of nodes. In the *Bordetellae* model the nodes are active (and have the value '1') or inactive (and have the value '0'). In contrast, in the Phospholipid network we use an additive rule. The additive rule can be explained as a function similar to memory. In the later case there exist many phospholipids at the same time and the effect on actin polymerization is the additive effect of all these individual phospholipids. So the simulator remembers the individual response and produces the total response (effect on actin polymerization) as a result of individual responses of Phospholipid. Similar logical formalism has been used to develop the tool Genetic Network Analyzer (GNA). This tool was then successfully implemented for the analysis of the network controlling the nutritional stress response in *Escherichia coli* (Batt et al., 2005). This tool is essentially used for the analysis of a genetic network where the genes active at time step t express the protein at time step t+1. The activation of genes is the function which uses Boolean operators. Such tools can be used for simple genetic networks, but can not be used at a systems level or for simulations of specific signal transduction networks or phospholipids networks which include allosteric interactions and metabolic transformations at the same time. The later networks need to be analyzed individually considering system specific parameters, however, the additive rule (Rene and Richard, 1990) allows already better qualitative description of the systems behavior.

All these approaches can be used in the presence of limited kinetic data and can be applied to predict mutation data, important parameters and regulatory hotspots. The approaches used in this work are essentially novel and try to address fundamental biological questions such as: 'How pathways are regulated?' 'At which places?' The success of these models highly depends on time scale used and their interpretation. For example from the experimental

observations we could estimate the time scale used in the model corresponding to 1.3 hours. For shorter time scales the predictions are better. More kinetic data obviously lead to better predictions. Such data nevertheless are difficult to get in many instances. The parameters used have to be modified with new experimental observations. Apart from these considerations it is necessary to remember that these models highly depend on the understanding of systems and the construction of correct networks.

11. Summary

In this century new experimental and computational techniques are adding an enormous amount of information, revealing many biological mysteries. The complexities of biological systems still broach new questions. Till now the main approach to understand a system has been to divide it in components that can be studied. The upcoming new paradigm is to combine the pieces of information in order to understand it at a global level.

In the present thesis we have tried to study infectious diseases with such a global 'Systems Biology' approach. In the first part the apoptosis pathway is analyzed. Apoptosis (Programmed cell death) is used as a counter measure in different infections, for example viral infections. The interactions between death domain containing proteins are studied to address the following questions: i) How specificity is maintained - showing that it is induced through adaptors, ii) how proliferation/ survival signals are induced during activation of apoptosis – suggesting the pivotal role of RIP. The model also allowed us to detect new possible interacting surfaces (Thakar, *et al*, "RIP death domain structural interactions implicated in a TNF-mediated proliferation and survival" in press in Protein: Structure, Function and Bioinformatics). The pathway is then studied at a global level in a time step simulation to understand the evolution of the topology of activators and inhibitors of the pathway. Signal processing is further modeled in detail for the apoptosis pathway in *M. musculus* to predict the concentration time course of effector caspases. Further, experimental measurements of caspase-3 and viability of cells validate the model (Juilee Thakar, Dorothee Walter, Christoph Borner and Thomas Dandekar, "Discrete time modeling of apoptosis pathway: comparison of topology and significance of critical components" (submitted to PLoS computational biology)).

The second part focuses on the phagosome, an organelle which plays an essential role in removal of pathogens as exemplified by *M. tuberculosis*. Again

the problem is addressed in two main sections: i) To understanding the processes that are inhibited by *M. tuberculosis*; we focused on the phospholipid network applying a time step simulation in section one, which plays an important role in inhibition or activation of actin polymerization on the phagosome membrane. (Mark Philipp Kühnel, Elsa Anes, Juilee Thakar, Evelyne Bos, Sezgin Erdogan, Katia Zanier, Michael Sattler, Roland Schwarz, Daniela Holzer, Britta Bruegger, Vladimir Rybin, Stefan Schuster, Jens Georg Reich, Thomas Dandekar and Gareth Griffiths, "Latex bead phagosomes - a system for the gobal analysis of membrane signaling networks", in preparation for Nature Biotechnology). ii) Furthermore, actin polymers are suggested to play a role in the fusion of the phagosome with lysosome. To check this hypothesis an *in silico* model was developed; we find that the search time is reduced by 5 fold in the presence of actin polymers. Further the effect of length of actin polymers, dimensions of lysosome, phagosome and other model parameter is analyzed. (Juilee Thakar, Chunguang Liang, Mark Philipp Kühnel, Gareth Griffith and Thomas Dandekar, "Spatial resolution model for phagosome- lysosome fusion", in preparation for BMC cell biology)

After studying a pathway and then an organelle, the next step was to move to the system. This was exemplified by the host pathogen interactions between *Bordetella pertussis* and *Bordetella bronchiseptica*. The limited availability of quantitative information was the crucial factor behind the choice of the model type. A Boolean model was developed which was used for a dynamic simulation. The results predict important factors playing a role in *Bordetella* pathology especially the importance of Th1 related responses and not Th2 related responses in the clearance of the pathogen. Some of the quantitative predictions have been counterchecked by experimental results such as the time course of infection in different mutants and wild type mice (Juilee Thakar, Mylisa Pilione, Eric Harvill and Réka Albert, "Modeling the interplay between *Bordetellae* and host immunity" in preparation for PLoS pathogens).

All these computational models have been developed in presence of limited kinetic data. The success of these models has been validated by comparison with experimental observations. Comparative models studied in chapters 6 and 9 can be used to explore new host pathogen interactions. For example in chapter 6, the analysis of inhibitors and inhibitory paths in three organism leads to the identification of regulatory hotspots in complex organisms and in chapter 9 the identification of three phases in *B. bronchiseptica* and inhibition of IFN-γ by TTSS lead us to explore similar phases and inhibition of IFN-γ in *B. pertussis*. Further an important significance of these models is to identify new components playing an essential role in host-pathogen interactions. *In silico* deletions can point out such components which can be further analyzed by experimental mutations.

12. Zusammenfasung

In diesem Jahrhundert haben neue experimentelle Techniken und Computer-Verfahren enorme Mengen an Information erzeugt, die bereits viele biologische Rätsel enthüllt haben. Doch die Komplexität biologischer Systeme wirft immer weitere neue Fragen auf. Um ein System zu verstehen, bestand der Hauptansatz bis jetzt darin, es in Komponenten zu zerlegen, die untersucht werden können. Ein neues Paradigma verknüpft die einzelnen Informationsteile, um sie auf globaler Ebene verstehen zu können. In der vorgelegten Doktorarbeit habe ich deshalb versucht, infektiöse Krankheiten mit globalen Methoden („Systembiologie") bioinformatisch zu untersuchen.

Im ersten Teil wird der Apoptose-Signalweg analysiert. Apoptose (Programmierter Zelltod) wird bei verschiedenen Infektionen, zum Beispiel bei Viruserkrankungen, als Abwehrmaßnahme eingesetzt. Die Interaktionen zwischen Proteinen, die ‚death' Domänen beinhalten, wurden untersucht, um folgende Fragen zu klären: i) wie wird die Spezifität der Interaktionen erzielt? – sie wird durch Adapter erreicht, ii) wie werden Proliferation/ Überlebenssignale während der Aktivierung der Apoptose eingeleitet? – wir fanden Hinweise für eine entscheidende Rolle des RIP Proteins (**R**ezeptor-**I**nteragierende Serine/Threonine-**P**roteinkinase 1).

Das Modell erlaubte uns, die Interaktions-Oberflächen von RIP vorherzusagen (Thakar *et al.*, "RIP death domain structural interactions implicated in a TNF-mediated proliferation and survival", im Druck in „*Protein: Structure, Function and Bioinformatic*s"). Der Signalweg wurde anschließend auf globaler Ebene mit Simulationen für verschiedene Zeitpunkte analysiert, um die Evolution der Aktivatoren und Inhibitoren des Signalwegs und seine Struktur besser zu verstehen. Weiterhin wird die Signalverarbeitung für Apoptosis-Signalwege in der Maus detailliert modelliert, um den Konzentrationsverlauf der Effektor-Kaspasen vorherzusagen. Weitere experimentelle Messungen von

Kaspase-3 und die Überlebenskurven von Zellen bestätigen das Modell (Juilee Thakar, Dorothee Walter, Christoph Borner und Thomas Dandekar, "Discrete time modeling of the apoptosis pathway: comparison of topology and significance of critical components" (eingeicht bei *PLoS computational biology*).

Der zweite Teil der Resultate konzentriert sich auf das Phagosom, eine Organelle, die eine entscheidende Rolle bei der Eliminierung von Krankheitserregern spielt. Dies wird am Beispiel von *M. tuberculosis* veranschaulicht. Die Fragestellung wird wiederum in zwei Aspekten behandelt: i) Um die Prozesse, die durch *M. tuberculosis* inhibiert werden zu verstehen, haben wir uns auf das Phospholipid-Netzwerk konzentriert, das bei der Unterdrückung oder Aktivierung der Aktin-Polymerisation eine große Rolle spielt. Wir haben für diese Netzwerkanalyse eine Simulation für verschiedene Zeitpunkte ähnlich wie in Teil eins angewandt. (Mark Philipp Kühnel, Elsa Anes, Juilee Thakar, Evelyne Bos, Sezgin Erdogan, Katia Zanier, Michael Sattler, Roland Schwarz, Daniela Holzer, Britta Bruegger, Vladimir Rybin, Stefan Schuster, Jens Georg Reich, Thomas Dandekar und Gareth Griffiths, "Latex bead phagosomes - a system for the gobal analysis of membrane signaling networks", in Vorbereitung für *Nature Biotechnology*). ii) Es wird vermutet, dass Aktin-Polymere bei der Fusion des Phagosoms mit dem Lysosom eine Rolle spielen. Um diese Hypothese zu untersuchen, wurde ein *in silico* Modell von uns entwickelt. Wir fanden heraus, dass in der Anwesenheit von Aktin-Polymeren die Suchzeit für das Lysosom um das Fünffache reduziert wurde. Weiterhin wurden die Effekte der Länge der Aktin-Polymere, die Größe der Lysosomen sowie der Phagosomen und etliche andere Modellparameter analysiert (Juilee Thakar, Chunguang Liang, Mark Philipp Kühnel, Gareth Griffith und Thomas Dandekar, "Spatial resolution model for phagosome- lysosome fusion", in Vorbereitung für *BMC cell biology*).

Nach der Untersuchung eines Signalwegs und einer Organelle führte der nächste Schritt zur Untersuchung eines komplexen biologischen Systems der

Infektabwehr. Dies wurde am Beispiel der Wirt-Pathogen Interaktion bei *Bordetella pertussis* /Mensch und *Bordetella bronchiseptica* / Maus dargestellt. Die geringe Menge verfügbarer quantitativer Daten war der ausschlaggebende Faktor bei unserer Modellwahl. Für die dynamische Simulation wurde ein selbst entwickeltes Bool'sches Modell verwendet. Die Ergebnisse sagen wichtige Faktoren bei der Pathologie von Bordetellen hervor, besonders die Bedeutung der Th1 assoziierten Antworten und dagegen nicht der Th2 assoziierten Antworten für die Eliminierung des Pathogens. Einige der quantitativen Vorhersagen wurden durch Experimente wie die Untersuchung des Verlaufs einer Infektion in verschiedenen Mutanten und Wildtyp-Mäusen überprüft (Juilee Thakar, Mylisa Pilione, Eric Harvill und Réka Albert, "Modeling the interplay between *Bordetellae* and host immunity" in Vorbereitung für *PLoS pathogens*).

Die begrenzte Verfügbarkeit kinetischer Daten war der kritische Faktor bei der Auswahl der computer-gestützten Modelle. Der Erfolg unserer Modelle konnte durch den Vergleich mit experimentellen Beobachtungen belegt werden. Die vergleichenden Modelle in Kapitel 6 und 9 können zur Untersuchung neuer Wirt-Pathogen Interaktionen verwendet werden. Beispielsweise führt in Kapitel 6 die Analyse von Inhibitoren und inhibitorischer Signalwege aus drei Organismen zur Identifikation wichtiger regulatorischer Zentren in komplexen Organismen und in Kapitel 9 ermöglicht die Identifikation von drei Phasen in *B. bronchiseptica* und der Inhibition von IFN-γ durch den Faktor TTSS die Untersuchung ähnlicher Phasen und die Inhibition von IFN-γ in *B. pertussis*. Eine weitere wichtige Bedeutung bekommen diese Modelle durch die mögliche Identifikation neuer, essentieller Komponenten in Wirt-Pathogen Interaktionen. *In silico* Modelle der Effekte von Deletionen zeigen solche Komponenten auf, die anschließend durch experimentelle Mutationen weiter untersucht werden können.

13. References

Ahmad, M., S.M. Srinivasula, L. Wang, R.V. Talanian, G. Litwack, T. Fernandes-Alnemri, and E.S. Alnemri. 1997. CRADD, a novel human apoptotic adaptor molecule for caspase-2, and FasL/tumor necrosis factor receptor-interacting protein RIP. *Cancer Res*. 57:615-9.

Alam, R., P. Forsythe, S. Stafford, and Y. Fukuda. 1994. Transforming growth factor beta abrogates the effects of hematopoietins on eosinophils and induces their apoptosis. *J Exp Med*. 179:1041-5.

Algrain, M., O. Turunen, A. Vaheri, D. Louvard, and M. Arpin. 1993. Ezrin contains cytoskeleton and membrane binding domains accounting for its proposed role as a membrane-cytoskeletal linker. *J Cell Biol*. 120:129-39.

Alla, H., and R. David. 1998. Continuous and hybrid petri nets. *Journal of Circuits, Systems and Computers*. 8:159-188.

Allen, L.H., and A. Aderem. 1995. A role for MARCKS, the alpha isozyme of protein kinase C and myosin I in zymosan phagocytosis by macrophages. *J Exp Med*. 182:829-40.

Ameisen, J.C. 1992. Programmed cell death and AIDS: from hypothesis to experiment. *Immunol Today*. 13:388-91.

Anes, E., M.P. Kuhnel, E. Bos, J. Moniz-Pereira, A. Habermann, and G. Griffiths. 2003. Selected lipids activate phagosome actin assembly and maturation resulting in killing of pathogenic mycobacteria. *Nat Cell Biol*. 5:793-802.

Aravind, L., V.M. Dixit, and E.V. Koonin. 1999. The domains of death: evolution of the apoptosis machinery. *Trends Biochem Sci*. 24:47-53.

Bang, S., E.J. Jeong, I.K. Kim, Y.K. Jung, and K.S. Kim. 2000. Fas- and tumor necrosis factor-mediated apoptosis uses the same binding surface of FADD to trigger signal transduction. A typical model for convergent signal transduction. *J Biol Chem*. 275:36217-22.

Barnewall, R.E., N. Ohashi, and Y. Rikihisa. 1999. Ehrlichia chaffeensis and E. sennetsu, but not the human granulocytic ehrlichiosis agent, colocalize with transferrin receptor and up-regulate transferrin receptor mRNA by activating iron-responsive protein 1. *Infect Immun*. 67:2258-65.

Batt, G., D. Ropers, H. de Jong, J. Geiselmann, R. Mateescu, M. Page, and D. Schneider. 2005. Validation of qualitative models of genetic regulatory networks by model checking: analysis of the nutritional stress response in Escherichia coli. *Bioinformatics*. 21 Suppl 1:i19-i28.

Beatty, W.L., and D.G. Russell. 2000. Identification of mycobacterial surface proteins released into subcellular compartments of infected macrophages. *Infect Immun*. 68:6997-7002.

Beinke, S., M.P. Belich, and S.C. Ley. 2002. The death domain of NF-kappa B1 p105 is essential for signal-induced p105 proteolysis. *J Biol Chem*. 277:24162-8.

Bentele, M., I. Lavrik, M. Ulrich, S. Stosser, D.W. Heermann, H. Kalthoff, P.H. Krammer, and R. Eils. 2004. Mathematical modeling reveals threshold mechanism in CD95-induced apoptosis. *J Cell Biol*. 166:839-51.

Bergeron, L., G.I. Perez, G. Macdonald, L. Shi, Y. Sun, A. Jurisicova, S. Varmuza, K.E. Latham, J.A. Flaws, J.C. Salter, H. Hara, M.A. Moskowitz, E. Li, A. Greenberg, J.L. Tilly, and J. Yuan. 1998. Defects in regulation of apoptosis in caspase-2-deficient mice. *Genes Dev*. 12:1304-14.

Berryman, M., R. Gary, and A. Bretscher. 1995. Ezrin oligomers are major cytoskeletal components of placental microvilli: a proposal for their involvement in cortical morphogenesis. *J Cell Biol*. 131:1231-42.

Bhalla, U.S., and R. Iyengar. 1999. Emergent properties of networks of biological signaling pathways. *Science*. 283:381-7.

Bhalla, U.S., P.T. Ram, and R. Iyengar. 2002. MAP kinase phosphatase as a locus of flexibility in a mitogen-activated protein kinase signaling network. *Science*. 297:1018-23.

Bottino, D.C., and L.J. Fauci. 1998. A computational model of ameboid deformation and locomotion. *Eur Biophys J*. 27:532-9.

Bretscher, A. 1989. Rapid phosphorylation and reorganization of ezrin and spectrin accompany morphological changes induced in A-431 cells by epidermal growth factor. *J Cell Biol*. 108:921-30.

Bretscher, A. 1999. Regulation of cortical structure by the ezrin-radixin-moesin protein family. *Curr Opin Cell Biol*. 11:109-16.

Bridgham, J.T., J.A. Wilder, H. Hollocher, and A.L. Johnson. 2003. All in the family: evolutionary and functional relationships among death receptors. *Cell Death Differ*. 10:19-25.

Brightman, F.A., and D.A. Fell. 2000. Differential feedback regulation of the MAPK cascade underlies the quantitative differences in EGF and NGF signalling in PC12 cells. *FEBS Lett*. 482:169-74.

Bugrim, A., T. Nikolskaya, and Y. Nikolsky. 2004. Early prediction of drug metabolism and toxicity: systems biology approach and modeling. *Drug Discov Today*. 9:127-35.

Burns, V.C., E.J. Pishko, A. Preston, D.J. Maskell, and E.T. Harvill. 2003. Role of Bordetella O antigen in respiratory tract infection. *Infect Immun*. 71:86-94.

Byrne, P., P. McGuirk, S. Todryk, and K.H. Mills. 2004. Depletion of NK cells results in disseminating lethal infection with Bordetella pertussis associated with a reduction of antigen-specific Th1 and enhancement of Th2, but not Tr1 cells. *Eur J Immunol*. 34:2579-88.

Carlier, M.F. 1998. Control of actin dynamics. *Curr Opin Cell Biol*. 10:45-51.

Carlier, M.F., C. Le Clainche, S. Wiesner, and D. Pantaloni. 2003. Actin-based motility: from molecules to movement. *Bioessays*. 25:336-45.

Caron, E., and A. Hall. 1998. Identification of two distinct mechanisms of phagocytosis controlled by different Rho GTPases. *Science*. 282:1717-21.

Chang, Y., E. Cesarman, M.S. Pessin, F. Lee, J. Culpepper, D.M. Knowles, and P.S. Moore. 1994. Identification of herpesvirus-like DNA sequences in AIDS-associated Kaposi's sarcoma. *Science*. 266:1865-9.

Chen, C.H., W.J. Wang, J.C. Kuo, H.C. Tsai, J.R. Lin, Z.F. Chang, and R.H. Chen. 2004. Bidirectional signals transduced by DAPK-ERK interaction promote the apoptotic effect of DAPK. *Embo J*.

Clemens, D.L. 1997. Mycobacterium tuberculosis: bringing down the wall. *Trends Microbiol*. 5:383-5.

Clemens, D.L., B.Y. Lee, and M.A. Horwitz. 2000. Deviant expression of Rab5 on phagosomes containing the intracellular pathogens Mycobacterium tuberculosis and Legionella pneumophila is associated with altered phagosomal fate. *Infect Immun*. 68:2671-84.

Clifton, D.R., R.A. Goss, S.K. Sahni, D. van Antwerp, R.B. Baggs, V.J. Marder, D.J. Silverman, and L.A. Sporn. 1998. NF-kappa B-dependent inhibition of apoptosis is essential for host cellsurvival during Rickettsia rickettsii infection. *Proc Natl Acad Sci U S A*. 95:4646-51.

Committee on Emerging Microbial Threats to Health in the 21st Century. Microbial Threats to Health in the United States: Emergence, D.a.R.e.S., M. S., Hamburg, M. A. & Lederberg, J.) (National Academy Press, Washington DC, 2003).

Cummings, C.A., M.M. Brinig, P.W. Lepp, S. van de Pas, and D.A. Relman. 2004. Bordetella species are distinguished by patterns of substantial gene loss and host adaptation. *J Bacteriol*. 186:1484-92.

de Hoog, C.L., and M. Mann. 2004. Proteomics. *Annu Rev Genomics Hum Genet*. 5:267-93.

Debbas, M., and E. White. 1993. Wild-type p53 mediates apoptosis by E1A, which is inhibited by E1B. *Genes Dev*. 7:546-54.

Debrabant, A., E. Ghedin, and D.M. Dwyer. 2000. Dissection of the functional domains of the Leishmania surface membrane 3'-nucleotidase/nuclease, a unique member of the class I nuclease family. *J Biol Chem*. 275:16366-72.

Defacque, H., M. Egeberg, A. Habermann, M. Diakonova, C. Roy, P. Mangeat, W. Voelter, G. Marriott, J. Pfannstiel, H. Faulstich, and G. Griffiths. 2000. Involvement of ezrin/moesin in de novo actin assembly on phagosomal membranes. *Embo J*. 19:199-212.

Desjardins, M., and G. Griffiths. 2003. Phagocytosis: latex leads the way. *Curr Opin Cell Biol*. 15:498-503.

Desjardins, M., L.A. Huber, R.G. Parton, and G. Griffiths. 1994. Biogenesis of phagolysosomes proceeds through a sequential series of interactions with the endocytic apparatus. *J Cell Biol*. 124:677-88.

Drath, R. 1998. Hybrid object nets: an object oriented concept for modeling complex hybrid systems. *Proc. Hybrid Dynamical Systems, 3rd International Conference on Automation of Mixed Processes, ADPM'98*:437-442.

Duan, H., and V.M. Dixit. 1997. RAIDD is a new 'death' adaptor molecule. *Nature*. 385:86-9.

Espinal, M.A. 2003. The global situation of MDR-TB. *Tuberculosis (Edinb)*. 83:44-51.

Felsenstein, J. 1997. An alternating least squares approach to inferring phylogenies from pairwise distances. *Syst Biol*. 46:101-11.

Galtier, N., M. Gouy, and C. Gautier. 1996. SEAVIEW and PHYLO_WIN: two graphic tools for sequence alignment and molecular phylogeny. *Comput Appl Biosci*. 12:543-8.

Garcia-Calvo, M., E.P. Peterson, D.M. Rasper, J.P. Vaillancourt, R. Zamboni, D.W. Nicholson, and N.A. Thornberry. 1999. Purification and catalytic properties of human caspase family members. *Cell Death Differ*. 6:362-9.

Gilmore, A.P., and K. Burridge. 1996. Regulation of vinculin binding to talin and actin by phosphatidyl-inositol-4-5-bisphosphate. *Nature*. 381:531-5.

Giuliano, M., P. Mastrantonio, A. Giammanco, A. Piscitelli, S. Salmaso, and S.G. Wassilak. 1998. Antibody responses and persistence in the two years after immunization with two acellular vaccines and one whole-cell vaccine against pertussis. *J Pediatr*. 132:983-8.

Golstein, P. 1997. Controlling cell death. *Science*. 275:1081-2.

Goodstadt, L., and C.P. Ponting. 2001. CHROMA: consensus-based colouring of multiple alignments for publication. *Bioinformatics*. 17:845-6.

Gorg, A., W. Weiss, and M.J. Dunn. 2004. Current two-dimensional electrophoresis technology for proteomics. *Proteomics*. 4:3665-85.

Goshima, G., F. Nedelec, and R.D. Vale. 2005. Mechanisms for focusing mitotic spindle poles by minus end-directed motor proteins. *J Cell Biol*. 171:229-40.

Gougeon, M.L., and L. Montagnier. 1993. Apoptosis in AIDS. *Science*. 260:1269-70.

Greenberg, S., J. el Khoury, F. di Virgilio, E.M. Kaplan, and S.C. Silverstein. 1991. Ca(2+)-independent F-actin assembly and disassembly during Fc receptor-mediated phagocytosis in mouse macrophages. *J Cell Biol*. 113:757-67.

Griffiths, G. 1996. On vesicles and membrane compartments. *Protoplasma*. 195:37-58.

Griffiths, G. 2004. On phagosome individuality and membrane signalling networks. *Trends Cell Biol*. 14:343-51.

Gronbaek, K., P.T. Straten, E. Ralfkiaer, V. Ahrenkiel, M.K. Andersen, N.E. Hansen, J. Zeuthen, K. Hou-Jensen, and P. Guldberg. 1998. Somatic Fas mutations in non-Hodgkin's lymphoma: association with extranodal disease and autoimmunity. *Blood*. 92:3018-24.

Guex, N., A. Diemand, and M.C. Peitsch. 1999. Protein modelling for all. *Trends Biochem Sci*. 24:364-7.

Guex, N., and M.C. Peitsch. 1997. SWISS-MODEL and the Swiss-PdbViewer: an environment for comparative protein modeling. *Electrophoresis*. 18:2714-23.

Hacker, H., and M. Karin. 2002. Is NF-kappaB2/p100 a direct activator of programmed cell death? *Cancer Cell*. 2:431-3.

Hanzel, D., H. Reggio, A. Bretscher, J.G. Forte, and P. Mangeat. 1991. The secretion-stimulated 80K phosphoprotein of parietal cells is ezrin, and has properties of a membrane cytoskeletal linker in the induced apical microvilli. *Embo J*. 10:2363-73.

Harvill, E.T., P.A. Cotter, and J.F. Miller. 1999. Pregenomic comparative analysis between bordetella bronchiseptica RB50 and Bordetella pertussis tohama I in murine models of respiratory tract infection. *Infect Immun*. 67:6109-18.

Harvill, E.T., A. Preston, P.A. Cotter, A.G. Allen, D.J. Maskell, and J.F. Miller. 2000. Multiple roles for Bordetella lipopolysaccharide molecules during respiratory tract infection. *Infect Immun*. 68:6720-8.

Hauf, N., W. Goebel, F. Fiedler, Z. Sokolovic, and M. Kuhn. 1997. Listeria monocytogenes infection of P388D1 macrophages results in a biphasic NF-kappaB (RelA/p50) activation induced by lipoteichoic acid and bacterial phospholipases and mediated by IkappaBalpha and IkappaBbeta degradation. *Proc Natl Acad Sci U S A*. 94:9394-9.

Haugh, J.M., A. Wells, and D.A. Lauffenburger. 2000. Mathematical modeling of epidermal growth factor receptor signaling through the phospholipase C pathway: mechanistic insights and predictions for molecular interventions. *Biotechnol Bioeng*. 70:225-38.

Heinrich, R., B.G. Neel, and T.A. Rapoport. 2002. Mathematical models of protein kinase signal transduction. *Mol Cell*. 9:957-70.

Heinrich, R., and S. Schuster. 1996. The regulation of cellular systems.

Henderson, S., D. Huen, M. Rowe, C. Dawson, G. Johnson, and A. Rickinson. 1993. Epstein-Barr virus-coded BHRF1 protein, a viral homologue of Bcl-2, protects human B cells from programmed cell death. *Proc Natl Acad Sci U S A*. 90:8479-83.

Henderson, S., M. Rowe, C. Gregory, D. Croom-Carter, F. Wang, R. Longnecker, E. Kieff, and A. Rickinson. 1991. Induction of bcl-2 expression by Epstein-Barr virus latent membrane protein 1 protects infected B cells from programmed cell death. *Cell*. 65:1107-15.

Hickman, J.A. 1992. Apoptosis induced by anticancer drugs. *Cancer Metastasis Rev*. 11:121-39.

Higgins, S.C., E.C. Lavelle, C. McCann, B. Keogh, E. McNeela, P. Byrne, B. O'Gorman, A. Jarnicki, P. McGuirk, and K.H. Mills. 2003. Toll-like receptor 4-mediated innate IL-10 activates antigen-specific regulatory T cells and confers resistance to Bordetella pertussis by inhibiting inflammatory pathology. *J Immunol*. 171:3119-27.

Hill, J.M., G. Morisawa, T. Kim, T. Huang, Y. Wei, and M.H. Werner. 2004. Identification of an expanded binding surface on the FADD death domain responsible for interaction with CD95/Fas. *J Biol Chem*. 279:1474-81.

Hofestad, R. 2000. Summer school on bioinformatics: information systems and network analysis of gene regulation and metabolism. *Biosystems*. 56:55-7.

Holler, N., R. Zaru, O. Micheau, M. Thome, A. Attinger, S. Valitutti, J.L. Bodmer, P. Schneider, B. Seed, and J. Tschopp. 2000. Fas triggers an alternative, caspase-8-independent cell death pathway using the kinase RIP as effector molecule. *Nat Immunol*. 1:489-95.

Holy, T.E., and S. Leibler. 1994. Dynamic instability of microtubules as an efficient way to search in space. *Proc Natl Acad Sci U S A*. 91:5682-5.

Horiuti, J., and T. Nakamura. 1957. Stoichiometric number and the theory of steady reaction. *Z. Phys. Chem. Neue Folge*. 11:358-365.

Howe, D., and L.P. Mallavia. 2000. Coxiella burnetii exhibits morphological change and delays phagolysosomal fusion after internalization by J774A.1 cells. *Infect Immun*. 68:3815-21.

Hsu, H., J. Huang, H.B. Shu, V. Baichwal, and D.V. Goeddel. 1996. TNF-dependent recruitment of the protein kinase RIP to the TNF receptor-1 signaling complex. *Immunity*. 4:387-96.

Hu, W.H., H. Johnson, and H.B. Shu. 2000. Activation of NF-kappaB by FADD, Casper, and caspase-8. *J Biol Chem*. 275:10838-44.

Huang, B., M. Eberstadt, E.T. Olejniczak, R.P. Meadows, and S.W. Fesik. 1996. NMR structure and mutagenesis of the Fas (APO-1/CD95) death domain. *Nature*. 384:638-41.

Huang, C.Y., and J.E. Ferrell, Jr. 1996. Ultrasensitivity in the mitogen-activated protein kinase cascade. *Proc Natl Acad Sci U S A*. 93:10078-83.

Ideker, T., O. Ozier, B. Schwikowski, and A.F. Siegel. 2002. Discovering regulatory and signalling circuits in molecular interaction networks. *Bioinformatics*. 18 Suppl 1:S233-40.

Jacobson, M.D., M. Weil, and M.C. Raff. 1997. Programmed cell death in animal development. *Cell*. 88:347-54.

Jahraus, A., M. Egeberg, B. Hinner, A. Habermann, E. Sackman, A. Pralle, H. Faulstich, V. Rybin, H. Defacque, and G. Griffiths. 2001. ATP-dependent membrane assembly of F-actin facilitates membrane fusion. *Mol Biol Cell*. 12:155-70.

Jeong, E.J., S. Bang, T.H. Lee, Y.I. Park, W.S. Sim, and K.S. Kim. 1999. The solution structure of FADD death domain. Structural basis of death domain interactions of Fas and FADD. *J Biol Chem*. 274:16337-42.

Kasof, G.M., J.C. Prosser, D. Liu, M.V. Lorenzi, and B.C. Gomes. 2000. The RIP-like kinase, RIP3, induces apoptosis and NF-kappaB nuclear translocation and localizes to mitochondria. *FEBS Lett*. 473:285-91.

Kataoka, T., R.C. Budd, N. Holler, M. Thome, F. Martinon, M. Irmler, K. Burns, M. Hahne, N. Kennedy, M. Kovacsovics, and J. Tschopp. 2000. The caspase-8 inhibitor FLIP promotes activation of NF-kappaB and Erk signaling pathways. *Curr Biol*. 10:640-8.

Katz, A.R., and D.M. Morens. 1992. Severe streptococcal infections in historical perspective. *Clin Infect Dis*. 14:298-307.

Kelliher, M.A., S. Grimm, Y. Ishida, F. Kuo, B.Z. Stanger, and P. Leder. 1998. The death domain kinase RIP mediates the TNF-induced NF-kappaB signal. *Immunity*. 8:297-303.

Kholodenko, B.N., O.V. Demin, G. Moehren, and J.B. Hoek. 1999. Quantification of short term signaling by the epidermal growth factor receptor. *J Biol Chem*. 274:30169-81.

King, K.L., and J.A. Cidlowski. 1995. Cell cycle and apoptosis: common pathways to life and death. *J Cell Biochem*. 58:175-80.

Kirimanjeswara, G.S., P.B. Mann, and E.T. Harvill. 2003. Role of antibodies in immunity to Bordetella infections. *Infect Immun*. 71:1719-24.

Kischkel, F.C., S. Hellbardt, I. Behrmann, M. Germer, M. Pawlita, P.H. Krammer, and M.E. Peter. 1995. Cytotoxicity-dependent APO-1 (Fas/CD95)-associated proteins form a death-inducing signaling complex (DISC) with the receptor. *Embo J*. 14:5579-88.

Kitano, H. 2002. Computational systems biology. *Nature*. 420:206-10.

Kitano, H. 2004. Biological robustness. *Nat Rev Genet*. 5:826-37.

Kjeken, R., M. Egeberg, A. Habermann, M. Kuehnel, P. Peyron, M. Floetenmeyer, P. Walther, A. Jahraus, H. Defacque, S.A. Kuznetsov, and G. Griffiths. 2004. Fusion between phagosomes, early and late endosomes: a role for actin in fusion between late, but not early endocytic organelles. *Mol Biol Cell*. 15:345-58.

Kruse, K., and F. Julicher. 2003. Self-organization and mechanical properties of active filament bundles. *Phys Rev E Stat Nonlin Soft Matter Phys*. 67:051913.

Kühnel, M., E. Anes, J. Thakar, E. Bos, S. Erdogan, K. Zanier, M. Sattler, R. Schwarz, D. Holzer, B. Bruegger, V. Rybin, S. Schuster, J. Reich, T. Dandekar, and G. Griffiths. Latex bead phagosomes - a system for the gobal analysis of membrane signaling networks. *Nat Biotechnol. Submitted*.

Landowski, T.H., N. Qu, I. Buyuksal, J.S. Painter, and W.S. Dalton. 1997. Mutations in the Fas antigen in patients with multiple myeloma. *Blood*. 90:4266-70.

Leckie, M.J., A. ten Brinke, J. Khan, Z. Diamant, B.J. O'Connor, C.M. Walls, A.K. Mathur, H.C. Cowley, K.F. Chung, R. Djukanovic, T.T. Hansel, S.T.

Holgate, P.J. Sterk, and P.J. Barnes. 2000. Effects of an interleukin-5 blocking monoclonal antibody on eosinophils, airway hyper-responsiveness, and the late asthmatic response. *Lancet*. 356:2144-8.

Lee, E.H., and Y. Rikihisa. 1996. Absence of tumor necrosis factor alpha, interleukin-6 (IL-6), and granulocyte-macrophage colony-stimulating factor expression but presence of IL-1beta, IL-8, and IL-10 expression in human monocytes exposed to viable or killed Ehrlichia chaffeensis. *Infect Immun*. 64:4211-9.

Lee, I., S.V. Date, A.T. Adai, and E.M. Marcotte. 2004. A probabilistic functional network of yeast genes. *Science*. 306:1555-8.

Lett, D., M. Hsing, and F. Pio. 2004. Interaction profile-based protein classification of death domain. *BMC Bioinformatics*. 5:75.

Letunic, I., R.R. Copley, S. Schmidt, F.D. Ciccarelli, T. Doerks, J. Schultz, C.P. Ponting, and P. Bork. 2004. SMART 4.0: towards genomic data integration. *Nucleic Acids Res*. 32 Database issue:D142-4.

Li, F., T. Long, Y. Lu, Q. Ouyang, and C. Tang. 2004. The yeast cell-cycle network is robustly designed. *Proc Natl Acad Sci U S A*. 101:4781-6.

Li, M.S., J.L. Farrant, P.R. Langford, and J.S. Kroll. 2003. Identification and characterization of genomic loci unique to the Brazilian purpuric fever clonal group of H. influenzae biogroup aegyptius: functionality explored using meningococcal homology. *Mol Microbiol*. 47:1101-11.

Lundstrom, K. 2005. Structural genomics of GPCRs. *Trends Biotechnol*. 23:103-8.

Mahon, B.P., B.J. Sheahan, F. Griffin, G. Murphy, and K.H. Mills. 1997. Atypical disease after Bordetella pertussis respiratory infection of mice with targeted disruptions of interferon-gamma receptor or immunoglobulin mu chain genes. *J Exp Med*. 186:1843-51.

Malinin, N.L., M.P. Boldin, A.V. Kovalenko, and D. Wallach. 1997. MAP3K-related kinase involved in NF-kappaB induction by TNF, CD95 and IL-1. *Nature*. 385:540-4.

Mangan, D.F., and S.M. Wahl. 1991. Differential regulation of human monocyte programmed cell death (apoptosis) by chemotactic factors and pro-inflammatory cytokines. *J Immunol*. 147:3408-12.

Mangeat, P., C. Roy, and M. Martin. 1999. ERM proteins in cell adhesion and membrane dynamics. *Trends Cell Biol*. 9:187-92.

Mann, P.B., K.D. Elder, M.J. Kennett, and E.T. Harvill. 2004. Toll-like receptor 4-dependent early elicited tumor necrosis factor alpha expression is critical for innate host defense against Bordetella bronchiseptica. *Infect Immun*. 72:6650-8.

Matsuno, H., Y. Tanaka, H. Aoshima, A. Doi, M. Matsui, and S. Miyano. 2003. Biopathways representation and simulation on hybrid functional Petri net. *In Silico Biol*. 3:389-404.

Mattoo, S., A.K. Foreman-Wykert, P.A. Cotter, and J.F. Miller. 2001. Mechanisms of Bordetella pathogenesis. *Front Biosci*. 6:E168-86.

McGuirk, P., B.P. Mahon, F. Griffin, and K.H. Mills. 1998. Compartmentalization of T cell responses following respiratory infection with Bordetella pertussis: hyporesponsiveness of lung T cells is associated with modulated expression of the co-stimulatory molecule CD28. *Eur J Immunol*. 28:153-63.

McGuirk, P., C. McCann, and K.H. Mills. 2002. Pathogen-specific T regulatory 1 cells induced in the respiratory tract by a bacterial molecule that stimulates interleukin 10 production by dendritic cells: a novel strategy for evasion of protective T helper type 1 responses by Bordetella pertussis. *J Exp Med*. 195:221-31.

Mendes, P. 1993. GEPASI: a software package for modelling the dynamics, steady states and control of biochemical and other systems. *Comput Appl Biosci*. 9:563-71.

Merrell, D.S., and S. Falkow. 2004. Frontal and stealth attack strategies in microbial pathogenesis. *Nature*. 430:250-6.

Meylan, E., F. Martinon, M. Thome, M. Gschwendt, and J. Tschopp. 2002. RIP4 (DIK/PKK), a novel member of the RIP kinase family, activates NF-kappa B and is processed during apoptosis. *EMBO Rep*. 3:1201-8.

Micheau, O., and J. Tschopp. 2003. Induction of TNF receptor I-mediated apoptosis via two sequential signaling complexes. *Cell*. 114:181-90.

Mills, K.H. 2001. Immunity to Bordetella pertussis. *Microbes Infect*. 3:655-77.

Mills, K.H. 2004. Regulatory T cells: friend or foe in immunity to infection? *Nat Rev Immunol*. 4:841-55.

Mills, K.H., A. Barnard, J. Watkins, and K. Redhead. 1993. Cell-mediated immunity to Bordetella pertussis: role of Th1 cells in bacterial clearance in a murine respiratory infection model. *Infect Immun*. 61:399-410.

Mills, K.H., and A.P. Boyd. Topley and Wilson's Microbiology and Microbial infections 10th edn (eds Kaufmann, S. H. & Steward, M.). Edward Arnold Publishers Ltd, London, in press.

Mills, K.H., M. Ryan, E. Ryan, and B.P. Mahon. 1998. A murine model in which protection correlates with pertussis vaccine efficacy in children reveals complementary roles for humoral and cell-mediated immunity in protection against Bordetella pertussis. *Infect Immun*. 66:594-602.

Mitchison, T., and M. Kirschner. 1984a. Dynamic instability of microtubule growth. *Nature*. 312:237-42.

Mitchison, T., and M. Kirschner. 1984b. Microtubule assembly nucleated by isolated centrosomes. *Nature*. 312:232-7.

Mogilner, A., and L. Edelstein-Keshet. 2002. Regulation of actin dynamics in rapidly moving cells: a quantitative analysis. *Biophys J*. 83:1237-58.

Mordue, D.G., and L.D. Sibley. 1997. Intracellular fate of vacuoles containing Toxoplasma gondii is determined at the time of formation and depends on the mechanism of entry. *J Immunol*. 159:4452-9.

Morris, D., and J.C. McDonald. 1957. Failure of hyperimmune gamma globulin to prevent whooping cough. *Arch Dis Child*. 32:236-9.

Mott, J., and Y. Rikihisa. 2000. Human granulocytic ehrlichiosis agent inhibits superoxide anion generation by human neutrophils. *Infect Immun*. 68:6697-703.

Musante, C.J., A.K. Lewis, and K. Hall. 2002. Small- and large-scale biosimulation applied to drug discovery and development. *Drug Discov Today*. 7:S192-6.

Musser, J.M., and R.K. Selander. 1990. Brazilian purpuric fever: evolutionary genetic relationships of the case clone of Haemophilus influenzae biogroup aegyptius to encapsulated strains of Haemophilus influenzae. *J Infect Dis*. 161:130-3.

Nagata, S. 1998. Fas-induced apoptosis. *Intern Med*. 37:179-81.

Naismith, J.H., and S.R. Sprang. 1998. Modularity in the TNF-receptor family. *Trends Biochem Sci*. 23:74-9.

Nakayama, H., T. Yamaga, and Y. Kunioka. 1998. Fine profile of actomyosin motility fluctuation revealed by using 40-nm probe beads. *Biochem Biophys Res Commun*. 246:261-6.

Niggli, V., C. Andreoli, C. Roy, and P. Mangeat. 1995. Identification of a phosphatidylinositol-4,5-bisphosphate-binding domain in the N-terminal region of ezrin. *FEBS Lett*. 376:172-6.

Novotny, P., A.P. Chubb, K. Cownley, J.A. Montaraz, and J.E. Beesley. 1985. Bordetella adenylate cyclase: a genus specific protective antigen and virulence factor. *Dev Biol Stand*. 61:27-41.

Ogasawara, J., R. Watanabe-Fukunaga, M. Adachi, A. Matsuzawa, T. Kasugai, Y. Kitamura, N. Itoh, T. Suda, and S. Nagata. 1993. Lethal effect of the anti-Fas antibody in mice. *Nature*. 364:806-9.

Page, R.D. 1996. TreeView: an application to display phylogenetic trees on personal computers. *Comput Appl Biosci*. 12:357-8.

Papin, J.A., T. Hunter, B.O. Palsson, and S. Subramaniam. 2005. Reconstruction of cellular signalling networks and analysis of their properties. *Nat Rev Mol Cell Biol*. 6:99-111.

Park, A., and V.R. Baichwal. 1996. Systematic mutational analysis of the death domain of the tumor necrosis factor receptor 1-associated protein TRADD. *J Biol Chem*. 271:9858-62.

Pishko, E.J., G.S. Kirimanjeswara, M.R. Pilione, L. Gopinathan, M.J. Kennett, and E.T. Harvill. 2004. Antibody-mediated bacterial clearance from the lower respiratory tract of mice requires complement component C3. *Eur J Immunol*. 34:184-93.

Ponti, A., P. Vallotton, W.C. Salmon, C.M. Waterman-Storer, and G. Danuser. 2003. Computational analysis of F-actin turnover in cortical actin meshworks using fluorescent speckle microscopy. *Biophys J*. 84:3336-52.

Pradines, J., L. Rudolph-Owen, J. Hunter, P. Leroy, M. Cary, R. Coopersmith, V. Dancik, Y. Eltsefon, V. Farutin, C. Leroy, J. Rees, D. Rose, S. Rowley, A.

Ruttenberg, P. Wieghardt, C. Sander, and C. Reich. 2004. Detection of activity centers in cellular pathways using transcript profiling. *J Biopharm Stat*. 14:701-21.

Preston, A., J. Parkhill, and D.J. Maskell. 2004. The bordetellae: lessons from genomics. *Nat Rev Microbiol*. 2:379-90.

Preuss, U., H. Bierbaum, P. Buchenau, and K.H. Scheidtmann. 2003. DAP-like kinase, a member of the death-associated protein kinase family, associates with centrosomes, centromers, and the contractile ring during mitosis. *Eur J Cell Biol*. 82:447-59.

Qin, H., S.M. Srinivasula, G. Wu, T. Fernandes-Alnemri, E.S. Alnemri, and Y. Shi. 1999. Structural basis of procaspase-9 recruitment by the apoptotic protease-activating factor 1. *Nature*. 399:549-57.

Rajasethupathy, P., S.J. Vayttaden, and U.S. Bhalla. 2005. Systems modeling: a pathway to drug discovery. *Curr Opin Chem Biol*. 9:400-6.

Ratner, A., and W.R. Clark. 1993. Role of TNF-alpha in CD8+ cytotoxic T lymphocyte-mediated lysis. *J Immunol*. 150:4303-14.

Reaven, E.P., and S.G. Axline. 1973. Subplasmalemmal microfilaments and microtubules in resting and phagocytizing cultivated macrophages. *J Cell Biol*. 59:12-27.

Reddy, V.N., M.L. Mavrovouniotis, and M.N. Liebman. 1993. Petri net representations in metabolic pathways. *Proc Int Conf Intell Syst Mol Biol*. 1:328-36.

Reder, C. 1988. Metabolic control theory: a structural approach. *J Theor Biol*. 135:175-201.

Rene, T., and D.A. Richard. 1990. Biological Feedback.

Rhoades, E., F. Hsu, J.B. Torrelles, J. Turk, D. Chatterjee, and D.G. Russell. 2003. Identification and macrophage-activating activity of glycolipids released from intracellular Mycobacterium bovis BCG. *Mol Microbiol*. 48:875-88.

Robubi, A., T. Mueller, J. Fueller, M. Hekman, U.R. Rapp, and T. Dandekar. 2005a. B-Raf and C-Raf signaling investigated in a simplified model of the mitogenic kinase cascade. *Biol Chem*. 386:1165-71.

Robubi, A., T. Mueller, J. Fueller, M. Hekman, U.R. Rapp, and T. Dandekar. 2005b. Supplementary material to the paper "B-Raf and C-Raf signaling investigated in a simplified model of the mitogenic kinase cascade". *Biol Chem*. 386:Sup36-Sup37.

Ross, P.J., E.C. Lavelle, K.H. Mills, and A.P. Boyd. 2004. Adenylate cyclase toxin from Bordetella pertussis synergizes with lipopolysaccharide to promote innate interleukin-10 production and enhances the induction of Th2 and regulatory T cells. *Infect Immun*. 72:1568-79.

Rouvier, E., M.F. Luciani, and P. Golstein. 1993. Fas involvement in Ca(2+)-independent T cell-mediated cytotoxicity. *J Exp Med*. 177:195-200.

Russell, D.G. 2001. Mycobacterium tuberculosis: here today, and here tomorrow. *Nat Rev Mol Cell Biol*. 2:569-77.

Ryan, M., G. Murphy, L. Gothefors, L. Nilsson, J. Storsaeter, and K.H. Mills. 1997. Bordetella pertussis respiratory infection in children is associated with preferential activation of type 1 T helper cells. *J Infect Dis*. 175:1246-50.

Sachs, L., and J. Lotem. 1993. Control of programmed cell death in normal and leukemic cells: new implications for therapy. *Blood*. 82:15-21.

Sanders, M.K., and D.A. Peura. 2002. Helicobacter pylori-Associated Diseases. *Curr Gastroenterol Rep*. 4:448-54.

Schorey, J.S., M.C. Carroll, and E.J. Brown. 1997. A macrophage invasion mechanism of pathogenic mycobacteria. *Science*. 277:1091-3.

Schuster, S., D.A. Fell, and T. Dandekar. 2000. A general definition of metabolic pathways useful for systematic organization and analysis of complex metabolic networks. *Nat Biotechnol*. 18:326-32.

Schwikowski, B., P. Uetz, and S. Fields. 2000. A network of protein-protein interactions in yeast. *Nat Biotechnol*. 18:1257-61.

Selter, H., and M. Montenarh. 1994. The emerging picture of p53. *Int J Biochem*. 26:145-54.

Shull, M.M., I. Ormsby, A.B. Kier, S. Pawlowski, R.J. Diebold, M. Yin, R. Allen, C. Sidman, G. Proetzel, D. Calvin, and et al. 1992. Targeted disruption of the mouse transforming growth factor-beta 1 gene results in multifocal inflammatory disease. *Nature*. 359:693-9.

Sinai, A.P., and K.A. Joiner. 1997. Safe haven: the cell biology of nonfusogenic pathogen vacuoles. *Annu Rev Microbiol*. 51:415-62.

Smith, G.R., and M.J. Sternberg. 2003. Evaluation of the 3D-Dock protein docking suite in rounds 1 and 2 of the CAPRI blind trial. *Proteins*. 52:74-9.

Souchelnytskyi, S. 2005. Bridging proteomics and systems biology: What are the roads to be traveled? *Proteomics*.

Squier, M.K., and J.J. Cohen. 1994. Cell-mediated cytotoxic mechanisms. *Curr Opin Immunol*. 6:447-52.

Stanger, B.Z., P. Leder, T.H. Lee, E. Kim, and B. Seed. 1995. RIP: a novel protein containing a death domain that interacts with Fas/APO-1 (CD95) in yeast and causes cell death. *Cell*. 81:513-23.

Stelling, J., S. Klamt, K. Bettenbrock, S. Schuster, and E.D. Gilles. 2002. Metabolic network structure determines key aspects of functionality and regulation. *Nature*. 420:190-3.

Stern, M., L. Meagher, J. Savill, and C. Haslett. 1992. Apoptosis in human eosinophils. Programmed cell death in the eosinophil leads to phagocytosis by macrophages and is modulated by IL-5. *J Immunol*. 148:3543-9.

Takeda, Y., H. Watanabe, S. Yonehara, T. Yamashita, S. Saito, and F. Sendo. 1993. Rapid acceleration of neutrophil apoptosis by tumor necrosis factor-alpha. *Int Immunol*. 5:691-4.

Telliez, J.B., G.Y. Xu, J.D. Woronicz, S. Hsu, J.L. Wu, L. Lin, S.F. Sukits, R. Powers, and L.L. Lin. 2000. Mutational analysis and NMR studies of the death domain of the tumor necrosis factor receptor-1. *J Mol Biol*. 300:1323-33.

Thakar, J., C. Liang, M. Kühnel, G. Griffith, and T. Dandekar. b. Spatial resolution model for phagosome- lysosome fusion. *BMC cell biology. in preperation*.

Thakar, J., M. Pilione, E. Harvill, and R. Albert. c. Modeling the interplay between Bordetellae and host immunity. *PLoS computational biology. in preperation*.

Thakar, J., K. Schleinkofer, C. Borner, and T. Dandekar. 2005. RIP death domain structural interactions implicated in TNF-mediated proliferation and survival. *Proteins: structure, function and bioinformatics*. *in press*.

Thakar, J., D. Walter, C. Borner, and T. Dandekar. Discrete time modeling of apoptosis pathway: comparison of topology and significance of critical components. *PLoS computational biology*. *Submitted*.

Thome, M., K. Hofmann, K. Burns, F. Martinon, J.L. Bodmer, C. Mattmann, and J. Tschopp. 1998. Identification of CARDIAK, a RIP-like kinase that associates with caspase-1. *Curr Biol*. 8:885-8.

Thompson, J.D., D.G. Higgins, and T.J. Gibson. 1994. CLUSTAL W: improving the sensitivity of progressive multiple sequence alignment through sequence weighting, position-specific gap penalties and weight matrix choice. *Nucleic Acids Res*. 22:4673-80.

Tilney, L. 1976. Actin: its aasociation with membranes and the regulation of its polymerization. *In Brinkley, B.R. and Porter, R.K. (eds), International Cell Biology. Rockfeller University Press, Boston, MA*:388-402.

Tilney, L.G., P.S. Connelly, L. Ruggiero, K.A. Vranich, and G.M. Guild. 2003. Actin filament turnover regulated by cross-linking accounts for the size, shape, location, and number of actin bundles in Drosophila bristles. *Mol Biol Cell*. 14:3953-66.

Tinel, A., and J. Tschopp. 2004. The PIDDosome, a protein complex implicated in activation of caspase-2 in response to genotoxic stress. *Science*. 304:843-6.

Tomita, M., K. Hashimoto, K. Takahashi, T. Shimizu, Y. Matsuzaki, F. Miyoshi, K. Saito, S. Tanida, K. Yugi, J.C. Venter, and C.A. Hutchison. 1997. E-CELL: Software Environment for Whole Cell Simulation. *Genome Inform Ser Workshop Genome Inform*. 8:147-155.

Tomita, M., K. Hashimoto, K. Takahashi, T.S. Shimizu, Y. Matsuzaki, F. Miyoshi, K. Saito, S. Tanida, K. Yugi, J.C. Venter, and C.A. Hutchison, 3rd. 1999. E-CELL: software environment for whole-cell simulation. *Bioinformatics*. 15:72-84.

van den Akker, W.M. 1998. Lipopolysaccharide expression within the genus Bordetella: influence of temperature and phase variation. *Microbiology*. 144 (Pt 6):1527-35.

Varfolomeev, E.E., M.P. Boldin, T.M. Goncharov, and D. Wallach. 1996. A potential mechanism of "cross-talk" between the p55 tumor necrosis factor receptor and Fas/APO1: proteins binding to the death domains of the two receptors also bind to each other. *J Exp Med*. 183:1271-5.

Verde, F., M. Dogterom, E. Stelzer, E. Karsenti, and S. Leibler. 1992. Control of microtubule dynamics and length by cyclin A- and cyclin B-dependent kinases in Xenopus egg extracts. *J Cell Biol*. 118:1097-108.

Verkhovsky, A., O. Chaga, S. Schaub, T. Svitkina, J. Meister, and G. Borisy. 2003. Orientational order of the lamellipodial actin network as demonstrated in living motile cells. *Mol Biol Cell*. 14:4667-75.

Wajant, H. 2002. The Fas signaling pathway: more than a paradigm. *Science*. 296:1635-6.

Wang, Y., H. Cui, A. Schroering, J.L. Ding, W.S. Lane, G. McGill, D.E. Fisher, and H.F. Ding. 2002. NF-kappa B2 p100 is a pro-apoptotic protein with anti-oncogenic function. *Nat Cell Biol*. 4:888-93.

Weber, C.H., and C. Vincenz. 2001. A docking model of key components of the DISC complex: death domain superfamily interactions redefined. *FEBS Lett*. 492:171-6.

Wells, A. 2000. Tumor invasion: role of growth factor-induced cell motility. *Adv Cancer Res*. 78:31-101.

White, E., P. Sabbatini, M. Debbas, W.S. Wold, D.I. Kusher, and L.R. Gooding. 1992. The 19-kilodalton adenovirus E1B transforming protein inhibits programmed cell death and prevents cytolysis by tumor necrosis factor alpha. *Mol Cell Biol*. 12:2570-80.

Woolf, P.J., and J.J. Linderman. 2004. An algebra of dimerization and its implications for G-protein coupled receptor signaling. *J Theor Biol*. 229:157-68.

Wyllie, A.H. 1997. Apoptosis: an overview. *Br Med Bull*. 53:451-65.

Xiao, T., K.H. Gardner, and S.R. Sprang. 2002. Cosolvent-induced transformation of a death domain tertiary structure. *Proc Natl Acad Sci U S A*. 99:11151-6.

Xiao, T., P. Towb, S.A. Wasserman, and S.R. Sprang. 1999. Three-dimensional structure of a complex between the death domains of Pelle and Tube. *Cell*. 99:545-55.

Yam, P.T., and J.A. Theriot. 2004. Repeated cycles of rapid actin assembly and disassembly on epithelial cell phagosomes. *Mol Biol Cell*. 15:5647-58.

Yu, P.W., B.C. Huang, M. Shen, J. Quast, E. Chan, X. Xu, G.P. Nolan, D.G. Payan, and Y. Luo. 1999. Identification of RIP3, a RIP-like kinase that activates apoptosis and NFkappaB. *Curr Biol*. 9:539-42.

Yu, X., and A.E. Carlsson. 2003. Multiscale study of counterion-induced attraction and bundle formation of F-actin using an Ising-like mean-field model. *Biophys J*. 85:3532-43.

Yuk, M.H., E.T. Harvill, P.A. Cotter, and J.F. Miller. 2000. Modulation of host immune responses, induction of apoptosis and inhibition of NF-kappaB activation by the Bordetella type III secretion system. *Mol Microbiol*. 35:991-1004.

Zevedei-Oancea, I., and S. Schuster. 2003. Topological analysis of metabolic networks based on Petri net theory. *In Silico Biol*. 3:323-45.

Contributions

Part I

Chapter 5

Professor Christoph Borner has carefully read the manuscript (accepted in Proteins: Structure, Fuction and Bioinformatics) and has given extremely important suggestions.
Medical cell research, Institute for Molecular Medicine, University of Freiburg, Stefan-Meier-Str. 17, 79104 Freiburg.

Karin Schleinkofer has guided for all structural analysis of proteins. She has also read the manuscript and provided suggestions.
Dept of bioinformatics, Biocenter, Am Hubland, University of Würzburg, 97074 Wuerzburg

Chapter 6

Dorothée Walter (PhD Student) has done all experimental work (section --) under the supervision of Professor Christoph Borner; which is used for the model validation.
Medical cell research, Institute for Molecular Medicine, University of Freiburg,
Stefan-Meier-Str. 17, 79104 Freiburg.

Part II

Chapter 7 and 8

Mark Kühnel (Post doctor fellow) has done all experimental work under the supervision of Dr. Gareth Griffith.
European Molecular Biology Laboratory, Postbox 102209, D-69012 Heidelberg, Germany.

Part III

Chapter 9

The work was performed in Pennsylvania State University, Department of Physics under the supervision of Professor Réka Albert. The fellowship

was awarded for three months (June-August 2005) by the Department of physics.
Department of Physics, Pennsylvania State University, 18902 Davey Laboratory, University park, PA 18902, USA.

Mylisa Pilione (Graduate student) and Professor Eric Harvill have given extremely important suggestions about *Bordetellae* pathology during the work.
Department of Veterinary and Biomedical Sciences, 18902 Henning Building, University park, PA 18903, USA.

All other work of the thesis including the drafts of manuscripts was done by Juilee Thakar under the guidance of Professor Thomas Dandekar, in the department of Bioinformatics, Wuerzburg.

Curriculum vitae

Personal information

Name	Juilee THAKAR
Date of Birth	21 April 1981
Place of Birth	Limerick, Republic of Ireland
Nationality	Irish
Address	Gneisenaus strasse 24B, 97074 Wuerzburg, Germany
Telephone	(0049) 017624553817
Email	Juilee.Thakar@biozentrum.uni-wuerzburg.de, juilee2000@yahoo.com
Occupation	Graduate student

Research interests Network modeling: to understand Biological networks

Educational Background

January 2004 – Present   PhD student in the group of Professor Thomas Dandekar, Department of Bioinformatics, University of Wuerzburg, Germany

August 2003 – December 2003   Research assistant in the group of Professor Bernhard Dobberstein, Zentrum für Molekular Biology, University of Heidelberg, Germany.

June 2001– June 2003   **Masters of Science** (honors - Microbiology) completed with **First class**, University of Pune, Abasaheb Garaware College, Pune, India.

June 2001 – June 2003   **Post graduate diploma in computational biology** (Part time) completed with 'A' grade (highest), Institute of Communication and Management, Abasaheb Garaware College, Pune, India.

June 1998 –April 2001   **Bachelors of Science** completed with **First class**, University of Pune, Abasaheb Garaware College, Pune, India.

June 1996 – March 1998   Higher secondary school completed with First class Distinction, Maharashtra State Board, India.

June 1986 – March 1996   Primary and Secondary school completed with First class Distinction, Maharashtra State Board, India.

Academic exchange during Phd

June 2005 – August 2005   Visiting scientist in the group of Professor Réka Albert, Department of Physics, Pennsylvania State University, USA. (Funded by fellowship)

November 2004   Visiting Scientist in the collaborating group of Professor Jens Timmer, Department of Physics, University of Freiburg, Germany. (Funded by BMBF)

Research experience (Before joining PhD)

1. "Simulation modeling of social behavior of myxobacteria" (July 2002 – April 2003) **Master's thesis 2**, in the group of Dr. M. Watve, Head, Microbiology Department, Maharshtra Education Society's Abasaheb Garware College, Pune.

2. "Characterization and localization of protein kinase D2" (April 2002 – June 2002) **Master's thesis 1**, in the group of Prof. Srinivas Ponnabalam, Biochemistry department, Leeds University, UK.

3. "Computational model for evolution of an sexual or asexual individual in co-operative group" (November 2001 – March 2002), in the group of Dr. M. Watve, Head, Microbiology Department, Maharshtra Education Society's Abasaheb Garware College, Pune.

4. "Studies on diffusion of proteins in lipid bilayer" (May 2001 – October 2001), in the group of Dr. Murli Sastry, National Chemical laboratory, Pune. (Scientific paper has been accepted in Colloids and surfaces B: Biointerfaces)

5. "Nectarless flowers: Floral and ecological co-relates and evolutionary stability" (January 2000 – January 2001), in the group of Dr. Milind Watve, Head, Microbiology Department, Abasaheb Garware College, Maharshtra Education Society, Pune. (Scientific paper has been published in Oecologia)

6. "Follow up study of Theory of mind in bee-eaters (*Merops orientalis*)" (May2000 - Aug 2000), in the group of Dr. Milind Watve, Head, Microbiology Department, Abasaheb Garware College, Maharshtra

Education Society, Pune. (Published in international Journal 'Animal Cognition")

7. "Study of Biodiversity in Western Ghats – *tamhani*" (June 1999 – March 2001), in the group of Prof. Milind Watve, Department of Microbiology and Dr. A. Padhye, Department of Zoology, Abasaheb Garware College, Maharshtra Education Society, Pune.
Director of the project: Prof. Madhav Gadgil, Center of Ecological Sciences, Indian Institute of Science, Bangalore.

8. "Comparison of behavior of queens of two species of Indian paper wasps, *Ropalidia cyathiformis* and *Ropalidia marginata*" (April 1999 – June 1999), in the group of Prof. R Gadagkar, Chairman, Center of Ecological Sciences, Indian Institute of Science, Bangalore. (Scientific paper has been published in Naturwissenschaften (2002) 89:176–179)

List of Publications

Publications associated with thesis

Juilee Thakar, Dorothee Walter, Christoph Borner and Thomas Dandekar "Discrete time modeling of apoptosis pathway: comparison of topology and significance of critical components" submitted to PLoS computational biology.

Mark Philipp Kühnel, Elsa Anes, **Juilee Thakar**, Evelyne Bos, Sezgin Erdogan, Katia Zanier, Michael Sattler, Roland Schwarz, Daniela Holzer, Britta Bruegger, Vladimir Rybin, Stefan Schuster, Jens Georg Reich, Thomas Dandekar and Gareth Griffiths "Latex bead phagosomes- a system for the global analysis of membrane signaling networks" in preparation for Nature Biotechnology.

Juilee Thakar, Mylisa Pilione, Eric Harvill and Réka Albert "Modeling interplay between Bordetellae and host immunity" submitted for PLoS pathogens

Juilee Thakar, Mark Kühnel, Gareth Griffith and Thomas Dandekar "Spatial resolution model for Phagosome-Lysosome fusion" in preparation for BMC cell biology.

Juilee Thakar, Karin Schleinkofer, and Thomas Dandekar "RIP death domain structural interactions implicated in TNF-mediated proliferation and survival" Proteins: Structure, Function and Bioinformatics, *in press* (accepted 2005 November)

Prior publications

Juilee Thakar, Krushnamegh Kunte, Anisha Chauhan and Milind Watve
"Nectarless flowers: Ecological correlates and evolutionary stability"
Oecologia 136:4,565-70 (2003).

Anand Gole, **Juilee Thakar** and Murli Sastry "Protein diffusion in to thermally
evaporated lipid films: role of protein charge/mass ratio." Colloids and surfaces
B: Biointerfaces 28(2-3):209-214 (2002).

Milind Watve, **Juilee Thakar**, Abhijit Kale, Shweta Puntambekar, Imraan
Shaikh, Kaustubh Vaze, Maithili Jog, Paranjape S "Bee-eater (*Merops orientalis*)
respond to what a predator can see" Animal cognition, 5:4, 253-259 (2002).

B. Smitha, **Juilee Thakar**, Milind Watve "Do bee-eaters have a theory of mind?"
Current Science 76:4, 574-577 (1999).

Conferences contributions

1. "BMBF status seminar – Network System Biology HepatoSys", Berlin,
   Germany (November 2005) **Poster presented** "Mathematical modeling of
   the Fas/CD95-induced signaling pathway in primary mouse hepatocyte"
   D. Walter, **J. Tharar**, C. Kreutz, S. McNelly, R. Nitschke, F. von
   Weizsäcker, J. Timmer, T. Dandekar and C. Borner.

2. "7th International EMBL PhD Student Symposium: Biology at work",
   Heidelberg, Germany (December 2005) **Poster presented** "Crucial death
   domain interactions in life and death" **J. Thakar**, K. Schleikofer, C. Borner
   and T. Dandekar.

3. "International Society for Computational Biology"(ISMB), Detroit,
   Michigan, USA (June 2005) **Poster presented** "Spatial resolution model
   for actin polymerization and fusion of lysosome phagosome." **J. Thakar**,
   M. Kuehnel, G. Griffiths, and T. Dandekar.

4. "Systems of Life- System biology meeting", Heidelberg, Germany. (April
   2005) **Poster presented** "Mathematical modeling of the Fas/CD95-induced
   signaling pathway in primary mouse hepatocytes." D. Walter, **J. Thakar**,
   C. Kreutz, K. Neubert, S. McNelly, F. Weizsäcker, J. Timmer, T. Dandekar
   and C. Borner.

5. "International conference on systems biology", Heidelberg, Germany. (October 2004): **Poster presented** "Modelling Fas ligand-induced apoptosis in primary mouse hepatocytes", L. Egger, C. Kreutz, **J. Thakar**, J. Timmer, T. Dandekar and C. Borner.

6. "Discussion meeting on behavioral ecology", University of Mysore, Karnataka, India. Convener by Prof R Gadagkar, and Prof H.A Ranganathan. (July 1999) (By invitation)

Distinctions

1. Fellowship awarded by BMBF (German ministry of science and technology) initiative in Systems Biology "HepatoSys", Germany from 2004 - 2006.
2. Fellowship awarded by the Pennsylvania state university, Department of Physics, for summer internship in 2005.
3. Fellowship awarded by the University of Leeds, Department of Biochemistry, for summer internship in 2002.
4. Scholarship awarded by the Association for the Study of Animal Behavior (ASAB), Edinburgh, UK, for "Follow up study of 'Theory of mind' in bee-eaters *(Merops orientalis)*" in 2001.

Language Skills

English, Marathi, Hindi (fluent)
German (Studied till intermediate level)

Interests

Wild life and nature conservation activities with environmental organizations:
1. Life Research Foundation, Pune (2001-2003): Newsletter editor.
2. World Wide Fund (WWF) for Nature India, New Delhi, Pune branch (1999 - 2003).
3. Bombay Natural History Society (BNHS), Mumbai (1995 - 2003).
4. "Nisargavedha" (Nature lover's organization), Pune (1995 - 2003).
5. Bhumata, (Nature lovers organization), Pune (1991 - 2003).